Degradation of plastics in the marine environment with reference to temperature and environmental factors

by

Delene Nel

Thesis presented in partial fulfilment
of the requirements for the Degree

of

MASTER OF ENGINEERING
(EXTRACTIVE METALLURGICAL ENGINEERING)

in the Faculty of Engineering
at Stellenbosch University

Supervisor

Prof Guven Akdogan

Co-Supervisors

Prof Christie Dorfling
Prof Annie Chimphango

December 2020

DECLARATION

By submitting this thesis electronically, I declare that the entirety of the work contained therein is my own, original work, that I am the sole author thereof (save to the extent explicitly otherwise stated), that reproduction and publication thereof by Stellenbosch University will not infringe any third party rights and that I have not previously in its entirety or in part submitted it for obtaining any qualification.

Date: *23 November 2020*

PLAGIARISM DECLARATION

1. Plagiarism is the use of ideas, material and other intellectual property of another's work and to present it is as my own.

2. I agree that plagiarism is a punishable offence because it constitutes theft.

3. I also understand that direct translations are plagiarism.

4. Accordingly, all quotations and contributions from any source whatsoever (including the internet) have been cited fully. I understand that the reproduction of text without quotation marks (even when the source is cited) is plagiarism.

5. I declare that the work contained in this assignment, except where otherwise stated, is my original work and that I have not previously (in its entirety or in part) submitted it for grading in this module/assignment or another module/assignment.

Student number: … ……..

Initials and surname: D. Nel ……..

Signature: ……..

Date: 23 November 2020 ……..

ABSTRACT

Plastic waste is an increasing problem, especially in the marine environment, where it has detrimental effects on the ecosystem . For a better comprehension of the environmental implications and eventual fate of plastic waste, research on the degradation is required. This project aimed to fill some of the knowledge gaps by completing a laboratory investigation on temperature associated plastic history, which refers to the degradation induced via temperature on plastics waste during their journey to the ocean, and the effect this has on the degradation behaviour of the plastic in the marine environment. Influences of various environments and plastic properties were also considered.

Tests at various temperatures were conducted to investigate the effect of temperature associated with plastic history. The tests were conducted at the following temperatures: 25˚C, 100˚C and a weekly cycle of 25˚C – 60˚C. In these tests, three plastics, namely, black polypropylene, clear polypropylene, and clear PET, were investigated in various sizes and shapes. For example, there were large and small, circle and rectangles shapes. The temperature, size, type of plastic and colour additive was found to have important effects on the degradation rate.

In the second set of tests to investigate what transpires under marine environmental conditions, samples collected after completion of the constant 25˚C and 100˚C initial tests were subjected to the following respective treatments: constant temperatures of 25˚C or 60˚C or 12-hour cycles of 65 W/m^2 or 130 W/m^2 UV radiance – submerged in either seawater or demineralised water, respectively. The UV radiance appeared to be predominantly responsible for greater and/or accelerated degradation compared to naturally expected temperatures, especially for clear polypropylene that exhibited physically visible embrittlement under 130 W/m^2 UV radiance. Nonetheless, prolonged exposure is recommended for investigating the 65 W/m^2 and 25˚C. For both the initial and secondary tests the colour additive is suspected of hindering mechanical property degradation. The 100˚C initial treatment is, however, suspected of passivating the colour additive; since after the 100˚C treatment, the colour additive did not hinder degradation effectively.

The investigation into the effect of environment indicated that under controlled conditions with identical temperatures the addition of water resulted in degradation rate increases. This suggests that the real-life phenomenon of lower degradation in the marine environment than on land could be due to water regulating the temperature. It was furthermore observed that salinity has an accelerating effect on the degradation of polypropylene. PET tended to react similarly to the salinity but the data were not conclusive enough to affirm this theory.

OPSOMMING

Plastiekafval is ’n toenemende probleem, veral in die see-omgewing, waar dit nadelige effekte op die ekosisteem het (Griffin *et al.,* 2018; Jambeck, 2018; Heimowska, Krasowska & Rutkowska, 2014; O’Brine & Thompson, 2010; Wellfair, 2008; Derraik, 2002). Om die omgewingsimpak en eventuele lot van plastiekafval beter te verstaan, word navorsing oor die degradering vereis. Hierdie projek het beoog om sommige van die kennisgate te vul deur ’n laboratoriumondersoek oor temperatuur geassosieerde plastiekgeskiedenis te voltooi, wat verwys na die degradasie wat teweeg gebring word deur temperatuur op plastiekafval gedurende hul reis na die see-omgewing, en die effek wat dit het op die degradasie gedrag in die see-omgewing. Die invloed van verskeie omgewings en plastiekeienskappe is ook oorweeg.

Toetse is by verskeie temperature uitgevoer om die effek van temperatuur geassosieer met plastiekgeskiedenis te ondersoek. Die toetse is uitgevoer by die volgende temperature: 25 °C, 100 °C, en ’n weeklikse siklus van 25 °C – 60 °C. In hierdie toetse is drie tipes plastiek, naamlik swart polipropileen, deursigtige polipropileen, en deursigtige PET ondersoek in verskeie groottes en vorms. Byvoorbeeld, daar was groot en klein, sirkel en reghoekige vorms. Dit is gevind dat die temperatuur, grootte, tipe plastiek en kleurselbymiddels belangrike effekte op die degradasietempo het.

In die tweede stel toetse, waar daar ondersoek is wat onder see-omgewingkondisies gebeur, is steekproewe bymekaar gemaak na die voltooiing van die konstante 25 °C en 100 °C aanvanklike toetse, en aan die volgende onderskeidelike behandelinge blootgestel: konstante temperature van 25 °C of 60 °C of 12-uur siklusse van 65 W/m^2 of 130 W/m^2 UV-straling – onderdompel in of seewater of gedemineraliseerde water, onderskeidelik. Dit het geblyk of die UV-straling hoofsaaklik verantwoordelik is vir meer en/of versnelde degradasie in vergelyking met verwagte natuurlike temperature, veral vir deursigtige polipropileen wat fisiese sigbare verbrossing getoon het onder 130 W/m^2 UV-straling. Terselfdertyd word verlengde blootstelling voorgestel vir die ondersoek van 65 W/m^2 en 25 °C. Dit word vermoed dat, vir beide die aanvanklike en sekondêre toetse, die kleurbymiddel die meganiese eienskap degradasie verhinder het. Dit word egter vermoed dat die aanvanklike behandeling van 100 °C die kleurbymiddel passief laat, aangesien die kleurbymiddel nie die degradasie effektief verhinder het na die 100 °C-behandeling nie.

Die ondersoek na die effek van omgewing het aangetoon dat in identiese temperature onder gekontroleerde kondisies die byvoeging van water die degradasietempo laat toeneem. Hierdie stel voor dat die verskynsel van laer degradasie in die natuurlike see-omgewing teenoor die land die gevolg kan wees van die water wat die temperatuur reguleer. Die polipropileen toon ook dat die effek van soutinhoud beduidend versnellend is. PET het ’n soortgelyke tendens getoon, maar die PET se data was nie beduidend genoem om die teorie te bevestig nie.

ACKNOWLEDGEMENTS

I would like to thank God for granting me the opportunity to do this project and giving me preservation and strength to overcome all the obstacles I encountered.

I would also like to express my gratitude to the following people, without whose contributions the study would not have been possible:

My supervisors, Prof G. Akdogan and Prof C. Dorfling, for the opportunity as well as their insights, guidance, motivation and support throughout the study, also Prof A. Chimphango for her guidance.

The personnel at the Department of Process Engineering, particularly Ms M. De Jager at administration, Mr J. Weerdenburg and Mr A. Cordier from the workshop and Mr A. Petersen at the Technical Department.

Dr H. Pfukwa and Dr D.D. Robertson from the Department of Chemistry and Polymer Science and Dr L. Loots from the Department of Natural Science, who provided equipment and machinery for the analysis of results. As well as M. Prof Kidd for statistical assistance.

Mr J.C. Rademeyer for proofreading of the thesis.

My family, especially my parents, grandparents and brother for their support, motivation, advice, encouragement and love throughout my life and in everything I undertook. Also, my uncle, who made me sensitive to the plastic waste problem long before I started this study.

Lastly, my friends and colleagues for their support and advice.

I would hereby also like to acknowledge the partial financial assistance of the National Research Foundation (NRF).

TABLE OF CONTENTS

LIST OF FIGURES

NOMENCLATURE

Acronyms and abbreviations	
ANOVA	Analysis of variance
APET	Amorphous polyethylene terephthalate
BPP	Black polypropylene
C=C	Alkene
C=O	Carbonyl
CH	Methanetriyl
CH_2	Methylene
CH_3	Methyl
CPP	Clear polypropylene
DSC	Differential Scanning Calorimetry
FTIR	Fourier-transform infrared spectroscopy
ID	Identification
OH	Hydroxyl
PET	Polyethylene terephthalate
PP	Polypropylene
PSU	Practical Salinity Unit
R	Represents any group or chain of atoms connected to the molecule
UV	Ultraviolet

DEFINITION OF KEY TERMS

ANOVA	Analysis of variance is a collection of statistical models used to determine and analyse the variances in means
Biodegradation	Refers to degradation of polymers by microorganisms see 2.2.
Cis	A category used to define torsion angle between molecules see 2.1.1
Degradation	refers to the total breakdown of the polymer structure see 2.2.
Deterioration	refers to the change or loss of physical properties of a polymer see 2.2.
Eclipse	A category used to define torsion angle between molecules see 2.1.1
Fragmentation	refers to the breaking of the material into smaller pieces see 2.2
Gauche	A category used to define torsion angle between molecules see 2.1.1
Macro plastics	Plastic particles larger than 2.5 cm
Meso plastics	Plastic particles between 0.5 mm and 2.5 cm
Microplastics	Plastic particles between 0.05 and 0.5 mm
Nano plastics	Plastic particles smaller than 1 micrometre
OMNIC	FTIR analysis software
pH	Scale for measuring acidity or basicity of a solution
STATISTICA	Statistical analysis software
TA Instrument Explorer	DSC analysis software
Thermoplastics	Plastic that will soften under high temperatures, allowing the plastic to be remoulded and harden into the new mould as it cools down
Thermoset plastics	Plastic that will not soften upon heating and cannot be remoulded
Trans	A category used to define torsion angle between molecules see 2.1.1
Universal Analysis	DSC analysis software
* Plastic size from (Bletter, Ulla, Rabuffetti & Garello, 2017).	

INTRODUCTION

1.1 Background

The world is currently facing a plastic problem. Plastics have multiple uses from the textile industry to the medical industry. Various products, including parts of technology, sewage systems, household items, medical implants and especially single-use items, are manufactured from plastic material. Plastics are economically favoured alternatives due to their ability to be produced cheaply along with their properties and performance characteristics.

The problem the world is facing is attributed to the excessive use of plastic materials that are ultimately discarded, and these discarded plastics usually end up in the marine environment. Whether it has been dumped directly into the ocean or has travelled via land, wind and rivers, once it reaches the ocean, it stays for an extended period due to the long lifespan and durability of plastic. It is stated that an estimate of 8 million tons of plastic ends up in the worlds' ocean every year (Jambeck, 2018; Griffin, Wilkins & Bowen, 2018). This has led to an enormous accumulation of plastic debris in the worlds' oceans. Numerous articles have been written on findings of plastic litter, waste and debris in marine life, as well as floating islands and plastic dunes at the bottom of the ocean. It has been stated that plastic is responsible for 60 – 80% of the floating debris and marine litter, and 95% of the marine litter on the ocean floor (Derraik, 2002; Gewert, Plassmann & MacLeod, 2015 & Fotopoulou & Karapanagioti, 2017). Some of the most common polluters are polypropylene (PP), polyethene terephthalate (PET), polyethene (PE), poly (vinyl chloride) (PVC) and polystyrene (PS) (Chamas, Moon, Zheng, Qiu, Tabassum, Jang, Abu-Omar, Scott & Suh, 2020; Fotopoulou & Karapanagioti, 2017; Martinko, 2017; Crawford & Quinn, 2016; Gewert, *et al*., 2015; Kamrannejad, Hasanzadeh, Nosoudi, Mai & Babaluo, 2014; Moore, Moore, Leecaster & Weisberg, 2001).

Besides being unaesthetic, oceanic plastic waste is detrimental to the marine ecosystem. Marine animals often end up entangled in plastic waste, causing deformation, diseases and painful deaths. Animals also confuse plastic for their natural food source, and after consumption starve to death. The consumption of plastic litter by marine animals can also lead to micro- and nanoparticles moving into the human food cycle, which contains multiple unknown health hazards. Other detrimental effects are floating plastics acting as transport vehicles for persistent organic pollutants (POPs) to travel and disrupt distant and sensitive ecosystems, as well as the toxic chemicals (BPA, phthalates, and flame retardants) in plastics that leach out during degradation (Griffin, *et al*., 2018; Jambeck, 2018; Heimowska, Krasowska & Rutkowska, 2014; O'Brine & Thompson, 2010; Wellfair, 2008; Derraik, 2002).

1.2 Problem statement and significance of the study

In a country such as South Africa, a large quantity of plastic litter travels via land, wind and/or rivers to the ocean. The effect of the travel time is essential in understanding the expected degradation behaviour of plastic. South Africa is a country known for its sunshine and heat, and these factors play a significant role in the initiating of plastic degradation during this journey. Various other factors such as plastic-type,

colour additives, size and shape of particles also affect the degradation associated with this journey, as well as the degradation endured in the marine environment. The effects of these factors are also essential in improving the understanding of the expected degradation behaviour of plastic.

Recent studies on plastic alternatives, innovative collection techniques, quantification and determination of plastic waste, the eventual fate of plastic and plastic degradation implications and influencing factors have increased . Nevertheless, there are still many underlying issues, pathways of degradation, rate of degradation that are not fully understood and urgently requires further research. Currently, insufficient data are available on the effect of temperature, radiation, size and shape of the samples on the rate of change in physical and chemical properties of plastics (Chamas, *et al*., 2020). Also, limited data are available regarding the interaction between plastics and ambient or natural conditions, as most studies are done at extreme conditions, and the effect various environments have on the rate of degradation (Fotopoulou & Karapanagioti, 2017; Gewert, *et al*., 2015). Other insufficient important information is the effects of the plastic history, referencing to the degradation associated with the journey of plastics to the ocean, and the effect this has on the plastic degradation in the marine environment.

This research project aims to answer some of these by investigating the degradation behaviour (i.e. the rate of change in physical and chemical properties) of plastics under marine environment conditions while considering the effect of temperature associated plastic history[1] as well as investigating the effects of various other factors on plastics degradation behaviour such as shape, size, subjection to water or light and plastic-type. It is believed that obtaining a better understanding of the influence of these factors on degradation, through this investigation, will assistfuture research, in understanding the complex processes and in defining more accurate models to predict environmental implications and eventual fate of plastics to ensure long term marine sustainability. The data obtained from this research should yield an indication on the significance of the effects along with expected changes in physical and chemical properties of plastic due to the temperature associated plastic history and other factors, such as plastic-type, colour additive and size. The data can be used to assist, define and refine models to predict environmental implications and eventual fate of plastics which could assist with answers to ensuring long term marine sustainability. The data should also lead to conclusions and suggestions for further research that will enhance the comprehension of the complex processes of degradation.

1.3 Project focus and objectives

This research project aims to investigate the degradation behaviour of plastics under marine environment conditions while considering the effect or influence of temperature associated with plastic history[1] and the various other factors that affect plastics degradation such as shape, size, plastic-type, subjection to water and/or light.

[1] Plastic history refers to the effects, changes and degree of degradation associated with the period between the discarding of the plastic and when it reaches the marine environment.

The objectives of the project were:

1. Complete a study on the effect of temperature associated with plastic history.
    a. The study should include an initial treatment dataset that investigates the effect of temperature on plastics when not submerged in water and mimics the "journey" to the ocean.
    b. The study should tie in with the marine environment study (Objective 2), to investigate what the effect of the initial temperature treatment (or temperature associated plastic history) is on the plastic's degradation behaviour when submerged in seawater.
    c. The investigation of plastics not submerged in water should include an investigation on the effect of shape and/or size of the plastics on the plastic's degradation behaviour.
2. Complete a study on what transpires in the marine environment and obtain a set of degradation data.
    a. The study should include an investigation of the difference in degradation behaviour based on the deterioration of plastic properties and chemical composition between two different plastic types and two different plastic colours.
    b. The study should also include an investigation on the effects of the various environmental factors such as the temperature and UV radiance.
3. Complete an investigation on the effect of environment on the plastic's degradation behaviour.
    a. The investigation must compare the plastic's degradation behaviour obtained from a condition constant in both studies to investigate the effect of land versus water environment.
    b. The investigation should also include a set of degradation data for plastics not submerged in seawater, to investigate the effect of the seawater salinity.

1.4 Research approach

This project is part of a more extensive study. It, therefore, excludes the biological effects on plastic degradation as well as UV radiance related plastic history. The project is limited to temperature associated plastic history, and the marine environment is constrained to the South African context with moderate and high ocean temperatures. This project investigated what the effect of temperatures plastics are exposed to would have on the degradation rate and behaviour of plastic properties, as the plastics travel to the ocean. Along with the influence's of plastic-type, shape, size, and colour would have on this effect. This project also investigated the influence of this effect once plastics has reached the marine environment, again considering the influences of various plastic properties and environmental factors.

Therefore three plastics, clear polyethylene terephthalate, clear polypropylene and black polypropylene was considered as these types are some of the most common polluters (Chamas *et al.*, 2020; Fotopoulou & Karapanagiati, 2017; Martinko, 2017; Crawford & Quinn, 2016; Gewert *et al*., 2015; Kamrannejad *et al*., 2014; Moore *et al*., 2001). The plastics were cut into two sizes and two shapes (therefore four different samples) and subjected to various temperature conditions. Data of hardness, degree of crystallinity and functional group index in the plastics over six weeks were collected. This data set was

used to investigate how the temperature affects plastics and the variance in effect between the two plastic types, the two plastic colours, the two sizes and two shapes.

After the initial investigation, some of the samples from these treatments were subjected to a second set of experiments. The second set focused on one shape and size. However, it investigated eight different treatments: two temperature and two UV radiance treatments in either seawater or demineralised water. Data of hardness, degree of crystallinity and functional group index in the plastics were collected over 6 six weeks. This data set was used to investigate how the initial treatment (or plastic history), the marine and freshwater environments and the different conditions (temperature and UV radiance) have affected the degradation behaviour and rate, all regarding the variance in effect between the two plastic types and colours.

1.5 Thesis chapter overview

The thesis is set out as follows: Chapter 1 introduces the study, with a background on why marine plastic waste is an environmental problem. Chapter 1 goes on the give the problem statement and focus of this project along with the objective and research questions, followed by why the study is significant, how it was approached, the scope and any limitations of the study.

Chapter 2 forms the literature review that starts with a quick overview of polymers. The first subsection in this overview focuses on the chemistry of how polymers are manufactured, what chemicals or additives can be added, the molecular orientation and structure of polymers. The following subsection gives particular reference to polypropylene and polyethylene terephthalate as these are the two plastics used in the investigation and is followed by a subsection on polymer analysis. The analysis subsection focuses on what functional groups, hardness and degree of crystallinity are and how it can be monitored during a polymer degradation study. Next, the literature review describes degradation, the various classes and the mechanisms followed by polypropylene and polyethylene terephthalate. The literature review ends with an overview of naturally expected environmental conditions in the South African context.

In Chapter 3, the research design and methodology are discussed. Chapter 3 also list all the materials and equipment used and followed by an explanation of the experimental design and procedure on how the tests were completed, as well as the analysis procedure on how the data were obtained. Chapter 3 ends with an explanation of how the data were processed to be able to be useful in analysing results.

Chapter 4 discussed the results. The result section starts with the results obtained from the initial tests and discusses any noteworthy trends or changes observed. This is followed by the results from the secondary set of tests after which a similar discussion on the secondary set of tests is given. Chapter 4 ends in a comparison between the various environments investigated.

The report is ended with Chapter 5, where the conclusions are drawn, and the recommendations made during the study are highlighted.

2 LITERATURE REVIEW

2.1 Polymers

Plastics, or polymers, are compounds of high molecular weight, that consists of long linear chains of linked, repeating monomers. Polymers are formed during the polymerisation of monomers. Monomers are generally organic molecules consisting of atoms such as carbon, hydrogen, oxygen and sometimes nitrogen and sulphide. This repeating monomer chain forms the backbone of the polymer. Linked to the backbone of the polymer are side chains or crosslinks, which affects the orientation of the polymer structure and order. Incorporated into the polymer are numerous additives and other impurities with various effects and purposes (Callister & Rethwisch, 2015; Wellfair, 2008).

2.1.1 Polymer chemistry

2.1.1.1 Polymerisation

As discussed at point 2.1, polymers consist of repeating monomer units in long chains. Therefore, to synthesise a polymer, these monomer units are polymerised by addition polymerisation or condensation polymerisation.

Addition polymerisation, also called chain reaction or chain growth, is mostly applied to monomers containing an alkene unit. An alkene unit, or double bond between two carbon atoms, contains one sigma bond and one pi bond. The reaction is initiated by an active initiator containing a free radical attacking the pi bond of the monomer molecule. The pi bond breaks and a new sigma bond is formed with one of the electrons, between the initiator and one of the carbon atoms. This leaves the other electron unpaired on the other carbon atom, causing another free radical. This results in the propagation step of polymerisation where the new radicals formed will attack another pi bond on other monomers. The reaction will terminate when two radicals react to form one linked chain or two dead ends (Callister & Rethwisch, 2015; Silber, 2013).

Condensation, or stepwise, polymerisation contains two functional groups and are commonly applied to synthesise copolymers. Usually, the monomer has the form of A-R-B where A and B are molecules or functional groups, that can be identical or not, and R is the rest of the molecule. The monomers will most commonly link when the A functional group on one of the monomers undergoes a dehydration-condensation reaction with the B group on another monomer. Usually, during this reaction, there is a low-molecular-weight by-product being eliminated. This process is repeated to form a linear molecule (Callister & Rethwisch, 2015; Silber, 2013).

During the polymerisation processes, various chemicals can be added to act as initiators, activators, promoters, modifiers, stabilisers, plasticisers and emulsifiers. The remnants of the initiators, activators and promoters, along with all the additives added will be caught in the polymer structure. These molecules are referred to as impurities, as they are not part of the “pure” monomer repeat unit the polymer is expected to consist. Other possible impurities to exist in the polymer are the monomer units

left that did not undergo polymerisation, non-polymerisable impurities caught in the monomer and functional groups that are not characteristic of the polymer but are present due to secondary reactions occurring. These impurities can be the initiators for degradation, and they can also cause crazing, discolouration, embrittlement and softening or influence polymer characteristics and ageing. In the case of additives, see 2.1.1.2, these impurities were purposefully added for the benefits of their effects, for example, colour additives, or UV stabilisers. However, it is essential to note that a polymer is never pure (Mark, 1948; Gewert *et al*., 2015).

2.1.1.2 Additives

An additive can be described as a substance incorporated into the polymer to achieve a technical effect on and is intended to be an essential part of, the finished product. (Ambrogi, Carfagna, Cerruti, & Marturano, 2017). General functions of additives are protection against weathering, heat stabiliser, flame retardant, a dye or pigment, plasticiser or impact modifier.

a) Stabilisers and protectors

Stabilisers and protectors are added to prolong the life of the polymer by increasing the resistance to degradation and slowing environment degradation down (Chamas, *et al*., Gewert, *et al*., 2015; Izdebska & Thomas, 2016). An anti-stabiliser, known as a pro-oxidant, can also be added to increase the plastics' sensitivity to degradation and has the opposite effect by decreasing the polymers' lifetime (Gewert *et al*., 2015). The stabilisers can be divided into three classes: protection against weathering, heat stabilisers and flame retardants, each contains multiple subclasses.

As discussed in 2.2, various natural factors attacks and affect polymer stability, causing degradation and failure of the polymer – this is sometimes referred to as weathering. Antioxidants are one of the additives that protect polymers against weathering by interfering with the thermal- and photo-oxidative cycles to obstruct or reduce the oxidative degradation process. Antioxidants can be categorised under primary and secondary antioxidants. Primary antioxidants such as phenols and amines act as hydrogen donors that terminate the oxidative chain reaction. The phenols have a reactive OH group while the amines have a reactive NH group, the reactive groups transfer a proton to the radical species. The resulting radical is stable and therefore, unable to disrupt the polymer chain by attracting a proton from the chain. The secondary antioxidants, such as phosphites and thioester, are referred to as hydroperoxide decomposers. Since the secondary antioxidants react with the peroxides and hydroperoxides to form stable, nonreactive and nonradical products, by doing so, they prevent the peroxides and hydroperoxides from splitting into reactive alkoxy and hydroxyl radicals (Ambrogi *et al*., 2017)..

Photo stabilisers are another type of additive that protects polymers against weathering, and they are divided into UV absorbers, quenchers and UV screeners. The UV absorbers impede the first step in photodegradation by absorbing the harmful UV radiation and converting it into harmless infrared radiation or heat. The energy can then be dissipated through the polymer without causing photooxidation. Examples of these are carbon black, rutile titanium oxide, benzophenones and

benzotriazoles. The quenchers react with an excited chromophoric group in a polymer to deactivate the excited state, by trapping the free radical that has been formed, before chain scission can occur. Thus, effectively preventing chain scission and limiting the photooxidation chain reaction process. Examples of these additives are metal complexes and hindered amine light stabilisers or HALS. UV screens prevent photooxidation from being initiated by reflecting the harmful light away from the surface of the polymer. To achieve this, the UV screens are incorporated as a coating or a pigment (see 2.1.1.2 b) – both with a high UV reflectance (Ambrogi *et al*., 2017).

Heat stabilisers' purpose is to either stop or prevent the thermal oxidation from occurring or from attacking the intermediate and decomposed products formed during oxidation to prevent propagation. Heat stabilisers can also be divided into three classes based on the bases of the stabilisers. They are metallic salts, that is generally based on zinc, cadmium, lead or barium, for example, barium-zinc and calcium-zinc. Next is the organometallic compounds, which is generally based on tin, for example, organotin. Lastly, there are non-metallic organic stabilisers which are generally based on phosphates, for example, bisphenol type epoxy resin and hydrolysed polyvinyl alcohol (Ambrogi *et al*., 2017).

Flame retardants are added to interfere with physics and/or the chemistry of the combustion process, causing the polymer to be less flammable. There are three classes of flame retardants, and they are divided by their technology, the three classes are halogen-based, phosphorus-based and metal-hydrates. The halogen-based flame retardants interfere with the chemical radical mechanism of the combustion process in the gas or vapour phase. Examples are brominated, fluorinated and chlorinates. The phosphorus-based flame retardants produce phosphoric acids during the combustion process. The phosphoric acids react with the polymer, which results in a char being produced that protects the polymer. An example is ammonium polyphosphate. The metal-hydrate flame retardants, for example, magnesium hydroxides and aluminium trihydroxides, release water upon being decomposed by heat and therefore impacts the combustion process (Ambrogi *et al*., 2017).

b) Other additives

Dyes, pigments and colourants are incorporated to impart colour or change the macroscopic appearance of the material. The main difference between a dye and a pigment is that dyes are soluble in water and/or other organic compounds while pigments are insoluble in both types. Since dyes are very soluble in plastics, they tend to migrate through the polymer, which can cause colour changes to appear. Other disadvantages include dyes having poor thermal and light stability. Dyes tend to be present as either single molecules or small clusters.

In contrast, pigments are discrete crystalline particles dispersed evenly throughout the polymer. Pigments can be organic or inorganic and tend to form clumps if not adequately dispersed. They are not as easy to migrate through the polymer as dyes and tend to not be as brilliant in colour. Examples of dyes are anthraquinone and azo. Examples of inorganic pigments are iron oxide, carbon black, molybdates lead chromate titanium dioxide, and examples of organic pigments are mono azo, quinacridone and

benzimidazolone. Examples of special effect pigments are fluorescent, pearlescent and metallic pigments (Ambrogi *et al*., 2017; Cramford & Quinn, 2016).

Plasticisers are generally added to alter material stability (Izdebska & Thomas, 2016). They make the plastic more flexible, durable and tough (Wellfair, 2008). They are normally divided into two classes, based on their chemical structures, named phthalates and non-phthalates. Since the plasticisers are not chemically bound to the molecule, they can leach out over time and poses a risk. Examples of phthalates are dioctyl-, di-isononyl- and di-n-butyl-phthalate. Examples of non-phthalates are adipates, benzoates, polyesters, phosphates and trimellitates (Ambrogi *et al*., 2017).

Impact modifiers are added to toughen the polymers and decrease the brittleness of plastics. The impact modifier should absorb impact energy and induce plastic deformation before cracking, and propagation can occur. There are different classes, and the first is the butadiene-based graft copolymers. They are extremely susceptible to thermal and oxidative degradation but have extremely low glass transition temperatures. The next is the ABS modifiers, they provide soft and rubbery plastics and have the polarity needed for interfacial compatibility with polymers. They also have hardness and chemical resistance, but they are vulnerable to UV degradation. Examples are Baymod A 52, BLENDEX 101 and ELIX TM 150 IG. The next impact modifier class are the MBS modifiers that also enhances toughness and clarity and have a significant effect at low temperatures. However, these are also vulnerable to UV degradation, and examples are CLEARSTRENGHT E950, PARALOID BTA-702S and Kane ace B382. The last class is the acrylic-based, along with enhancing toughness, which also provides high impact strength, good heat and thermal stability and moderate weathering resistance, unlike the MBS and ABS. Examples are ADD-AIM-100, DURASTRENGHT and Paraloid EXL-2314 (Ambrogi *et al*., 2017).

Fillers are incorporated into plastics to reduce production costs. However, they can also be used to accelerate the chemical degradation of a polymer (Wellfair, 2008). At the same time, compatibilists are incorporated to promote the formation of homogenous blends between two thermodynamically immiscible polymer structures (Ambrogi *et al*., 2017).

Additives can leach out due to it not being covalently bonded to the polymer structure posing as a risk (Gewert *et al*., 2015), and that is why bio-based additives are being increasingly studied. A bio-based additive can be any type, stabilisers, plasticisers and pigments. The purpose of the bio-based additive is the same as the purpose of the classified type. However, it has the added purpose of making the polymer either more recyclable (by preventing leaching of dangerous chemicals during the recycling) or biodegradable. Examples are epoxidised soybean oil (used as a light stabiliser/UV absorber), polyhydric alcohol (a flame retardant) and fatty acid ester (a plasticiser) (Ambrogi *et al*., 2017).

2.1.1.3 Molecular orientation

The molecular orientation in the polymer is influenced by the side chains (or branching) and the complex backbone structure of the polymer. The branching or side-chains exists as a result of side reactions occurring during synthesis. Other chains of molecules may be connected to the main linear chain or

backbone and protrude to the side. This will lead to what is known as a branched polymer (Callister & Rethwisch, 2015). Many different types of branching exist, and they refer to the way the branch deviates from the linear structure. Examples of different types of branching are the star polymer, the comb polymer and the brush polymer (Crawford & Quinn, 2016).

Crosslinking between the chains may also occur either during synthesis or by a non-reversible chemical reaction. In a crosslinked polymer the adjacent chains are joined via covalent bonds at various locations on the chains. Another molecular structure possibility is active covalent bonds forming between three or more multifunctional monomers, resulting in a three-dimensional network, classified as a network polymer. A highly crosslinked polymer may also be classified as a network polymer. Usually, polymers do not have a singular distinctive structure. They can exhibit a mixture of the structures as mentioned above; for example, a primarily linear polymer may have partially crosslinking and limited branching (Callister & Rethwisch, 2015).

The polymer backbone is formed during polymerisation and can be very complex based on the monomers and their arrangement and/or bonding during synthesis. Polymers in which the repeating units are identical monomers, referred to as homopolymers, are generally less complex than copolymers, which exists of different monomers repeating throughout the chain. In copolymers, the monomers can be arranged randomly, alternating, in blocks or grafted that the backbone is one monomer and the chains the other. Again, various forms of these exist, such as the palm tree, the star block and the pom-pom (Crawford & Quinn, 2016; Callister & Rethwisch, 2015). The homopolymers can also exhibit various molecular configurations even in the same plastic sample since the monomers can be connected either head-to-tail or head-to-head.

This causes the polymer to have some sort of stereoisomerism, referring to the spatial arrangement of the monomers that are linked in the same order. The stereoisomerism refers to both the configuration and conformation of the polymer chain. The configuration, or tacticity, refers to the arrangement of the molecules along the backbone of the chain and that cannot be altered or rotated without serving and reforming the bonds. The three configurations are isostatic, syndiotactic and atactic. An isostatic configuration denotes a chain where all of the R groups (R represents a side branch/group or an atom other than hydrogen) are situated on the same side of the chain, while in a syndiotactic configuration the R groups are on alternate sides of the chain. An atactic configuration also exists where the R groups are positioned randomly around the chain (Callister & Rethwisch, 2015). At the same time, the confirmation refers to the outline, shape or angular relationship of the chain molecules and is produced by rotation or twisting around the sigma bonds (Robert & Caserio, 2019; Hunt, 2006). Conformational isomers are categorised by their angular relationship, also known as their torsion angle. A graph to define the four ranges of torsion angles for the four categories, synperiplanar or cis-, antiperiplanar or trans-, ±synclinical or gauche and ±anticlinical or eclipse is given in Figure 1 (Moss, 1996).

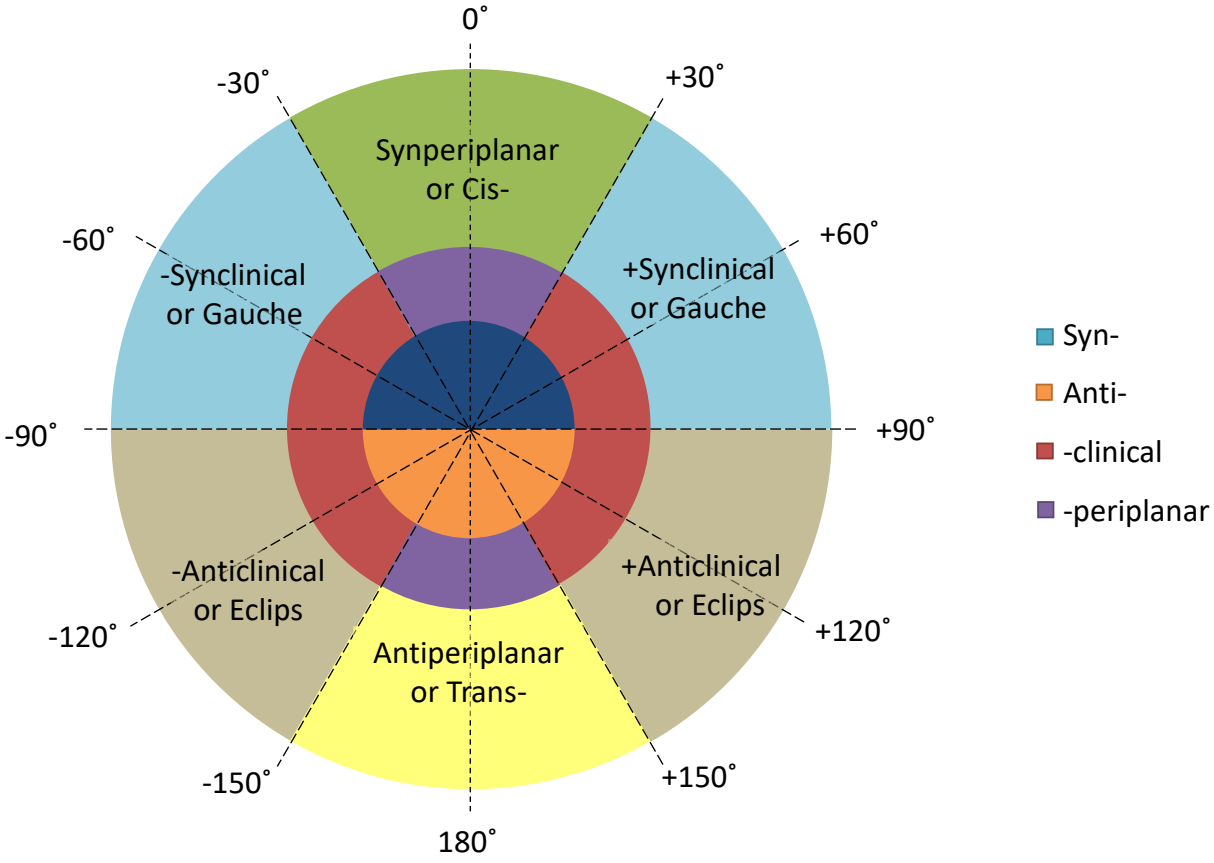

Figure 1: A Newman Projection formula to showcase the torsion angle range and categories. Redrawn from Moss, G., 1996. Basic Terminology Of Stereochemistry. *International union of pure and applied Chemistry,* 68(12), pp. 2193-2222

For tracking PET degradation, Gok (2016) stated that the trans- and gauche conformers of the ethylene glycol unit of PET is essential. Therefore, to have a better three dimensional visual understanding of Figure 1 and by default, a concept of the trans- and cis- form of the ethylene glycol unit of PET, Figure 2 a schematic representation of the gauche and trans conformers of the ethylene glycol unit in PET, is given.

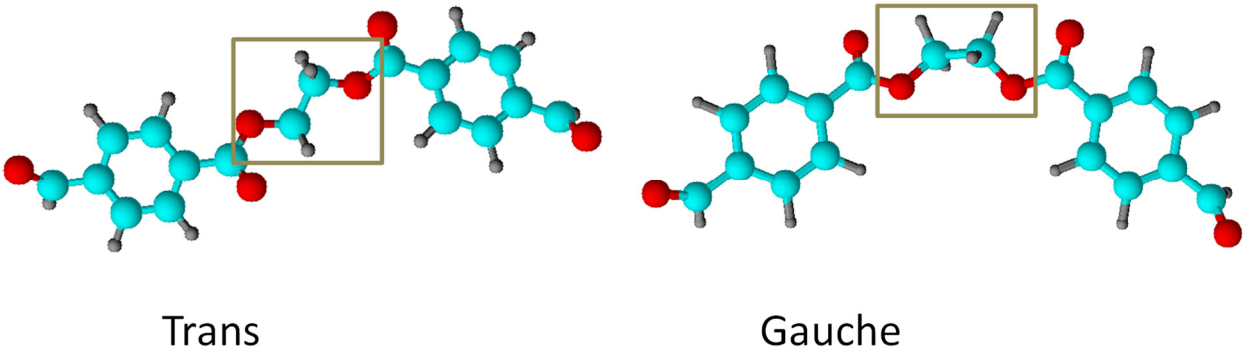

Figure 2: Schematic representation of the gauche and trans conformers of the ethylene glycol unit in PET, redrawn from Gok, A., 2016. *Degradation pathway model of poly(ethylene terephthalate) under accelerated weathering conditions*

All the above-mentioned affects the polymers' properties and characteristics and indicates just how complex polymer compounds are. The exact pathway of the reaction of the whole polymer can therefore not always be predicted as a polymer does not only exhibit a singular configuration and /or conformation but a variety of each, each of which could react differently.

2.1.1.4 Crystallinity

The main chains produced during polymerisation will either form highly organised crystalline structures or end in a disordered and tangled mass. The abovementioned such as additives, impurities, molecular orientation, branching or anything that affects the spatial regularity, intermolecular forces or hinders close alignment of the polymer chains affects the ability of the polymer to form highly organised crystalline structures (Meyer & Keurentjes, 2005; University of Cambridge, 2004-2020). The term used to refer to this structural order and degree of alignment of polymer chains is crystallinity, and the more ordered the structure, the higher the degree of crystallinity.

Generally, polymers exist as a combination of these highly organised structures, referred to as crystalline parts, and the disordered tangled mass referred to as amorphous parts. When the majority of the polymer are crystalline, the polymer is referred to as semi-crystalline (Crawford & Quinn, 2016), when the polymer exhibit only weak or no crystalline structures it is referred to as amorphous (Michler & Goerg, 2008).

As stated, the crystallinity is affected by anything that hinders the close alignment of the polymer chains. For example, functional groups that are capable of polar interactions and increase intermolecular forces allow for closer packing, which will increase crystallinity. Similarly, block copolymers, which contains large segments of regular structure that is capable of participating in crystallisation, exhibit a higher tendency to crystallise than random copolymers (Meyer & Keurentjes, 2005) while branching prevents molecules from being closely packed and therefore lowering the crystallinity (Crawford & Quinn, 2016). The stereoregularity and the regularity of the copolymer configuration also affect the polymer chains' potential to pack together closely and orderly. The more regular the copolymer, and the more stereoregularity in the chain, the easier the chains will pack together closely and orderly (University of Cambridge, 2004-2020). For example, as explained by Gok (2016), the crystalline region of PET prefers the transform of the ethylene glycol unit in PET. During degradation, the crosslinking and chain scissions can lower the degree of crystallinity (Huang, 1989), as this will cause more branching and less regular copolymer configuration and stereoregularity. However, sometimes chain-scissions results in the scission of the side branches, which could result in an initial increase in the degree of crystallinity. Thus, a variance in the degree of crystallinity is expected to be an indication of degradation.

Crystallinity can also be affected by temperature. Polymers have a glass transition temperature at which the chains in the amorphous regions are sufficiently mobile to allow repositioning/reordering. Between this temperature and the melting point of the polymer, the chains in the amorphous regions fold and

align themselves to become more crystalline (Crawford & Quinn 2016; Chen, 2012; Crawford & Thorne, 2002).

2.1.2 Specific plastics/polymers

Plastic is a material that is used in a wide variety of fields with specific requirements. Therefore numerous specialised plastics are produced, resulting in the existence of a wide range of plastics. From this range, common polluters are polypropylene (PP), polyethene terephthalate (PET) (which is also a type of polyester (PES)) and polyethene (PE) (Martinko, 2017; Crawford & Quinn 2016; Moore *et al*., 2001. Usually, these are petrochemical-based thermoplastics and not very readily biodegradable, although there are bio-based versions available. Therefore this research will focus on polypropylene and PET as they are two of the most common consumer used plastics as well as most commonly found plastic waste in the marine environment (Chamas *et al*., 2020; Fotopoulou & Karapanagioti, 2017; Martinko, 2017; Crawford & Quinn, 2016; Gewert *et al*., 2015; Kamrannejad *et al*., 2014; Moore *et al*., 2001).

2.1.2.1 Polypropylene

Polypropylene (PP) is a thermoplastic with a carbon-carbon backbone and the chemical formula $(C_3H_6)_n$ (Crawford & Quinn, 2016; Gewert *et al*., 2015). It is a type of chain-growth polymer that is classified as a polyolefin, based on the fact that it is produced during the polymerisation of propene, at around 50 – 80˚C and 5 – 20 atm (Fotopoulou & Karapanagioti, 2017; Crawford & Quinn, 2016; Rubin, 1990). See Figure 3 for molecule representatives. The production process typically includes the cracking of naphtha, a crude oil, making polypropylene a petrochemical-based plastic. However, bio-based polypropylene from sugarcane, beet and corn are also available on the market (Gotro, 2013).

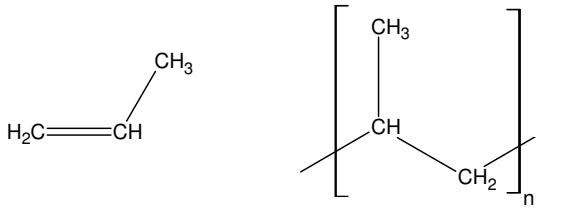

a) Propene b) Polyproylene monomer

Figure 3: Propene and polypropylene monomer molecule representatives

Polypropylene is a semi-crystalline plastic, that can be produced in all three possible geometric forms, with isotactic and syndiotactic being responsible for the crystalline areas and atactic for the amorphous areas (Hindle, 2019; Subramanian, 2017; Crawford & Quinn, 2016; Rubin, 1990). Commercially available polypropylene generally has a mixture of 75% isotactic to 25% atactic molecular structure configuration (Crawford & Quinn, 2016). When polypropylene is in the isotactic form, all methyl groups are on the same side of the polymer chain. For the syndiotactic form, the methyl groups alternate around the polymer chain, and for atactic, the methyl groups are positioned randomly around the polymer chain, see Figure 4 for visual representation (Rubin, 1990).

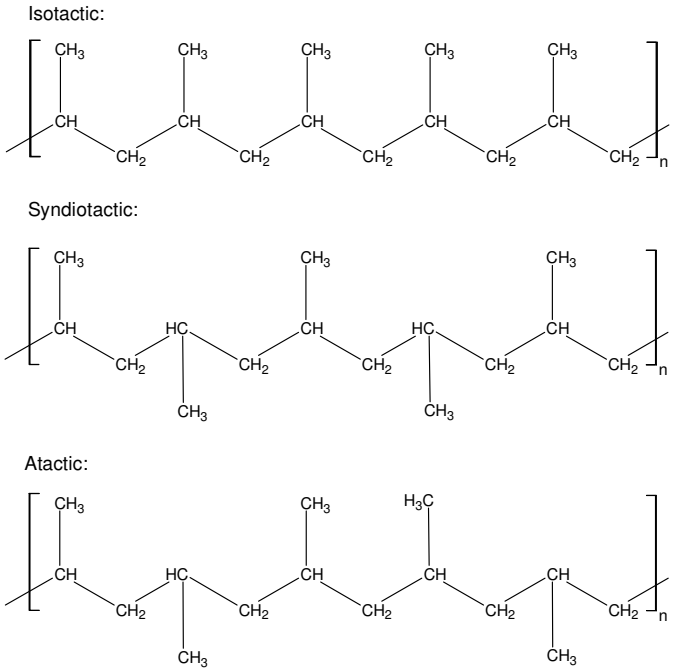

Figure 4: Propylene geometric forms, redrawn from Rubin, I. I. (Ed.). (1990). *Handbook of Plastic Materials and Technology*. John Wiley & Sons, Inc.

Polypropylene is a very versatile material, with good heat and chemical resistance, good transparency, good balance between impact strength and rigidity as well as high stiffness, a relatively low density of 0.903 – 0.905 g/cm^3 and thermal conductivity of around 0.12 W/m·K (Hindle, 2019; Crawford & Quinn, 2016; Callister & Rethwisch, 2015; Rubin, 1990). The melting point of polypropylene is at 160˚C and higher, and the glass transition temperature is between -20˚C and -3˚C. Both are dependent on the degree of crystallinity (Callister & Rethwisch, 2015; Androsch & Wunderlich, 2001; Rubin, 1990). However, polypropylene has low UV resistance and at cold temperatures it exhibits poor resistance to bending, breaking and crushing as well as brittleness around 0˚C (Hindle, 2019; Crawford & Quinn, 2016; Rubin, 1990).

All plastics contain some impurities and/or additives, and it is these impurities in polypropylene that permits the formation of a radical that will react with oxygen initiating degradation (Gewert *et al*., 2015). From there the tertiary carbons, to which the methyl groups are attached, are vulnerable to degradation as they are a site for oxidation and will form another radical to react with oxygen (Crawford & Quinn, 2016). Several, of both, reactions will lead to random chain scissions, crosslinking and will produce carboxylic acid and aldehydes and especially forming functional groups such as carbonyl and hydroperoxides (Crawford & Quinn, 2016; Gewert *et al*., 2015). The presence of carbonyl groups is, therefore, an indication that oxidation has taken place and renders the material susceptible to further degradation. Since the hydroperoxides that were formed along with the carbonyl groups are thermally and photolytically unstable and will produce two radicals upon decomposition. Both of these radicals will participate in the chain reaction process of degradation that is transpiring (Fotopoulou & Karapanagioti, 2017).

According to various studies on degradation in literature, these reactions will lead to lower molecular weight. It will also result in the formation of fine cracks on the surface that will deepen and grow more severe over time. It will cause reductions and decreases in tensile strength, elongation break and intrinsic viscosity. The carbonyl group formation will continue to increase. The crystallinity will decrease except for samples with nanocomposites, in which case the crystallinity is expected to increase (Fotopoulou & Karapanagioti, 2017; Crawford & Quinn, 2016; Gewert *et al*., 2015).

2.1.2.2 Polyethylene terephthalate

Polyethene terephthalate (PET) is a thermoplastic with a heteroatom[2] in the backbone and the chemical formula $(C_{10}H_8O_4)_n$. It is a type of polyester, based on the fact that it contains an ester functional group in the main chain. The production of PET begins with one of two processes, either via esterification of terephthalic acid and ethylene glycol with water as a by-product (see Figure 5) or via trans-esterification of ethylene glycol and dimethyl terephthalate with methanol as a by-product (see Figure 6). After the initial reaction is completed a second and sometimes third (depending on the molecular weight required) polymerisation step is performed to yield the final products also seen in Figure 5 and Figure 6 (Fotopoulou & Karapanagioti, 2017; Webb, Arnott, Crawford & Ivanova, 2013). The first reaction takes place at 250 – 280°C and 2 – 3 kPa, and the second polymerisation step occurs at 270 – 280°C and 50 – 100 kPa. After the second step, PET with lower molecular weight chains has been formed. If higher molecular weights are required, the PET is subjected to the third step at 200 – 240°C and 100 kPa (Webb *et al*., 2013).

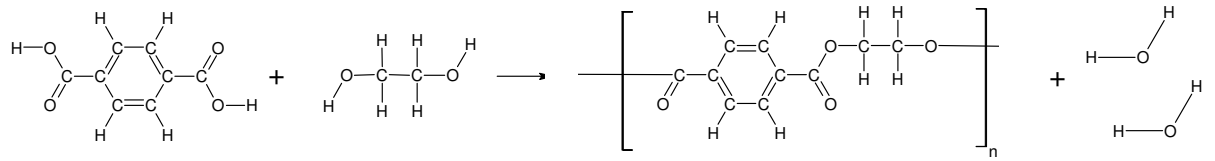

Figure 5: Molecule representatives for the esterification reaction for PET

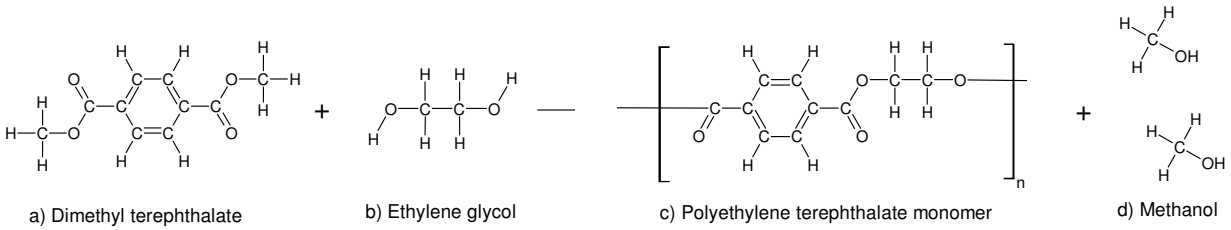

Figure 6: Molecule representatives for the trans-esterification reaction for PET

PET is a semi-crystalline polymer since a fraction of the polymer is un-crystallised (Subramanian, 2017; Crawford & Quinn 2016; Sichina, 2000). Depending on the degree of crystallisation, the PET will be referred to as CPET, crystalline PET, or APET, amorphous PET (Clearpak, 2017). The crystallinity affects various properties of the PET such as the density, thermal stability and hardness. However, the generally

[2] Heteroatoms refers to any atom that is not a carbon or hydrogen atom.

expected density of PET is around 1.4 g/cm$^{-3,}$ and 0.15 W/m·K for the thermal conductivity. The expected glass transition and melting point temperatures are in the ranges 67 – 81˚C and 254 – 265˚C, respectively. Furthermore, PET is generally known as a strong and durable polymer, that is chemically stable with good resistance to ageing, wear and tear, impact and shatter. PET is also lightweight, proves to be a good gas and moisture barrier and has transparency to visible light and microwaves (Crawford & Quinn 2016; Callister & Rethwisch, 2015; Webb *et al*., 2013).

Due to the compact structure of PET, and specifically, its aromatic group, it is highly resistant to environmental biodegradation and relatively resistant to photo-oxidative degradation (Fotopoulou & Karapanagioti, 2017; Gewert *et al*., 2015). This heteroatom backbone also causes the PET to be thermally more stable than a carbon-carbon backbone polymer. However, it renders the polymer vulnerable to hydrolytic degradation. Therefore, when submerged in water or under wet and/or humid conditions, oxonium or hydrogen ions can be produced by the carboxyl end groups which can cause a scission reaction that breaks the primary bonds of the chain and results in irreversible damage (Crawford & Quinn, 2016). During this hydrolysis process, carboxylic acid and alcohol functional groups are formed (Gewert *et al*., 2015). See Figure 12 in 2.2.1.3, for the hydrolyse degradation mechanism of PET and the resulting molecules. Even though PET is relatively resistant to degradation, it is still moderately susceptible to oxidative degradation. During the oxidative degradation, a hydroperoxide is formed at the methylene group which will mainly result in a chain scission, resulting in end groups that promote both thermo-oxidative and photo-oxidative degradation (Gewert *et al.*, 2015). See Figure 10 and Figure 11 in 2.2.1, for an overview of this mechanism as well as other possibilities and the resulting molecules. These degradation processes will cause discolouration and embrittlement of the PET polymer, as well as an increase in carboxylic end groups and a reduction in molecular weight (Chamas *et al*., 2020; Gewert *et al*., 2015).

2.1.2.3 Comparing polypropylene and PET

Polypropylene and PET are two very different polymers. They consist of different molecules, and they follow different degradation pathways resulting in different degradation results and have different densities, hardness and degrees of crystallinity etc. In chapter 4 Results and discussion, it is notable how they react differently and in some instances produce different values. This subsection is dedicated to highlighting some of these differences.

a) General variances

When examining the chemical molecular structure of the different plastics, it is noticeable that the polypropylene has methyl and methylene functional groups but no carbonyl functional groups. In contrast, PET has no methyl functional groups, but it does have carbonyl functional groups in the molecular structure.

Physical observable differences between the plastics used in the investigation were that the PET was more transparent than the clear polypropylene (CPP), which was translucent. This is attributed to the

degree of crystallinity, as a higher degree of crystallinity leads to a decrease in transparency (Crawford & Quinn, 2016). It was indeed observed during analysis at the start of experimentation that the degree of crystallinity for the polypropylenes was higher than the degree of crystallinity for the PET and that the PET has a higher hardness value than the polypropylenes.

b) Expected variance during degradation

During degradation, it is expected that both plastics will exhibit an increase in the hydroxyl (OH) index and decreases in hardness and crystallinity (see section 2.2) except for the PET subjected to the 100˚C treatment, as this is above the crystallisation temperature for the PET. Therefore, it will increase the crystallinity and hardness. With regards to FITR analysis, the carbonyl (C=O), hydroxyl (OH), alkene (C=C) and methanetriyl, methylene and methyl (CH_3, CH_2, and CH) indices are typically tracked as degradation indicators (Chamas *et al*., 2020; Fotopoulou & Karapanagioti, 2017; Smith, 2017; Rouillon, Bussiere, Desnoux, Collin, Vial, Therias & Gardette, 2016; Gewert *et al*., 2015; Kamrannejad *et al*., 2014; Wellfair, 2008; Kaczmarek, S´wic¸catek and Kamin´ ska, 2004). However, polypropylene already contains methyl (CH_3) groups. Similarly, PET already contains carbonyl (C=O) and alkene (C=C) groups. Therefore it can be predicted that the respective indices will vary greatly during the degradation process' propagation step as new groups form and former groups are disbanded.

Furthermore, during the degradation of the plastics, the polypropylene, regardless of the type of degradation, will ultimately result in chain scission. This results in the formation of a carbonyl and/or an alkene – along with some other products such as methyl and hydroxyl. Unless in alkaline conditions, where a hydroxyl group will be added to the chain, or when two radicals react to form a branched structure or crosslink (see section 2.2). Therefore, variances in the carbonyl and alkene indices are good indicators of degradation for polypropylene. With hydroxyl and methyl, methane and methylene indices being the secondary indicators.

However, PET already contains carbonyl groups and alkenes in the molecular structure, which can complicate the observation of degradation when considering these indices. During degradation, PET is most likely to be attacked at the carbonyl group or the ethylene glycol unit of PET (Gok, 2016; Scheirs & Gardette, 1997). This will form alkenes, resulting in changes to the ethylene glycol unit, and especially hydroxyl functional groups, with a high probability of causing end groups to be carboxylic acids. It is, therefore, better to use the hydroxyl index as a primary indicator of degradation for PET along with the carbonyl, methylene and alkene indices as secondary indicators. With reference to the orientation and morphology of the alkenes, as these could be an indication of where the alkenes are situated and whether the ethylene glycol unit of PET has undergone degradation.

2.1.3 Analysing polymers

Numerous polymer types exist with a variety of complex chemistry, molecular structures and pathways for degradation or reactions which results in structural and chemical changes leading to property enhancement, alteration or deterioration. Methods to identify the type, verify the standards and to

monitor any alterations is, therefore, a necessity. The approaches to analysing polymers include monitoring chemical changes, calculating the elimination of small molecules, measuring changes in material properties and evaluating physical changes (Chamas *et al*., 2020).

In this study, the monitoring of chemical changes, through FTIR analysis, and measuring changes in material properties, through hardness and degree of crystallinity, will be applied, and thus discussed in the following section.

2.1.3.1 Functional groups

The polymers formed during polymerisation will consist of various functional groups either from the monomer or produced during polymerisation. A functional group is a group of atoms that are clustered together in a particular way and is responsible for consistent and specific behaviours and/or reactions (Muscato, 2015; Silberg, 2013). They occur in polymers as part of the chain, the end-group, as micro-unsaturation functional groups or as part of additives and/or impurities in the polymer (Crompton, 1993). Some of these groups are very susceptible to attacks by microbial enzymes, light, water and heat. Thus, it initiates and propagates degradation in the polymer while other groups are the result of a degradation reaction that created new functional groups (Chamas *et al.,* 2020, Fotopoulou & Karapanagioti, 2017).

Therefore, it can be useful to track functional groups, as they could be molecular indications of degradation taking place. A wide range of physical and chemical techniques exists that can be employed to determine and track the formation and/or ratio of the functional groups. These methods are classified under two categories, either chemical or physical methods. The chemical methods include techniques such as halogenation, hydrogenation and colourimetric procedures, titration, saponification values procedures based on acetylation., The physical methods are based on infrared, Raman and nuclear magnetic resonance spectroscopy and saponification (Crompton, 1993). In this investigation, Fourier Infrared Spectroscopy (FTIR) was used and will thus be the method discussed further.

The functional groups that are useful to track depend on the plastic-type. Most literature studies track the carbonyl and hydroxyl functional groups (Chamas *et al*., 2020; Fotopoulou & Karapanagioti, 2017; Smith, 2017; Rouillon *et al*., 2016; Gewert *et al*., 2015; Kamrannejad *et al*., 2014; Wellfair, 2008; Signor Chin & Vanlandingham, 2003). Other functional groups that literature indicated useful to track was the methanetriyl, methylene and methyl groups (Rouillon *et al*., 2016; Kaczmarek *et al.,* 2004). In this investigation, the alkene groups were also tracked due to the expected formation of this group during the degradation mechanism of polypropylene. It was also found that it is useful to track the vibrations and conformations of specific functional groups when considering PET degradation, as discussed by Gok (2016) since PET already contains some of the functional groups expected in degradation products in the original chain.

The carbonyl group refers to the functional group composed of a carbon atom double-bonded to an oxygen atom (see Figure 7). Due to the massive electronegativity difference between carbon and oxygen the bonds are highly polar, with the carbon having a large partial positive charge and the oxygen of the

carbonyl having a large partial negative charge. The carbonyl group is easy to detection by infrared (IR) spectroscopy, due to the intense stretching vibration peak caused by this charge and the fact that the carbonyl group appears in a unique wavenumber range (Smith, 2017). The carbonyl group is relatively easy to track and more useful in tracking polypropylene degradation than that of PET. PET is more complex as the polymer chain already contains a carbonyl group and for some pathways, the carbonyl group will be decomposed while for others an addition carbonyl group will form (see Figure 10 and Figure 11 in 2.2.1 and Figure 12 in 2.2.1.3).

The hydroxyl, also known as alcohol, group refers to the oxygen and hydrogen bond (see Figure 7). It is expected to form during any oxidative degradation and hydrolysis. For this reason, it is an excellent functional group to track (see Figure 9, Figure 10, Figure 11 and Figure 12 in 2.2.1 and 2.2.1.3).

Methanetriyl (CH), methylene (CH_2) and methyl (CH_3) functional groups refers to a carbon bonded to a hydrogen atom or atoms, see Figure 7. Variances in these groups can indicate that chain scissions and other degradative mechanisms are occurring (see Figure 9, Figure 10, Figure 11 and Figure 12 in 2.2.1 Degradation mechanisms and 2.2.1.3 Hydrolysis).

Alkene functional group refers to a carbon-carbon double-bonded atom (see Figure 7). These are indicators of chain scissions (as part of oxidative degradation or on its own), fragmentation and disproportion in polypropylene and therefore useful to track. Again, PET is more complex as the PET molecule already contains a benzene ring consisting of double bonds. Although this is also a possible product of chain scission in PET, it is not worthwhile to track because there are other functional groups which are more likely to form that are easier to track.

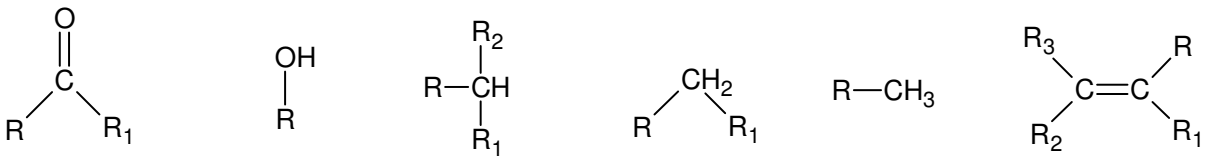

Figure 7: Representatives of functional groups, with R denoting any group or chain of atoms connected to the functional group

FTIR is a fast, non-destructive and mechanically simple technique with high sensitivity, making it reliable and cost-effective. For these reasons, it is one of the frequently employed techniques in polymer degradation studies (Beltrán-Sanahuja, Casado-Coy, Simó-Cabrera & Sanz-Lázaro, 2020; Chamas *et al.*, 2020; Jung, Horgen, Orski, Rodriguez, Beers, Balazs, Jones, Work, Brignac, Royer, Hyrenbach, Jensen & Lynch, 2018; Olesen, Van Alst, Simon, Vianello, Liu, & Vollertsen, 2018; Wellfair, 2008; Celina, Ottesen, Gillen & Clough, 1997; Scheirs & Gardette, 1997). One of the other main reasons FTIR analysis is employed in polymer degradation studies is because not only can it be used to identify the molecules and/or functional groups, the orientation and conformations of the polymer chains are also identifiable on the spectrum (Gok, 2016; Wellfair, 2008).

During infrared spectroscopy, a beam of infrared light is passed through a sample of material. Some of the radiation will be absorbed and converted to rotational and/or vibrational energy by molecules in the sample material. The rest of the radiation will pass through, i.e. transmitted. The radiation that passes through is detected by the detector of the sensitive FTIR spectrometer. The detector will convert the signal received to present a spectrum of %transmittance or absorbance against wavelength. This resulting spectrum acts as a fingerprint for the sample as each molecule, chemical structure or functional group will produce an absorption peak that corresponds to the unique frequencies of vibrations between the bonds that makes up that molecule, chemical structure or functional group.

FTIR analysis is therefore qualitative, as the absorbance or %transmittance spectrum allows for identification of new or disappearing functional groups. However, it can also be quantitative as the size of the peak is an indication of the amount of that molecule, chemical structure or functional group present (RTI Laboratories, 2015; Bradley, 2013; Celina *et al*., 1997). To be able to use the FTIR analysis quantitively the peaks under investigation must be normalised to a peak that does not exhibit significant changes during degradation. This quantitative value is called the index of the functional group, for example, the carbonyl index. There are various ways to normalize this index as discussed by Dony, Ziyani, Drouadaine, Pouget, Faucon-Dumont, Simard, Mouillet, Poirier, Gabet, Boulange, Nicolai, & Gueit (2016). However, the two most common methods employed by literature is the area calculation and the peak calculation.

The area method consists of calculating the area under the absorbance curve for the peak being investigated and then dividing by the calculated area under the absorbance curve for the reference peak (Beltrán-Sanahuja *et al*., 2020; Rogeaux, Carter, Perraton and Daoudi, 2019; Hofko, Porot, Falchetto-Cannone, Poulikakos, Huber, Lu, Mollenhauer, Grothe, 2018). The peak method firstly identifies the maximum absorbance value for the peak in that wavelength region, for both the reference peak and the peak of the functional group investigated, and then divides the peak value for the investigated peak by the peak value for the reference peak (Yan, Xiao, Huang, Lv, 2018; Ángeles-López, Gutiérrez-Mayen, Velasco-Pérez, Beltrán-Villavicencio, Vázquez-Morillas & Cano-Blanco, 2017; Mylläri, Ruoko & Syrjälä, 2015; Rouba, Sadoun, Boutagrabet, Kerrouche, Zadi & Mimi, 2015; Xu, Yin, He, Zhao & Wang, 2012; Mellor, Moir & Scott, 1973).

2.1.3.2 Hardness

Hardness is defined as the resistance of a material against localised plastic deformation by abrasion or by surface indentation (Callister & Rethwisch, 2015; Briscoe & Sinha, 1999). Hardness can be classified as a mechanical property (Kaufmann, 2003; Green & Perry, 2007). It is related to other strength and elastic characteristics such as tensile strength and yield strength (Brantley, Berzins, Iijima, Tufekçi & Cai, 2017; Callister & Rethwisch, 2015; Ainbinder & Laka, 1966).

Hardness is normally calculated as a ratio between the applied load or force and the projected area or depth of the plastic deformation produced by the indenter (Herrmann, 2011). Therefore, the smaller the

indentation area or the indentation depth, the higher the hardness number and thus the harder the material. However, the hardness number is relative to the test method, force and dwell time used. Therefore, care must be taken when comparing values ensuring the values are comparable and/or convert the values from one hardness scale to the other (Callister & Rethwisch, 2015).

The four most common tests used to determine the hardness are the Brinell, Vickers, Rockwell and Knoop test. Alternatively, named after their indenter geometry, they are known as the cone and sphere (Rockwell), sphere (Brinell) and pyramid (Vickers) tests (Briscoe & Sinha, 1999). The test can be classified by either the indentation load (or applied force) or the measurement method used (Kaufmann, 2003).

For the measurement method, there are two classes, the visual observation method and the indentation depth measurement. For the visual observation method, the indentation diameter must be measured; Vickers, Knoop and Brinell tests falls in this category. The indentation depth measurement method is employed in the Rockwell and some nanoindentation testers (Kaufmann, 2003).

Based on the indentation load method, there are also two classes, a “macro” test and a “micro” test. A macro test refers to a test with an applied load of more than 1 kg, and a micro-test refers to a test with an applied load of 1 kg or less. Some micro-tests can go to loads such as 0.01 g and will then be referred to as nanoindentation or ultralight tests (Kaufmann, 2003). A micro-test usually also leads to an indentation where the is depth is less than 70 – 100 µm (Sundararajan & Roy, 2001). Knoop falls in the micro test category while Brinell and Rockwell fall in the macro test category. Vickers can fall in either category depending on the size of indenter and applied load (Kaufmann, 2003).

For this project, the Vickers microhardness test method was selected since the pyramidal diamond indenter produces a square indentation that leads to an easy, accurate and optimal measurement of the microhardness. The diamond pyramid geometry of the indenter also provides a contact pressure which is more unaffected by the elastic release than the rounded geometry of other indenters. The Vickers test also leaves an indentation that is deeper than the Knoop’s test indentation, which will lead to a lesser sensitivity to surface defects (Lopez, 1993).

Hardness is expected to change as the polymer degrades, due to the change in molecular structure. It is expected that the hardness will ultimately decrease over time with degradation, along with the degree of crystallinity (O’Brine & Thompson, 2010; Rosario & Dell, 2010; Lopez, 1993). However, literature has reported various diverging tendencies of the hardness change. For example Izdebska and Thomas (2016) stated that hardness will increase with crosslinking and only start decreasing when crosslinking becomes excessive. Similarly, Rouillon *et al.* (2016) reported that the hardness increased markable before dramatically dropping with an ageing time of 400 hours. In contrast, Signor *et al.* (2003) reported only an increase in hardness over 4 000 hours while O’Brine & Thompson (2010) reported an overall decreasing trend, with a zigzagging pattern in the data.

The Vickers microhardness test is a micro indentation-testing method that determines the hardness of a material by computing the ratio between the indentation load and the size of the impression produced

(Deepa, Jayakrishna & Rajiyalakshmi, 2018; Callister & Rethwisch, 2015). The method is referred to as a microhardness test due to the size of the indenter and the size of the indentation left; usually, the applied load is less than 1kg force (Kaufmann, 2003).

The Vickers test indenter has the geometry of a symmetrical, pointed, pyramid-shaped diamond and the pyramid's opposite faces have an included angle of 136˚(Sundararajan & Roy, 2001). A schematic sketch of the indenter can be seen in Figure 8. The applied load is usually somewhere in between 1 – 1000 g for a dwell time of up to 20 seconds, although 15 seconds is commonly used (Deepa *et al*., 2018; Callister & Rethwisch, 2015; Smallman & Ngan, 2014).

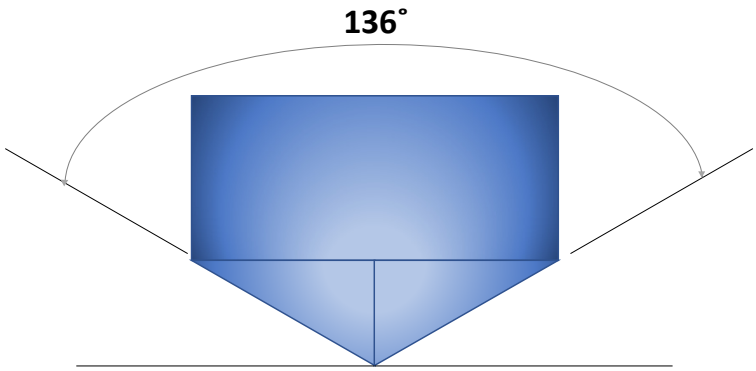

Figure 8: Schematic sketch of a side view of the Vickers hardness test indenter, redrawn from Callister, W. D. & Rethwisch, D. G., 2015. *Materials Science and Engineering.* 9th ed. s.l.: John Wiley & Sons

2.1.3.3 Degree of crystallinity

The degree or percentage of crystallinity represents the relationship between the amount of the crystalline component and the amorphous component in the polymer (Sichina, 2000). The higher the percentage crystallinity, the more crystalline (structurally ordered) the polymer. Therefore, the percentage of crystallinity has a direct effect on the polymer's mechanical, optical, chemical and thermal properties (Crawford & Quinn, 2016; Sichina, 2000; Blaine, n.d.). This is because, in the amorphous areas, the disorder and entanglement of the polymer chains hinder the movement of the polymer, causing the polymer to be brittle and rigid. The more crystalline areas have increased hardness and density over amorphous areas as the ordered structures are stronger and more closely packed. Therefore, the higher the crystallinity, the more flexible, harder and denser and less transparent the polymer (Crawford & Quinn, 2016).

A molecular chain alteration produces a variance in the degree of crystallinity. Consequently, the degree of crystallinity can be tracked as an indication of polymer degradation. However, the degree of crystallinity can also be an indication of other reactions, such as crystallization occurring. Because when an amorphous area is heated, it induces molecular motion allowing the chains to move and re-order, resulting in an increase in crystalline regions or an increase in the degree of crystallinity (Crawford & Quinn, 2016).

The percentage of crystallinity can be calculated with Equation 12. Where ΔH_m^o is the reference heat/enthalpy of melting, that is the value of the heat of melting should the polymer be 100% crystalline. The commonly established reference heat of melting values for polypropylene and PET is 207.1 J/g and 140.1 J/g respectively (Sichina 2000; Blaine, 1990). The ΔH_m and ΔH_c represents the enthalpy/heat of melting or fusion and the enthalpy/heat of crystallization, respectively. These values can be determined with a differential scanning calorimetry analysis. However, sometimes, due to the polymer sample's thermal history, a cold crystallization peak may not be observed. In these cases the enthalpy/heat crystallization cannot be determined and the ΔH_C is taken as 0 J/g (Sichina, 2000).

$$\%Crystallinity = \frac{\Delta H_m - \Delta H_c}{\Delta H_m^o} \times 100\% \qquad [1]$$

Differential Scanning Calorimetry, or DSC, is a thermal analysis technique that measures the energy flow into or from the sample as a function of time or temperature under controlled conditions. The results can yield various information such as the heat of fusion, enthalpy of crystallization, glass transition temperature and the melting temperature. These results are meaningful as they can be linked to degradation in polymers.

The melting temperature of a polymer is dependent on the molecular weight of the polymer. Literature expresses that the melting point decreases with a decrease in molecular weight (Predecki & Karr, 1978). Since degradation is defined as a breakage of the polymer chains (Crawford & Quinn, 2016), it means that a decrease in average molecular weight, and thus a decrease in melting point temperature, indicates degradation of the polymer. Another approach to linking degradation and the DSC results is through the degree or percentage of crystallinity (Beltrán-Sanahuja *et al*., 2020).

To determine the heats of fusion and cold crystallization (in J/g), integration of the area of the cold crystallization and melting peaks of the calorimetric curves from the DSC analysis must be applied. This means that the DSC analysis must have a final temperature of at least 30˚C above the melting temperature of the polymer (Sichina, 2000). Usually, in literature, an analysis will start at room temperature and employ a heating rate of 10˚C/minute (Beltrán-Sanahuja *et al.,* 2020; Rouillon *et al.,* 2016; Sichina, 2000; Blaine, n.d.). The calorimetric curve, of heat flow (in W/g) against temperature (in ˚C), is examined. Computer software is used to integrate the area of the peaks to determine the heats of fusion and cold crystallization.

2.1.3.4 Other analyses

Tensile strength and mass loss are other properties frequently used to track polymer degradation. While it was decided to exchange the tensile tests for hardness tests, the mass loss investigation was continued. Hardness was used since Callister & Rethwisch (2015) states that the hardness can be (directly) related to tensile stress with a conversion factor depending on the material investigated. For the mass loss investigation, a milligram scale accurate to two decimal numbers was used. However, due to water reactions on surface, and both the absorbance of water and degradation occurring simultaneously, the

weight loss results were not conclusive and are not presented in the report. Chamas, et al. (2020), Zhao, Li, Chen, Shi & Zhu (2007) and others similarly reported results for mass loss to be inconclusive. An example of weight losses recorded for plastic degradation in water by Heimowska *et al.* (2014) are less than 0,6% after 48 weeks.

2.2 Degradation

Literature frequently uses degradation, deterioration, fragmentation and biodegradation to describe what happens to polymers over time. Therefore, each of these terms will be explained as to how it was perceived in this research. The degradation mechanisms considered in this research will be limited to the degradation mechanisms that occur in a natural environment under natural conditions and in the presence of oxygen.

Degradation refers to the breakdown of the polymer structure leading to a change in physical and chemical properties as a result of a significant change in its chemical structure (Fotopoulou & Karapanagioti, 2017; Wellfair, 2008; Andrady, 1990). However, biodegradation refers to the conversion of the polymer to non-toxic molecules such as carbon dioxide and water by microorganisms (Rosario & Dell, 2010). Deterioration refers to the change or loss of physical properties of a polymer regardless of the mechanism causing the change, and not necessarily impacting the chemical structure (Fotopoulou & Karapanagioti, 2017; Andrady, 1990). Fragmentation refers to the breaking of the material into smaller pieces (Wellfair, 2008).

While polymers are durable materials that are resistant to degradation, fundamentally, they are constructed from chemical bonds that can be broken. Polymers contain impurities of different kinds that can initiate or propagate degradation. When polymers are exposed to sun rays, oxygen or oxidants, varying temperatures, water, moisture or humidity, acid rain or other atmospheric pollution and environmental and physical stresses, radical formation is initiated. The formed radicals will react with other molecules on the polymer chain, in a complex chain reaction of radical processes, causing the initiation and propagation of degradation. Degradation can also occur through the bacteria, and moulds polymers are exposed to, these microorganisms can attack and feed on the plastics converting them into non-toxic molecules (Lee & Coote, 2016; Gewert *et al.,* 2015; Kaczmarek *et al*., 2004; Signor *et al.,* 2003). It is a fact that polymers will weather and degrade over time. It is also expected that microplastics will degrade faster than meso- and macroplastics. This is expected because they have a higher surface to volume ratio, and the plastic surface is more exposed to the abovementioned factors; and thus, more vulnerable to chemical or enzymatic attacks (Gewert *et al.,* 2015).

There are various degradation mechanisms, and they are classified based on the factors initiating the degradation. These mechanisms are chemical (such as atmospheric oxidation and hydrolytic degradation), physiochemical (such as photo-degradation, thermal degradation, and mechanical degradation) or biological processes (Fotopoulou & Karapanagioti, 2017; Reich & Stivala, 1971). However since various factors initiate and affect degradation in the environment, as well as enhance each other

and/or co-occur, the mechanism and products may be more diverse than those expected from a specific pathway (Gewert *et al.,* 2015).

In the environment under natural conditions with near-ambient temperatures, polymer degradation typically involves hydrolysis or oxidation (Chamas *et al.,* 2020; Fotopoulou & Karapanagioti, 2017; Gewert *et al*., 2015). Generally, these are initiated by light, heat or other abiotic factors and can be accelerated by microbial action, heat, light, or combinations thereof (Chamas *et al.,* 2020).

During degradation, the hydrogen and carbon and carbon-carbon bonds break, as well as radical intermediates and products recombine and cause crosslinking and formation of new chromophores, in the polymer structures (Chamas *et al.,* 2020; Kaczmarek *et al.,* 2004). Other chemical changes at a molecular level such as oxidation and bond cleavage lead to the creation of new molecules, that usually have much shorter chain lengths (Chamas *et al.,* 2020). It is therefore clear that the degree of crystallinity and functional group concentrations will change with degradation. Since the chemical and molecular structure is responsible for the properties of the polymer, the properties will also change. Some of the expected physical and visual effects of the degradation occurring are discolouration, cracking, flaking, embrittlement, disintegration as well as reductions in tensile strength and loss of surface area (Chamas *et al.,* 2020; Gewert *et al*., 2015; O'Brine & Thompson, 2010). However, various studies have shown that mechanical properties exhibit an improvement during the early stages of degradation before deteriorating. It has been stated that a possible reason for this could be that the crosslinking of the polymer chains enhances the properties and that the mechanical properties only start deteriorating when the crosslinking becomes excessive (Izdebska & Thomas, 2016; Rouillon *et al*., 2016).

2.2.1 Degradation mechanisms

The degradation mechanisms are classified under the factor that initiated the process. For the chemical degradation mechanisms, atmospheric oxidation is initiated by ozone, acid rain or other pollutants in the atmosphere while water molecules initiate hydrolysis (Fotopoulou & Karapanagioti, 2017; Crawford & Quinn, 2016; Signor *et al*., 2003). For biological degradation, it is living organisms, such as microorganisms that perform the degradation. For the physiochemical degradation such as mechanical degradation, shear forces, tension and/or compression initiate the degradation (Capone, Di Landro, Inzoli, Penco & Sartore, 2007). While photo- and thermal- oxidative degradation is generally very similar, being initiated by oxygen and light or oxygen and elevated temperatures, respectively (Andrady, 1990).

Under normal circumstances, mechanical factors are not major initiators of degradation in the marine environment, but they play an active role in the acceleration and contribution of the degradation. It acts in synergy with other environmental parameters, such as the water, temperature and UV rays (Capone *et al.*, 2007). Atmospheric oxidation usually is also not a prime initiator. While hydrolysis is a major initiator and degradation mechanism, for plastics vulnerable to hydrolysis since water molecules are in abundance in the marine or river environments and humid conditions are common in the natural environment. As for the photo- and thermal- degradation, under normal marine conditions photo-

oxidative and thermal-oxidative degradation are similar and two of the primary initiators and degradation mechanisms experienced by polymers (Chamas *et al.*, 2020; Fotopoulou & Karapanagioti, 2017). It is assumed that photolysis (or photodegradation) only occurs during the absence of oxygen, and thus only photo-oxidative degradation will be considered in this investigation (Gok, 2016). This review will only focus on the mechanisms primarily responsible for polymer degradation in the natural environment; except for biodegradation, as living organism did not fall within the project scope. Therefore, only discussions on hydrolysis and photo-oxidative and thermal-oxidative degradation will be continued (Gewert *et al*., 2015; O'Brine & Thompson, 2010).

The chemistry for polymer degradation is plastic specific. The general pathway for polymer degradation is initiation, propagation and termination. An initiator such as heat or light causes the formation of a radical during the initiation step. Propagation occurs when that radical reacts to form a peroxide- or hydroxyl-radical or hydroperoxide which will decompose to form free radicals. These newly formed radicals will attack the polymer chain and cause a complex chain reaction which will keep forming new radicals until termination occurs. Termination occurs when two radicals react to recombine, disproportionate, form a crosslinked or branched polymer, form two stable molecules or when a hydrogen donor enters the reaction (Lee & Coote, 2016; Sobków & Czaja, 2003; Crompton, 1993).

More specifically, for an oxidative reaction, the general pathway is that oxygen reacts with the hydrocarbons and forms unstable peroxides or hydroperoxides. This will induce complex chain reaction degradation through radicals (Chamas *et al.,* 2020; O'Brine & Thompson, 2010; Crompton, 1993). Since the thermo-oxidative and photo-oxidative mechanism are similar, it will only be presented once. Figure 9 represents the possible pathways for polypropylene degradation. For PET no generally accepted degradation pathway has been fully reported on, the pathways proposed here, in Figure 10, is a combination of various sources. Because PET is a complex molecule and the products and intermediates from the pathways can interact, resulting in secondary reactions and products, Figure 11 represents some small molecules that can be expected to form during PET degradation ultimately (Chamas *et al.,* 2020; Kaczmarek *et al.,* 2004; Buxbaum, 1968).

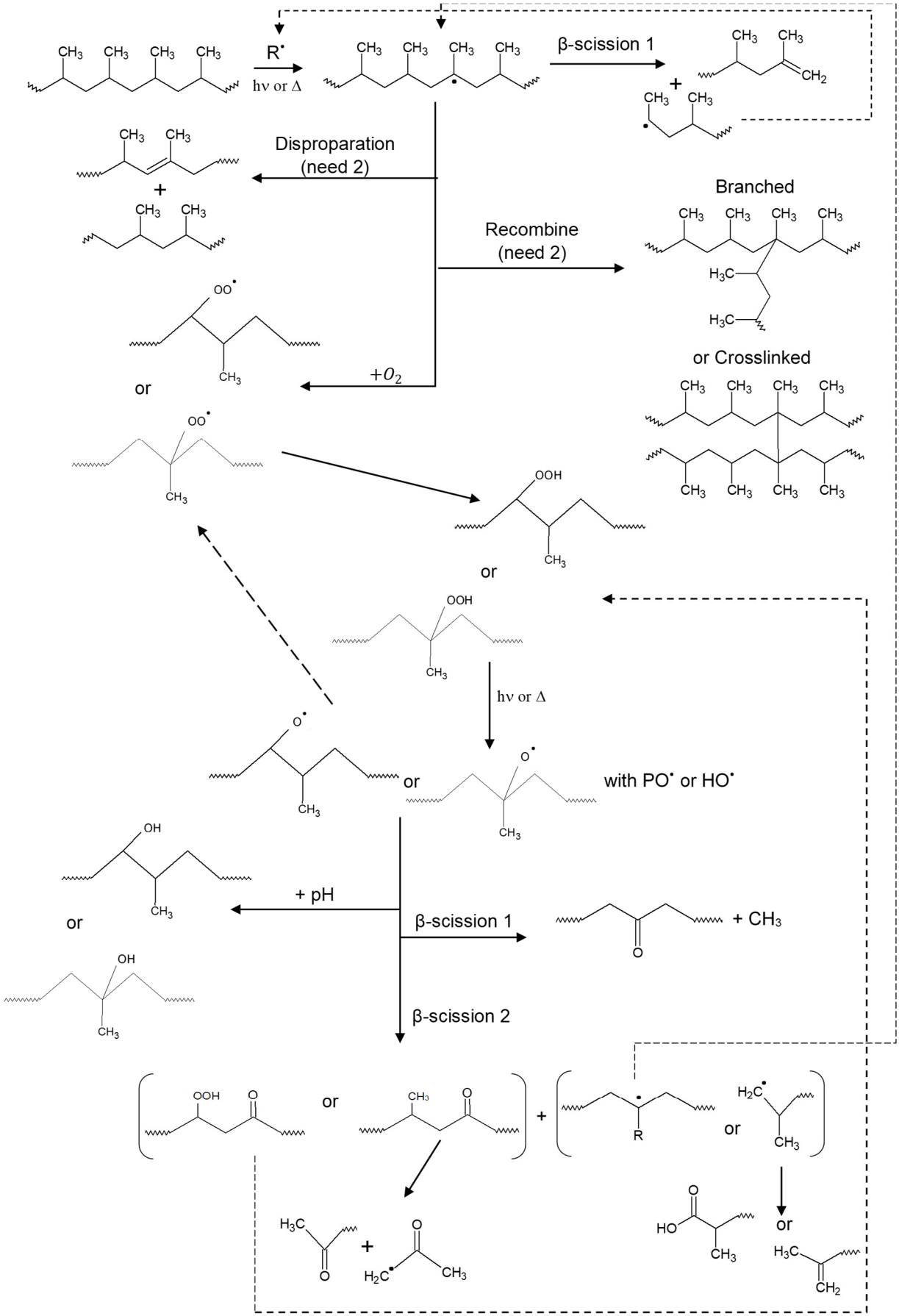

Figure 9: Proposed mechanisms for polypropylene degradation. Redrawn from Fotopoulou and Karapanagioti (2017); Izdebska and Thomas (2016); Rouillon *et al.* (2016); Gewert *et al.* (2015); Gijsman, 2008; Vaillant, Lacoste and Dauphin, (1994)

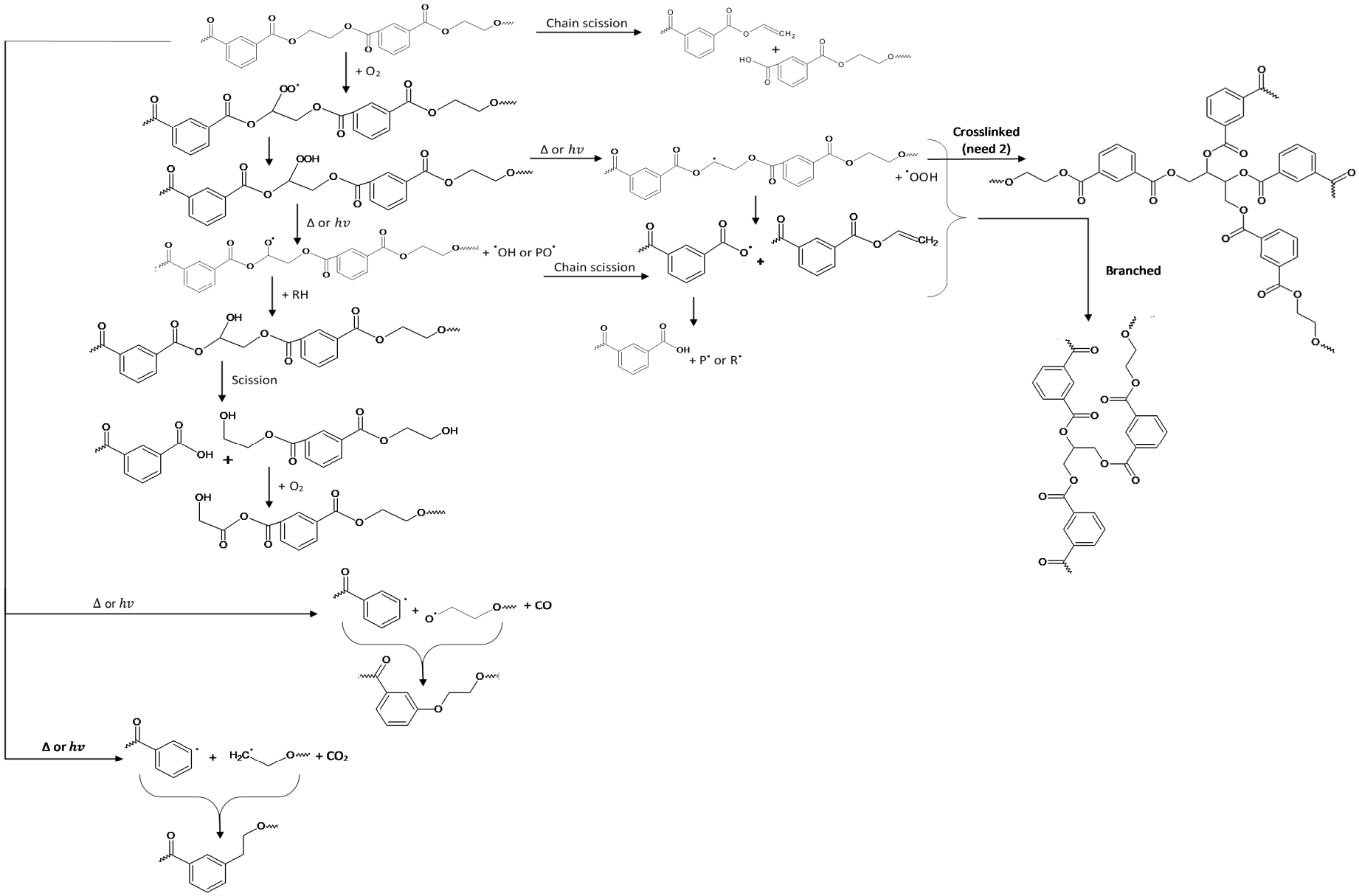

Figure 10: Proposed mechanisms for PET degradation. Redrawn from Chamas *et al.* (2020); Michiels, Van Puyvelde and Sels (2017); Izdebska & Thomas (2016); Venkatachalam, Nayak, Labde, Gharal, Rao and Kelkar (2012); Romão, Franco, Corilo, Eberlin, Spinace and De Paoli (2009), Holland & Hay (2002); Buxbaum (1968)

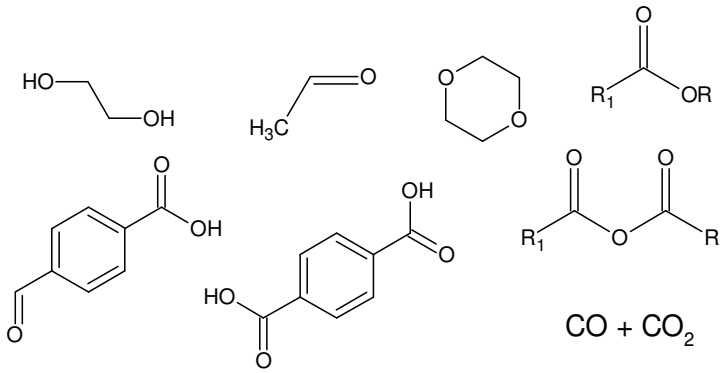

Figure 11: Small molecules representatives that can form during PET oxidative degradation redrawn from Chamas *et al.*, 2020. Degradation Rates of Plastics in the Environment. *ACS Sustainable Chemistry & Engineering,* 8(9), pp. 3494-3511

2.2.1.1 Thermo-oxidative degradation

Thermo-oxidative degradation refers to oxidative degradation being initiated by heat. Even though it mainly occurs at elevated temperatures, slow thermo-oxidative degradation is known to occur at moderate temperatures as well, as long as oxygen is abundant (Fotopoulou & Karapanagioti, 2017; Crompton, 1993; Andrady, 1990). Polymers may even undergo a "heat build-up". This will result in the polymer having a significantly higher temperature than its surroundings which will also induce thermo-oxidative degradation (Andrady, 1990; Summers, Rabinovitch & Qeensbury, 1983). It is generally expected to be more likely for thermo-oxidation to occur sequentially or simultaneously with photo-oxidation and hydrolysis under normal ambient conditions. Especially since it has been noted that photo-oxidative and thermal-oxidative degradation are similar under normal conditions and that their products have a catalytic or promoting effect on themselves and each other (Fotopoulou & Karapanagioti, 2017; Gewert *et al.,* 2015).

The pathway is plastic specific, but the general pathway is that oxygen reacts with the hydrocarbons and forms unstable peroxides or hydroperoxides that will induce the complex chain reaction degradation through radicals (Chamas *et al.*, 2020; Crompton, 1993). Figure 9 is a possible representative of the mechanism for polypropylene. Since photo-oxidative degradation follows a similar mechanism, it can be challenging to identify the degradation initiator from the products in an environmental situation (Fotopoulou & Karapanagioti, 2017; Gewert *et al*., 2015).

2.2.1.2 Photo-oxidative degradation

Photo-oxidative degradation refers to the oxidative degradation reaction initiated by light (Binuja 2018; Fotopoulou & Karapanagioti, 2017; Andrady, 1990). It is thought to be initiated when a molecule in the polymer accumulates enough energy, through the absorption of light, to be activated into an excited singlet or triplet state (Binuja, 2018). According to Wellfair (2008) and Ángeles-López *et al. (*2017), UV light in the wavelength range 290 nm to 315 nm is primarily responsible for the degradation. It is said to be one of the main mechanisms responsible for polymer degradation in ambient and natural conditions (Fotopoulou & Karapanagioti, 2017; Gewert *et al*., 2015; Signor *et al*., 2003). Photo-oxidative and thermal-oxidative degradation are stated to be very similar and enhance each other (Ambrogi *et al*., 2017;

Fotopoulou & Karapanagioti, 2017; Gewert *et al.,* 2015; Andrady, 1990). Due to photo-oxidation being dependant on the sun rays and the ability or efficiency of the radiation penetration of the rays, photo-oxidation is usually only dominant on the surface of the polymer and especially in the amorphous area of the polymer (Ambrogi *et al*., 2017; Izdebska & Thomas, 2016)

Photo-oxidation occurs by the absorption of light by molecules in the polymer, that are photocleaved into free radicals when they have accumulated enough energy to be activated into an excited state. They can also transfer that energy causing neighbouring molecules to become excited. When photocleaved, the formed radicals will initiate a complex chain reaction, as well as secondary reactions which will lead to the degradation of the polymer (Binuja, 2018; Ambrogi *et al*., 2017; Kaczmarek *et al*., 2004). This photo-oxidative degradation, although it is said to mostly result in chain scissions (Binuja, 2018; Rouillon *et al*., 2016; O'Brine & Thompson, 2010; Gewert *et al*., 2015), causes cross-linking, chain scission and oxidation to occur (Chamas *et al*., 2020; Izdebska & Thomas, 2016). This ultimately results in new chromophores forming, causing discolouration, polymer embrittlement and reduction of molecular weight and increase in surface area (Chamas *et al*., 2020; Fotopoulou & Karapanagioti, 2017; Heimowska *et al.,* 2014).

PET is an immensely complex molecule for photo-oxidative degradation since it contains both carbonyl groups and a benzene ring. This is because while the benzene ring acts as a photo stabiliser, due to the ability of the de-localized electron "cloud" to absorb the energy from the photons. In contrast, the carbonyl group acts as a photo-oxidative enhancer since the carbonyl group is a primary absorber of light causing excitation of its molecules, or transferring their excitation energy to nearby molecules. This results in initiation of photo-oxidation degradation and secondary photochemical processes (Izdebska & Thomas, 2016; Kaczmarek *et al*., 2004; Wellfair, 2008).

2.2.1.3 Hydrolysis

Hydrolysis refers to degradation due to water (Wellfair, 2008; Andrady, 1990). When a polymer absorbs water, it might have a plasticization effect, and this could also result in the matrix having increased accessibility to atmospheric oxygen, resulting in increased degradation rates. This increase could also be caused due to the stabilising additives being leached out (Andrady, 1990). However, the most crucial effect of water being absorbed into a polymer is the initiation of hydrolytic cleavage (or hydrolysis), predominantly when the polymer main chain consists of both carbon and heteroatoms (Gewert *et al*., 2015). PET is very susceptible to hydrolysis (hydrolytic cleavage) for this reason (Fotopoulou & Karapanagioti, 2017; Crawford & Quinn, 2016; Gok, 2016; Gewert *et al*., 2015).

Even though PET is susceptible to thermal-oxidative and photo-oxidative degradation, hydrolysis is one of the main mechanisms in PET degradation in the marine environment. Depending on the availability of light or temperature, hydrolysis will occur sequentially, simultaneously or separately with thermal-oxidative and photo-oxidative degradation (Fotopoulou & Karapanagioti, 2017; Gewert *et al*., 2015). The hydrolysis rate is said to be slow but increases substantially with temperature. It is also affected by the moisture content available, initial morphology, crystallinity as well as initial carboxylic end group content.

As crystalline regions act as a barrier for water diffusion, it is believed that hydrolysis occurs in the amorphous regions of the polymer by the water that diffused into this amorphous region (Fotopoulou & Karapanagioti, 2017; Gok, 2016).

The PET hydrolysis pathway is not fully understood, and at least four kinetics schemes have been proposed (Fotopoulou & Karapanagioti, 2017). The generally accepted pathway for hydrolysis is given below in Figure 12. From the pathway, there is a formation of new functional groups, especially hydroxyl end groups, and chain scissions. Along with these, it is stated that hydrolysis will result in changes to the CH_2 bands' vibrations and conformation (Fotopoulou & Karapanagioti, 2017; Gok, 2016). It is also stated that hydrolysis leads to reductions in molecular weight and initial decreases in amorphous fraction, resulting in initial crystallinity increases. However, it is thought that this could be attributed to the plasticization effect of water (Gok, 2016; Gewert *et al*., 2015).

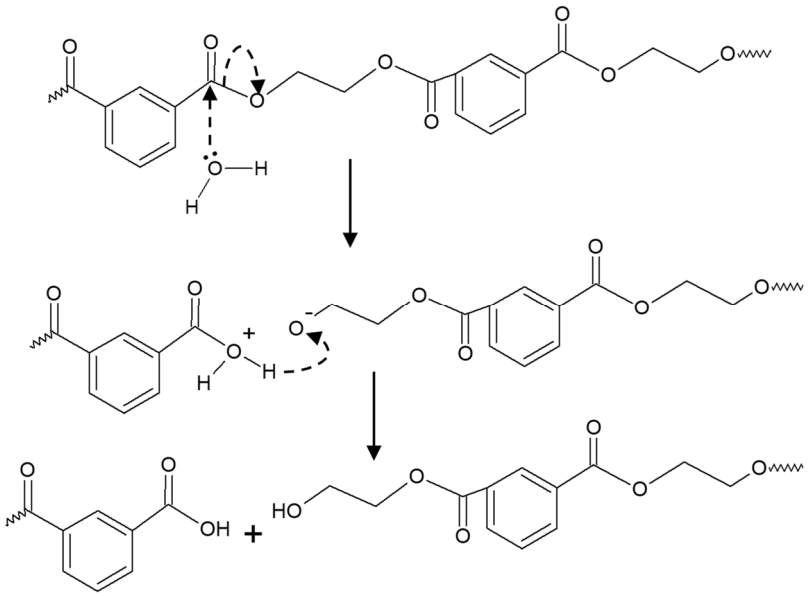

Figure 12: Proposed hydrolysis mechanism for PET, redrawn from (Chamas *et al*., 2020; Gok, 2016; Pirzadeh, Zadhoush & Haghighat, 2007)

2.2.2 Degradation rate

The number of varying pathways with varying results in the mechanisms along with their ability to occur sequentially or simultaneously to enhance and promote the effects of each other and proceed at varying rates makes defining the degradation rate difficult. It becomes even more complicated due to the tendency of the polymer properties to exhibit varying mechanical properties (Kamrannejad *et al.,* 2014). Such as occasionally exhibit increases before exhibiting the expected decreases, or different properties exhibiting opposing tendencies (Izdebska & Thomas, 2016; Rouillon *et al*., 2016; O'Brine & Thompson, 2010).

In literature studies various units for degradation rate was considered, such as mass loss over time, carbonyl group increase over time, surface area increases on micro- or nano- scale over time, tensile

strength decreases over time, etc. The studies, also included what was observed regarding various other functional groups, degree of crystallinity and hardness (Chamas *et al*., 2020; Fotopoulou & Karapanagioti, 2017; Smith, 2017; Gok, 2016; Rouillon *et al*., 2016; Gewert *et al.,* 2015; Kamrannejad *et al.,* 2014; Longo, Savaris, Zeni, Brandalise & Grisa, 2011; Wellfair, 2008; Kaczmarek *et al.,* 2004; Signor *et al*., 2003). From these studies, it was concluded that it is more accurate to consider a variety of these together, instead of a singular degradation rate unit which is still undefined. Therefore, in this investigation, the various analysis results will be considered together rather than having a singular defined degradation rate. The results will be analysed/viewed together to form a supporting theory on what occurred during the investigation.

The overall influence of plastic properties on the rate of degradation is reported on with higher confidence. These included the degree of crystallinity, as amorphous polymers or region is stated to degrade more easily, the molecular structure as branched polymers degrade at a slower rate than linear structures. The various functional groups allow or increase in the degradation rate, and many others such as the effect of water, salt ions and temperature increases (Ma, Yu, Xia & An, 2019; Gok, 2016; Izdebska & Thomas, 2016; Rouillon *et al*., 2016; Gijsman, 2008; Wellfair, 2008; Pirzadeh *et al*., 2007; Kaczmarek *et al*., 2004).

2.2.3 Previous degradation studies

There have been various studies on plastic degradation in the marine environment; a summary of these is given in Table 1. These studies tended to investigate buried polymers and polymers deep underwater. Studies of floating polymers (plastic bags in PET boxes), and polymers placed in a net in the ocean have also been investigated. However, none of these studies considered the South African environment's heat and temperature, or investigated the effect of the plastic history.

Table 1: Table of previous / similar polymer degradation studies

Research focus	Reference
Weathering of LDPE, PP, netting material, latex rubber balloons, foamed PS and degradable PE in natural conditions in air and floating in seawater in North Carolina.	(Andrady, 1990)
Monitoring degradation of four commercial polymer blends on the seafloor and in a water column, by simulating conditions in a laboratory at 16˚C.	(Beltrán-Sanahuja, Casado-Coy, Simó-Cabrera & Sanz-Lázaro, 2020)
Degradation of clear, green and pink coloured PET bottles filled with drinking water and carbonated drinks with long sunlight exposure on the roof of a building.	(Chaisupakitsin, Chairat-utai & Jarusiripot, 2019)

Table 1 continued: Table of previous and/or similar, polymer degradation studies

Research focus	Reference
The use of prodegradant additives on PET to enhance/accelerate the thermo-oxidative degradation at 70˚C.	(Chelliah, Subramaniam, Gupta & Gupta, 2017)
Investigated hydrolysis of PET.	(Güçlü, Yalçınyuva, Özgümüş & Orbay, 2003)
Investigated PET and pure and modified PE in natural conditions 2 m deep in the Baltic sea water and simulated laboratory environment at around 20˚C.	(Heimowska, Krasowska & Rutkowska, 2014, 2014)
Degradation of PP and Bioriented Polypropylene (BOPP) buried in a landfill.	(Longo, Savaris, Zeni, Brandalise & Grisa, 2011, 2007)
Determining biodegradability of two polymers, Willow Ridge Plastics – PDQ-H additive and Ecosafe Plastic – TDPA additive, in simulated and natural composting conditions at temperatures 35˚C - 50˚C.	(Mohee & Unmar, 2007)
Degradation and breakdown of two oxy-biodegradable, a compostable and a standard PE carrier bag in natural conditions 0.6m under the water in Devon in the UK.	(O'Brine & Thompson, 2010).
Investigated accelerated photoaging and weathering on a PET/PC melt extruded blend between 14˚C and 34˚C, at a UV intensity of 0.35 W/m^2 and a wavelength of 340 nm for 2 000 hours.	(Pires, Mendes, Cestari & Pita, 2015)
Thermal and hydrolytic degradation of PET in a waterbed and an oven above and below the glass transition temperature.	(Pirzadeh, Zadhoush & Haghighat, 2007)
Investigated erosion as a possible mechanism for the decrease of size of plastic pieces floating in oceans by weathering PP samples in seawater in a stainless-steel water tank with wave simulator and mercury lamp for UV radiation.	(Resmeriță,A.-M.,Coroaba, A., Darie, R., Doroftei, F., Spiridon, I., Simionescua, B. & Navard P., 2018)
Thermo-oxidative and thermo-mechanical degradation mechanisms of bottle-grade PET in temperatures up to 280 ±10˚C for 120 hours.	(Romão, Franco, Corilo, Eberlin, Spinace & De Paoli, 2009)
Photo-oxidation and photolysis of PEN, PBN and PET under 60˚C and mercury lamps with a wavelength of 300 nm.	(Scheirs & Gardette, 1997)

Table 1 continued: Table of previous and/or similar, polymer degradation studies

Research focus	Reference
Degradation of plastic carrier bags in the pelagic, eulittoral and sandy sublittoral zones as well as bottom of the deep sea and buried by sediment.	(Tosin, Weber, Siotto, Lott, & Innocenti, 2012).
Investigated the degradation of plastic carrier bags in saltwater, tap water and salt water in darkness as well as buried in sand or mud.	(Wellfair, 2008)
Investigated photocatalytic degradation of PE with TiO_2 under daily solar radiation and radiation under four 8W UV lamps at 25˚C.	(Zhao, Li, Chen, Shi & Zhu, 2007)

2.3 Natural environment conditions

Plastic waste is exposed to natural environmental conditions, and these conditions act as factors influencing the rate or initiating the degradation or weathering of plastics. The natural conditions this investigation was concerned with was mostly temperature, the marine environment and therefore seawater, as well as UV radiation from the sun rays. The following section is centred around the expectations for these conditions in the South African environment and especially the Cape Town region.

2.3.1 Temperature

Temperature varies due to position on the globe, change of season, time of day and amount of sunlight. Various online resources, such as Meteo Blue Climate Cape Town (2020), World Weather Online (2020), World Sea Temperature (2020) and Climates To Travel World Climate Guide (n.d.), exist where one can track and/or obtain historical weather and climate data of a place. These resources have recorded years of minimum and maximum daily temperatures of various places on earth and have calculated average temperatures, precipitation, UV index, rainfall etc. Using this data one can determine the expected average temperature and sunlight hours for any month or season for anywhere in the world.

South Africa falls in the Southern Hemisphere, causing its summer season and therefore warmer months to fall over December and the beginning of the year, January and February. South Africa has a moderately warm climate with the average maximum summer temperature for South Africa being between 25˚C and 27˚C, and the average minimum winter temperature is between 7˚C and 10˚C. However, temperatures can reach well over the 30˚C, sometimes pushing 40˚C, and fall below 5˚C sometimes pushing freezing point (Meteo Blue Climate Cape Town, 2020; World Weather Online, 2020; World Sea Temperature, 2020; Climates To Travel World Climate Guide, n.d.).

2.3.2 Ultraviolet radiation (UV)

Ultra-violet (or UV) radiation is part of the electromagnetic spectrum emitted by the sun. The UV rays are invisible to the human eye, as their wavelengths fall below the visible light range. UV-A is the largest with

a wavelength of 315 – 400 nm, UV-B has a wavelength of 280 – 315 nm, and UV-C has a wavelength of 200 – 280 nm (SA Weather (WX) Forecasts, 2020; Fioletov, Kerr & Fergusson, 2010; (Kool-a-sun, n.d.). Of these UV-C is almost completely absorbed by atmospheric oxygen and ozone and is therefore prevented from reaching the earth's surface, it also absorbs about 90% of UV-B radiation while very little UV-A is absorbed. Since the UV radiation radiates from the sun, the intensity is dependent on the distance between the earth and the sun. Therefore during January, when the earth is closest to the sun, the intensity of the radiation is about 7% more than in July when the sun is the furthest from the earth. However, the variability in radiation itself is less than 1% (Fioletov *et al.,* 2010). Similarly to temperature, the UV radiance varies with geo-orbital factors, such as latitude, season and time. However, UV radiance also varies with environmental factors such as clouds, the ozone layer, pollutant and reflection from the earth's surface (Marionnet, Tricaud & Bernerd, 2015).

The UV radiance is also part of the climate history, similarly to temperature, and online resources, as mentioned in 2.3.1, also contains forecasts and historical data of UV radiation on various places on earth. Average expected daylight hours for South Africa is about 12 hours, with the summertime exhibiting an average of about 13 hours and the winter an average of 11 hours, even though in summertime the daylight can reach over 14 hours and in wintertime fall to 9 hours. Depending on the resource, the UV-radiation can be given as a UV index, W/m^2 or $mW/(cm^2 \cdot nm)$. From data obtained over the years 2016-2020, the average daily index can be anything from 50 W/m^2 in winter months to about 300 W/m^2 in the summertime, with an overall average of around 150 W/m^2 (Meteo Blue Climate Cape Town, 2020; Marionnet *et al*., 2015; Climates To Travel World Climate Guide, n.d.; Weather Atlas, n.d.; Weather Spark, n.d.).

2.3.3 Seawater

Seawater is roughly 96.5% water with the rest being various salts, sand, broken seashells and an assortment of other substances and gases (Mackenzie, Duxbury & Byrne, 2018). The exact concentration of these varies with geometric position. The literature data obtained for seawater contents and variances for this project will focus on the South African content as the investigation will be completed in seawater from the South African coast.

According to the South African water quality guidelines for coastal marine waters given by the South African government (Department of Environmental Affairs, 2018), the pH of seawater ranges between 7.9 and 8.3 depending on the region – with the fynbos region (west and south coasts) being more acidic – and the CO_2 in the atmosphere or surface waters. The further away from river inlets, the less the variability, due to the increased concentrations of salt that serves as buffering ions.

The salinity of the ocean not only varies with the coastal region but with temperature as well. The South African government and Data Centre for Oceanography (Department of Environmental Affairs, 2018; SADCO, 1999) published that the salinity of the South African coastline varies between 34.4-35.6 PSU.

The higher salinities was detected to the north in the Indian Ocean, due to the warmer waters which is a result of the subtropical conditions and warm ocean current.

Due to position on globe and change of season, the water temperature of the earth's ocean varies. As explained previously, the change in temperature can affect degradation. It is therefore important to identify and collect the global position and seasonal temperature data for the project data to apply to a real-life scenario. Using various online, expected temperature and weather, sources such as World Sea Temperature and Climates To Travel World Climate Guide, the average sea temperature during summer or winter could be estimated as 23˚C and 19˚C for the coastline of South Africa.

3 RESEARCH DESIGN AND METHODOLOGY

3.1 Materials

The materials acquired for the investigation included seawater from Gordon's Bay Boat Angling Club located at the coast of the Western Cape of South Africa and demineralised water from the process engineering department in Stellenbosch University. Commodity thermoplastics sheets used for the production of single-use plastic products were obtained from Zibo plastics. The three plastic sheets obtained from Zibo plastics were clear APET (amorphous polyethylene terephthalate), black polypropylene that contains a black pigment as a photo stabiliser and cloudy polypropylene. Cloudy polypropylene instead of clear polypropylene was obtained since Zibo plastics stated they add a clarifier additive to the clear polypropylene. However, they claimed to not add additives to the cloudy polypropylene. The cloudy polypropylene are therefore thought to be better for comparison purposes as Zibo plastics also claim not to add clarifying additives to the PET. The plastic sheets were cut into specific shapes, as seen in Table 2. Other materials were CONSOL glass flasks of 350 ml, bottle product number: 01538101, as flasks for bench tests and Hulett aluminium foil freezer trays as trays for initial tests.

Table 2: Plastic material, shapes and sizes used in the investigation

Plastic-type	Colour	Sheet thickness (error ±0.02mm)	Shapes		Supplier
PET	Clear	0.31 mm	Small circle	5 mm	Zibo plastics
			Large circle	12.7 mm	
			Small rectangle	8 mm x 3.5 mm	
			Large rectangle	20 mm x 9 mm	
PP	Clear/ Cloudy	0.48 mm	Small circle	5 mm	Zibo plastics
			Large circle	12.7 mm	
			Small rectangle	8 mm x 3.5 mm	
			Large rectangle	20 mm x 9 mm	
PP	Black	0.32 mm	Small circle	5 mm	Zibo plastics
			Large circle	12.7 mm	
			Small rectangle	8 mm x 3.5 mm	
			Large rectangle	20 mm x 9 mm	

3.2 Equipment

The experimental and analytical equipment required for the project is summarized in Table 3. In Table 3, a custom build UV chamber is mentioned. The dimensions of the stainless-steel UV chamber are length 500 mm, width 500 mm and height 500 mm, and the distance between the lamps and wire rack was 400 mm. In Figure 13, a schematic representation of the UV chamber is given, during runs at 65 W/m^2 a singular lamp was placed at “possible light placement for singular lamp runs”. In contrast, during

135 W/m^2 runs two lamps, as indicated in Figure 13 were used. In the UV chamber, airflow is added to the side to cool down the chamber as the temperature can easily reach 90^{o}C due to the energy given off by the lights if no precautions are taken. However, with no door and air blowing through, the temperature can be brought down to between 30˚C and 40˚C or less depending on the outside temperature and amount of lights switched on.

In Figure 13 reference is made to light ignitors. When using high-performance halogen metal halide lamps the gases inside needs to be ignited for the lights to work. The light ignitors provide an initial brief, high voltage pulse that ignites the gases inside the lamps and regulates the initial inrush current that occurs when the lamps turn on; this allows the lamps to turn on and ensure reliable and smooth starting behaviour as well as increasing efficiency (RS Components, n.d).

Table 3: Experimental and analytical equipment utilised in the investigation

Experimental equipment	Analytical equipment
• Custom build UV cycle chamber (see Figure 13) • MRC Refrigerated Incubator LOM-150 obtained from United Scientific • Fridge • Timer controller • Oven • Light bulbs: Supratec HTC400 241 R7s	• Differential scanning calorimetry machine: Instrument DSC Q200 V24.10 Build 122 • Fourier transform infrared spectroscopy Thermo Nicolet instrument • UHL VHMT Microhardness tester • STATISTICA version 13.5.0.17

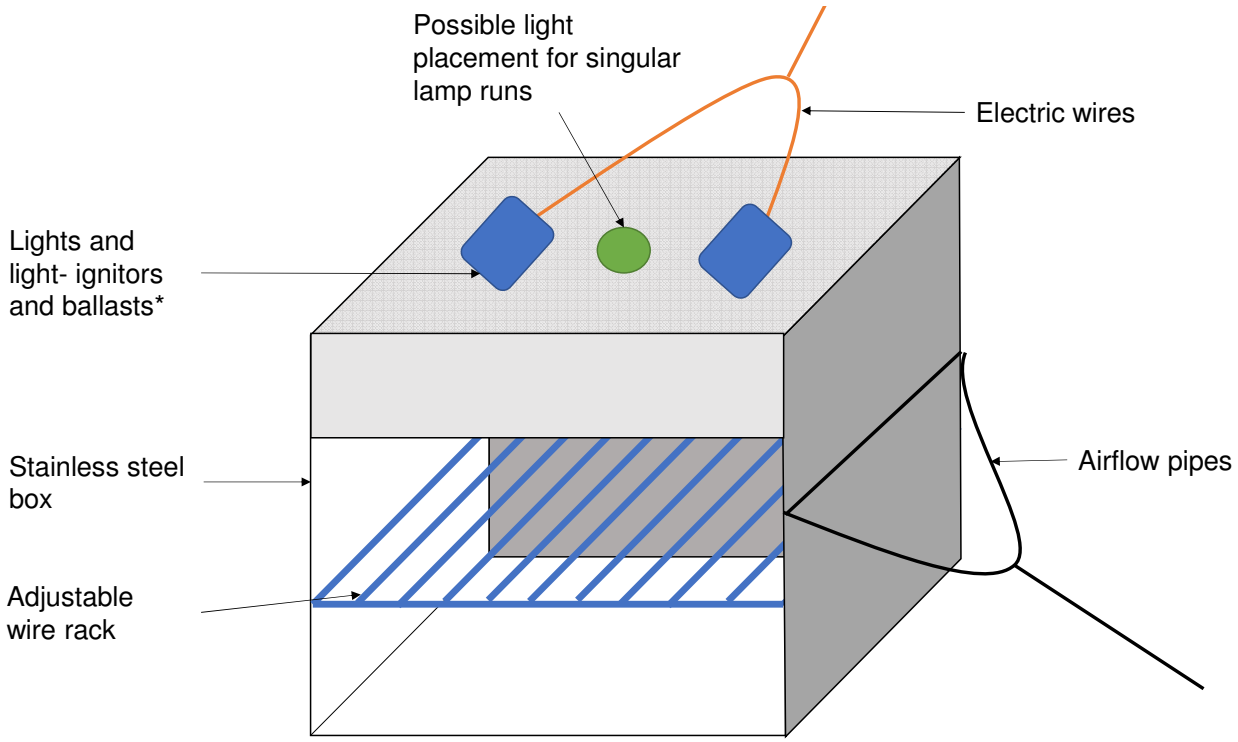

Figure 13: Custom build UV chamber

3.3 Methods

3.3.1 Experimental design

The experiment was designed to be divided into two sections, as seen in Figure 14. The first section being the initial experiments, also referred to as the pre-treatment, and the last section being secondary experiments, also referred to as the bench tests.

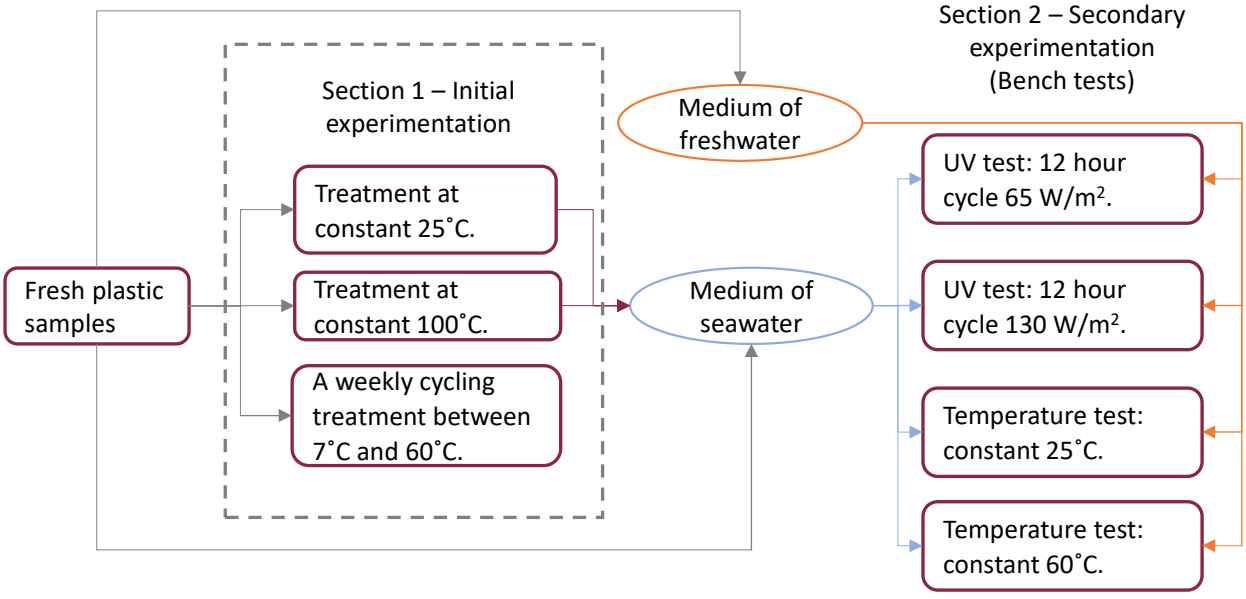

Figure 14: Experimental design flowchart

The specific plastics used in the experiment were selected as these are some of the most common plastic waste types found in the ocean. The selection also incorporated a colour change to allow an investigation into the effect of colour additive on degradation.

3.3.1.1 Initial experiments

The initial experiments served to simulate the degree of thermal degradation associated with the journey of plastics into the ocean. The initial experiments were also used to investigate the influences of various plastic properties such as the plastic-type, colour, size and shape as well as natural conditions such as temperature on the degradation. Thus, the initial experiments expanded over all the plastic types, colours and shapes. In the initial experiments, the plastic particles were subjected to the temperature conditions in Table 4, in dark conditions, for six weeks. The temperature was controlled by either a temperature controlled oven or an incubator. During the experiments bi-weekly sampling for FTIR and initial and final sampling for hardness and DSC tests were completed. Two different shapes and sizes were incorporated to investigate the size and shape effect or surface area to volume ratio.

Table 4: Temperature conditions for initial experiments

Temperature	Motivation for selection	Frequency of adjustment
25˚C	Simulate a moderate average day temperature during summertime for South Africa.	Constant throughout
100˚C	High temperature causes physical deformation or degradation and possibly exhibits accelerated degradation change.	Constant throughout
7˚C – 60˚C	The highest and lowest setting on the incubator to cause the greatest effect possible.	Weekly cycle

The purpose of the initial experiments' design was to be able to investigate and/or compare the effects of temperature, plastic-type, colour, shape and size on the degradation rate and/or behaviour of properties of the plastic.

3.3.1.2 Secondary experiments (Bench tests)

The secondary experiments, or bench tests, served to stimulate the degree of degradation associated with the marine environment considering the influence of the initial experiments. The secondary experiments were also used to account for and/or investigate the influence of plastic-type, colour and natural conditions such as temperature and UV radiation or effect of freshwater versus marine water on the degradation. The bench test expanded over all the plastics types and colour of the small circular shape, from both high and low initially treated conditions as well as untreated plastics, in both sea and freshwater. In the bench tests, the plastic particles were subjected to the treatments in Table 5, for six weeks during which bi-weekly sampling for FTIR and hardness and initial and final sampling for DSC tests were completed. The purpose of the bench tests' design was to be able to investigate and/or compare

the effects of water conditions, plastic history, plastic-type and colour as well as the effects of heat and radiation on the degradation of plastic.

Table 5: Temperature and UV radiation conditions for bench tests.

Treatment	Motivation for selection	Frequency of adjustment
25˚C with no light	Simulate a moderate average day temperature during summertime for South Africa and compare to initial experiments.	Constant throughout
60˚C with no light	A high temperature to possibly exhibit accelerated degradation changes that would be helpful to define parameters in modelling.	Constant throughout
0 W/m^2 – 65 W/m^2	Simulate average UV radiation while accounting for various geo-orbital and environmental factors, such as winter, clouds or the plastics being submerged deeper under water than used in the investigation.	24-hour light and darkness cycle
0 W/m^2 – 135 W/m^2	Simulate average UV radiation in the summer.	24-hour light and darkness cycle

3.3.2 Experimental procedure

3.3.2.1 Preparation

For the plastic preparation CPP, BPP and PET obtained from Zibo plastics were used to punch:

- 500 small circular shapes with a diameter of ± 5 mm, with a Genmes medium punch.
- 150 large circular shapes with a diameter of ± 12,7 mm, with punch tools.
- 150 small rectangles with a size of 3,5 mm x 8 mm, with a paper binder machine.
- 150 large rectangles with a size of 9 mm x 20 mm, manually measured, with a paper guillotine.

These plastic particles were separated into groups of 10 each. Each group was placed and sealed in a Ziplock bag. The envelopes were marked accordingly and placed in the refrigerator at a constant temperature of 4˚C. The purpose of the Ziplock bags was to isolate the plastics from the air, and more specifically oxygen, in an attempt to impede the oxidization and thus degradation of plastics during storage.

3.3.2.2 Initial experiments

All samples used required during initial experiments or for analysis of initial values were extracted from the stockpile in the refrigerator.

Determination of initial values was done by randomly selecting three samples of CPP, BPP and PET plastic with small circular, small rectangular, large circular and large rectangular shape for FTIR analysis. Six more

samples each, of CPP, BPP and PET plastic with small circular shape were drawn, three for hardness tests and three for DSC analysis.

For each of the initial experiments, CPP, BPP and PET plastic samples of small and large circular and rectangular shape were placed in three separate Hulett aluminium foil freezer trays.

For the initial experiments under the 100˚C conditions, the aluminium pans containing the plastics samples were placed in an oven set to a constant temperature of 100˚C. It was then left for six weeks, while the bi-weekly sample extraction procedure was followed. Similarly, for the initial experiments under the 25˚C conditions, the aluminium foil trays containing the plastics samples were placed in the incubator. The incubator was set to a constant temperature of 25˚C and left for six weeks, while the bi-weekly sample extraction procedure was followed. For the initial experiments under the 7˚C – 60˚C weekly cycle conditions, the incubator was set to 60˚C and changed to 7˚C after one week, at week two the temperature was changed back to 60˚C and so the cycle continued by being changed every week; while the bi-weekly sample extraction procedure was still followed.

Every two weeks, three samples of CPP, BPP and PET plastics of the small circular, small rectangular, large circular and large rectangular shape were extracted with a stainless-steel tweezer. These samples were placed inside a Ziplock bag and then placed in an envelope. After six weeks, six additional samples of CPP, BPP and PET plastics of small circular shape were extracted – three samples were used for to hardness tests and three for DSC analysis. The rest of the samples were also extracted, marked accordingly and stored in Ziplock bags at a constant 4˚C until required for the bench tests.

3.3.2.3 Secondary experiments (Bench tests)

Every bench test commenced with extracting 24 untreated BPP, CPP and PET plastic samples of small circular shape from the refrigerator and placing the samples in three separate 375 ml CONSOL flasks with lids, filled with 100 ml freshwater each. Another 24 untreated and 24 initially treated at 100˚C and 25˚C respectively, plastic samples of BPP, CPP and PET with a small circular shape are then extracted from the refrigerator and placed in nine separate flasks filled with 100 ml seawater each.

The UV treatments of 65 W/m^2 and 130 W/m^2 was performed by positioning the twelve flasks horizontally in the UV chamber. The UV chamber was set to the appropriate setting of either 65 W/m^2 or 130 W/m^{2,} and the timer controller was set on a 12-hour-on-12-hour-off cycle; both were then switched on. The experiments were left for six weeks with weekly aeration and co-ordinated interchangement of jars to ensure equally distributed UV radiation and replenish oxygen for degradation via oxygenation.

The temperature treatment was performed by positioning the twelve flasks upright in the incubator and setting the incubator on the appropriate setting of either 25˚C or 60˚C. The incubator was switched on, and the experiments were left for six weeks with weekly aeration to replenish oxygen for degradation via oxygenation.

Every two weeks, all jars were removed from the UV chamber and incubator to extract six plastic samples from each with a stainless-steel tweezer. The samples were dried and placed inside Ziplock bags and then placed in an envelope. The envelopes were marked with the bench test and initial experiment conditions, bench test medium, time of extraction and plastic-type and colour. These samples were then subjected to FTIR and hardness analysis. The water in the jars for the rest of the samples was renewed, and the jars were returned to their respective conditions in the UV chamber or incubator. After six weeks, an additional three samples were extracted for DSC analysis.

3.3.3 Analysis procedure

3.3.3.1 FTIR analysis

To employ the technique, the crystal on the FTIR machine was cleaned with acetone and allowed to dry before completing a background scan to obtain the atmospheric print. Next, a sample from the stockpile was clamped onto the FTIR machine's crystal. For handling of the sample, a stainless-steel tweezer, cleaned with acetone and allowed to dry, was used to prevent contamination. The infrared radiation was then passed through the sample, with wavelengths between 400 cm^{-1} – 4000 cm^{-1}, the FTIR machine completed 32 scans before yielding the %transmittance spectrum. The OMNIC program utilised automatically subtracts the atmospheric print from the sampling print obtained, resulting in an accurate dataset for the sample. The spectrum is advantageous as it can be converted from absorbance to transmittance and vice versa with Equation 2, where A represents absorbance and %T represents %transmittance. After completion of the scan, the spectrum was saved, and the sample overturned and clamped at another location. The analysis was repeated, and the spectrum saved under a new sample number. Before continuing to the next sample, the crystal was again cleaned, and a new background scan completed.

$$A = 2 - \log(\%T) \qquad [2]$$

After obtaining the spectrums, the next step was identifying the molecules, chemical structure and/or functional groups from the spectrum. Various infrared identification by frequency regions tables exist that can assist with these. The wavelength regions used to identify the functional groups in this investigation can be seen in Table 6, sometimes references identified different regions for peaks resulting in an overlapping of wavelength regions. References for Table 6 are Chamas *et al.* (2020), Merck (2020), LibreTexts (2019), Fotopoulou & Karapanagioti (2017), Smith (2017), Gok (2016), Rouillon *et al*. (2016), Gewert *et al*. (2015), Kamrannejad *et al*. (2014), Longo *et al*. (2011), Wellfair (2008), Kaczmarek *et al*. (2004), Signor *et al.* (2003), UCLA College Chemistry & Biochemistry (2001), and University of Puget Sound (n.d).

Table 6: List of the vibrations, conformational isomers and absorptions of functional groups against the corresponding infrared spectroscopy frequency ranges

Functional group	**Wavelength region (in cm^{-1})**
Carbonyl	1500 – 1780
Hydroxyl	3000 – 3700
Methanetriyl	2800 – 3000 and 1350 – 1390
Methylene	1420 – 1480
Methyl	1350 -1390 and 1420 – 1480
Alkene	700 – 1050
* Trans oxy-ethylene group in the ethylene glycol unit	955 – 990
* Trans CH_2 rocking of ethylene glycol	840 – 850
* Gauche oxy-ethylene group in the ethylene glycol unit	1030 – 1050
* Gauche CH_2 rocking of ethylene glycol	895 – 905
*Vibrations and conformational isomers of molecules for tracking PET degradation (Gok, 2016).	

3.3.3.2 Hardness tests

To perform the test the hardness tester was set to a force of 300 gf, an indention time of 15 s, a speed of 15 µm/s and the measuring lines were calibrated. A sample from the stockpile was extracted with a stainless-steel tweezer and placed on the hardness tester's platform for samples. The optical microscope was set on a magnification of "50x", and the lens and platform height was adjusted to give a clear view of the location were indentation will be performed.

The machine performs the test by pressing the indenter against the sample, at the selected force and dwell time. The optical microscope was then employed to measure the diagonal lengths (D1 and D2) of the resulting indentation, as seen in Figure 15. The diagonal lengths were recorded in micron metres as D1 and D2 specific to the sample. After which the sample was overturned, and another hardness test was performed and recorded at another location on the sample.

The projected area of indentation was calculated from the diagonal lengths. The Vickers hardness number was computed as the ratio of the applied force to the projected area (Smallman & Ngan, 2014; Sundararajan & Roy, 2001; Briscoe & Sinha, 1999) as explained in the following paragraphs.

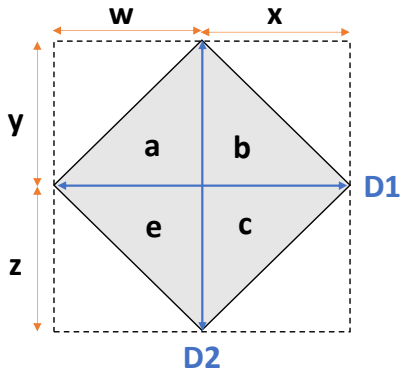

Figure 15: Schematic sketch of the indentation left by Vickers hardness test

The projected area of the indentation equals the sum of the areas of the triangles (a, b, c and e) in Figure 15 – where the area of a triangle is the product of the perpendicular height and ½ of the basis. The derivation for the projected indentation area is represented by Equations 3 – 7.

$$Projected\ area = \sum areas\ of\ triangles = \frac{1}{2} \times w \cdot y + \frac{1}{2} \times x \cdot y + \frac{1}{2} \times w \cdot z + \frac{1}{2} \times x \cdot z \quad [3]$$

$$Projected\ area = \frac{1}{2} \times (wy + xy + wz + xz) \quad [4]$$

And:

$$D1 \times D2 = (w + x) \times (y \times z) \quad [5]$$

$$D1 \times D2 = wy + xy + wz + xz \quad [6]$$

Therefore when substituting Equation 6 into Equation 4 it's observed that the projected area of indentation is half of the product of the diagonals as represented by Equation 7.

$$Projected\ area\ of\ indentation = \frac{1}{2} \times (D1 \times D2) \quad [7]$$

The hardness value can, therefore, be determined by Equation 8 as Vickers microhardness is calculated as a ratio between the indentation load and the projected area.

$$HV = \frac{Applied\ load}{0.5 \times D1 \times D2} \quad [8]$$

3.3.3.3 DSC analysis

The first step in preparing the sample for DSC analysis was weighing the sample on a five decimal gram scale. The weight was recorded and entered along with the sample ID into the TA Instrument Explorer program of the computer attached to the DSC machine. The first step in the analysis was to set the DSC machine equipment to a heating rate of 10˚C per minute under nitrogen atmosphere, with a starting temperature of 25˚C, and maximum end temperatures of 300˚C for PET and 200˚C for the polypropylenes via the computer. The cycle was started to allow the DSC machine to reach the specified starting temperature. While the DSC machine cooled down to 25˚C, the sample preparation continued, by placing

the identified sample into aluminium DSC heating pans. The aluminium lids, which contains a small hole in the top to release gasses, was placed on top of the heating pans and pressed closed to prevent the melted plastic from escaping. A reference aluminium pan with lid was also assembled containing nothing. Once the required starting temperature of 25˚C was reached, both pans were placed inside the DSC machine, and the data recording process in the analysis were started. The DSC machine recorded the heat flow in W/g against temperature in ˚C. Once the maximum temperature was reached, the calorimetric curve recorded was saved. The DSC machine was left to cool down before removing the sample and repeating the process with another of the identified samples.

All communication with the DSC machine was done via the TA Instrument Explorer program, and all handling of either the plastic sample or the aluminium pan was done with a stainless-steel tweezer to prevent contamination.

3.3.4 Data and data processing

3.3.4.1 FTIR analysis

The %transmittance graphs were studied and converted to absorbance graphs. An automatic baseline correction was done on all graphs. The literature reviewed referred to two methods for calculating the different indices; therefore, both methods were applied in the project. The two methods where compared to determine which method is more appropriate. The comparison was made by investigating the changes in the FTIR analysis graphs throughout the experiment and to compare trends in the mean graphs for both methods. For both methods, the wavelength range or frequency region considered for every functional group investigated is given in Table 6 in 3.3.3.1. While the reference peak region was considered to be the 2156.5 – 2175 cm^{-1} region. For both methods all the indices, of all samples with repeats, has been individually calculated and labelled in Excel.

The first method is to determine the indices by examining the peak values. To determine the respective indices with peaks, the maximum absorbance value of the peak that falls within the range specified for that functional group is used. Equation 9 represents the formula used to calculate the index with peaks.

$$Functional\ group\ index = \frac{Max\ peak\ value\ in\ functional\ group\ range}{Max\ peak\ value\ in\ reference\ \ range} \quad [9]$$

The second method is to determine the indices by examining the areas under the peak values. For this, the area below the absorbance graph must be calculated. For the calculation of the area under the curve, numerical integration using the midpoint rectangle method in combination with the Riemann sum method was applied. The Δx used for the Riemann calculation was 0.4821 cm^{-1} the same as the datapoint collection interval used by the FTIR analysis machine. Equation 10 represents the formula used to calculate the index with peaks.

$$Functional\ group\ index = \frac{Absorbance\ area_{Functional\ group}}{Absorbance\ area_{reference}} \quad [10]$$

3.3.4.2 Hardness tests

The data obtained from the samples were entered into Excel. These include the labels of samples and repeats as well as the dimensions for each. The dimensions were then used to calculate the hardness, as seen in Equation 11. The calculated hardness's was also sorted and tabulated in Excel to facilitate the use of STATISTICA later.

$$HV = \frac{300}{1000} \div \left(\left(\frac{D1}{1000} \times \frac{D2}{1000}\right) \times 0.5\right) \quad [11]$$

3.3.4.3 DSC analysis

The calorimetric curves were analysed with Universal Analysis 2000 version 4.5A to obtain the onset temperature, the peak temperature and the heat of fusion and crystallization as seen in Figure 16. The program determines these values when applying the function "Sigmoidal Horizontal Peak Integration" between a specific temperature range. The temperature range used for the polypropylenes were 120˚C–180˚C and for PET 110˚C–150˚C and 200˚C–270˚C. Once the values were obtained they were entered into Excel along with the sample ID and used to calculate the % crystallinity with Equation 12.

$$\%Crystallinity = \frac{\Delta H_m - \Delta H_c}{\Delta H_m^o} \times 100\% \quad [12]$$

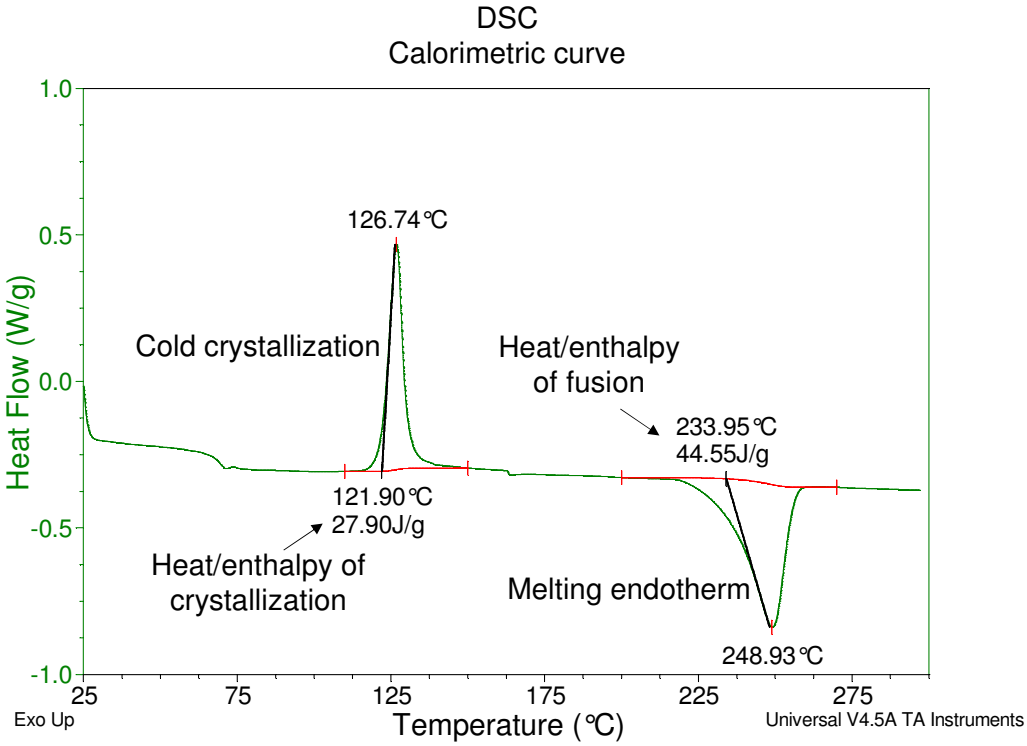

Figure 16: Example of determining heats of fusion and cold crystallization

3.3.4.4 STATISTICA

The advance analytic software STATISTICA version 13.5.0.17 was employed in the analysis and graphing of all data. Data required for the specific analysis or comparison were imported from Excel.

The "ANOVA" and "LS means with CI" analysis under the "Variance Estimation and Precision" option in STATISTICA was completed on the data using the REML estimating method, with Type III sum of squares and a 95% confidence interval. The ANOVA methods were also applied by O'Brine and Thompson (2010) and Mohee and Unmar (2007). The ANOVA compares the means of the main effects with the purpose of identifying if there is a difference in the means and if the difference is statistically significant. It also tests the differences or variances between the various factors, to identify if the differences/variances are independent of each other. The "LS means", or least-square means, are a graphing method that fits a graph to the means by minimizing the differences of the sum of the squares between the observed values and the values estimated by the formula of the graph. The "with CI", or with confidence intervals, ensures that the graph includes error bars for a 95% confidence interval of the data.

4 RESULTS AND DISCUSSION

In Table 7 a comparison between published properties for the respective plastics and the properties measured during the analysis of the raw samples (samples at week zero) in this study is given. Since the degree of crystallinity is not generally given as a polymer property value, the onset temperature was used instead. The onset temperature is also obtained from the DSC thermogram and is therefore a substitute for the degree of crystallinity while still allowing comparison of DSC thermogram data. Appendix A provides details about the conversion between hardness and tensile strength. Literature values for tensile strength were obtained from Shah (2007) and Cambridge University Engineering Department (2003), the conversion table were obtained from Guanyu Tube (2020) and the onset temperatures were obtained from Longo *et al*. (2011) and Güçlü, Yalçınyuva, Özgümüş and Orbay (2003). Without exception, the properties measured in this study fall within the typical property ranges reported in literature for the respective plastics.

Table 7: Comparison of literature values to plastic samples used

Property	PP		PET	
	Raw samples analysed	Literature range	Raw samples analysed	Literature range
Tensile strength [MPa]	51.5 - 57.2	41 - 69	60.7 - 61.6	48.3 - 72.4
Vickers Hardness (HV) [kgf/mm^2]	11.2 ± 0.21	6.95-15.8	13.38 ± 0.14	2.3-16.9
Onset temperature (melting) [^{0}C]	153.04 ± 0.30	135.5-166.2	234.26 ± 0.18	227.4-266.2
Onset temperature (cold crystallization) [^{0}C]	NA	NA	122.04 ± 0.10	115-137

4.1 Initial experiments

4.1.1 Crystallinity

The degree of crystallinity, as seen in Figure 17, exhibits no significant change for the black polypropylene (BPP) samples. The CPP samples also exhibited a similar trend with no change for the cycling and 25˚C treatments, but a significant increase, about 4% ± 0.4%, when samples are subjected to 100˚C. The PET samples subjected to cycling temperature treatment exhibited a slight increase, about 2.5% ± 1.4%, while samples at 100˚C exhibited a significant and substantial increase, about 19.3 % ± 1.3%. Crawford and Quin (2016) state that an amorphous polymer does not have a distinct melting point. Since 60˚C (from the cycling temperature treatment) approaches the crystallization temperature of crystalline PET, it is theorised that the amorphous regions in the APET underwent some degree of crystallization. At the same time, the increases indicating crystallization at 100˚C were anticipated, as 100˚C exceeds the crystallization temperature for PET. Please note that all figures have been staggered for ease of interpretation and visibility. Therefore, in essence, all the data points around a certain week are at that week, e.g. the data points around week 6 are at week 6.

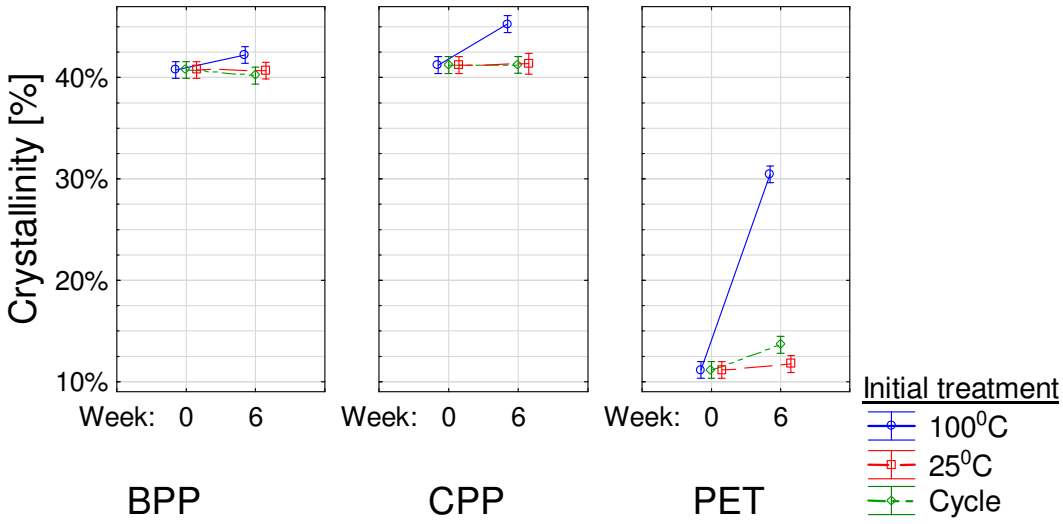

Figure 17: Percentage crystallinity mean graphs for the initial treatments

4.1.2 Hardness

The hardness results in Figure 18 indicates no significant variances for BPP samples, between either the various initial treatments or the initial and final values. Along with the data obtained from the degree of crystallinity analysis, it suggests that BPP did not undergo significant deterioration. The PET samples exhibited increases in hardness for the 100˚C and cycling treatment (about 5.7% ± 1.3% and 1.7% ± 1.2%, respectively). These increases are linked to the structural change and hardening of PET during crystallization. The CPP exhibited significant decreases in hardness for all treatments (between 1.3% ± 1.2% and 2.75% ± 1.2%), with the samples treated at 100˚C exhibiting the lowest decrease and the samples from the cycling temperature treatment the most. Normally it is expected that degradation will lead to a decrease in both hardness and crystallinity. However, since the hardness decreased and the degree of crystallinity increased for CPP subjected to 100˚C, a possible theory is that degradation occurred mostly in the form of chemicrystallization. Chemicrystallization is normally associated with photo-oxidative degradation, but Fayolle, Richaud, Colin, & Verdu (2008) state that during thermal ageing, chemicrystallization and annealing effects can occur and coexist. This would cause increases in crystallization while decreasing hardness. The possibility exists that BPP has also undergone some chemicrystallization but not significantly enough to exhibit deterioration of plastic properties.

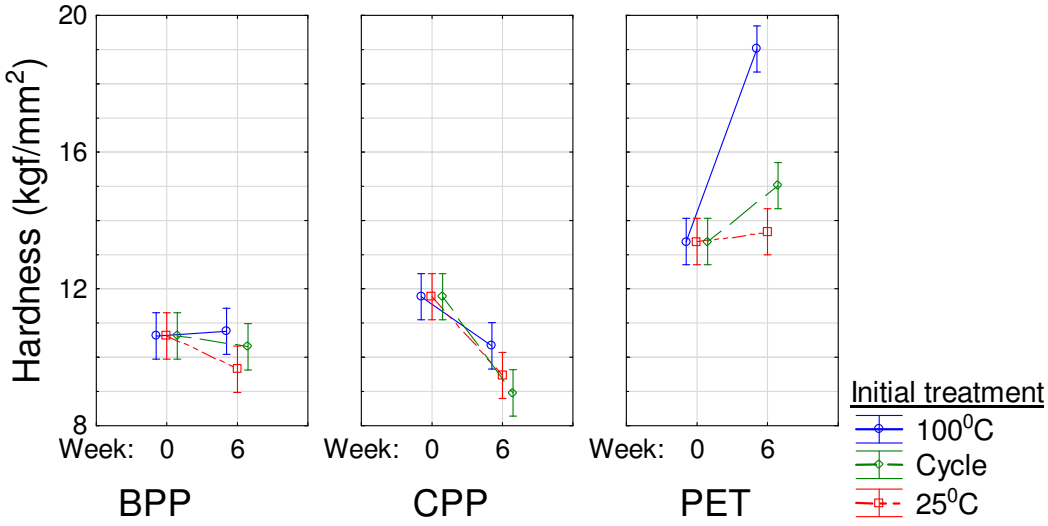

Figure 18: Hardness value mean graphs for the initial treatments

4.1.3 FTIR indices

To affirm the theories obtained from the hardness and crystallinity data, the FTIR results are consulted. Chen (2012), found that the carbonyl index, as well as that the peaks in the 1430 - 1460 cm^{-1} range decrease with PET crystallization. From Figure 19, the carbonyl index for the PET subjected to the 100˚C and cycling treatment, where the suspected crystallization occurs, drops over the first two weeks and thus supports the theory. The increases and other variances viewed after the second week is possibly due to degradation occurring after the crystallization was completed. Similarly, over the first two weeks, the methylene index that was measured in the 1420 - 1485 cm^{-1} range also drops, as seen in Figure 19. This suggests that the second requirement is also fulfilled and confirming the crystallization of PET at both temperature treatments. In the 100˚C treatment, it is also possible to observe the significant increases in both the transforms, which Gok (2016) stated, to be favoured by crystalline regions.

Along with initial decreases in the gauche forms, which stated by Gok (2016), are favoured by the amorphous regions—indicating a clear shift from amorphous to crystalline. Similarly, the gauche forms exhibited initial decreases in the cycling treatment, indicating and supporting the decrease in amorphous regions theory. The increases and other variances viewed after the second week is possibly due to degradation occurring after the crystallization was completed.

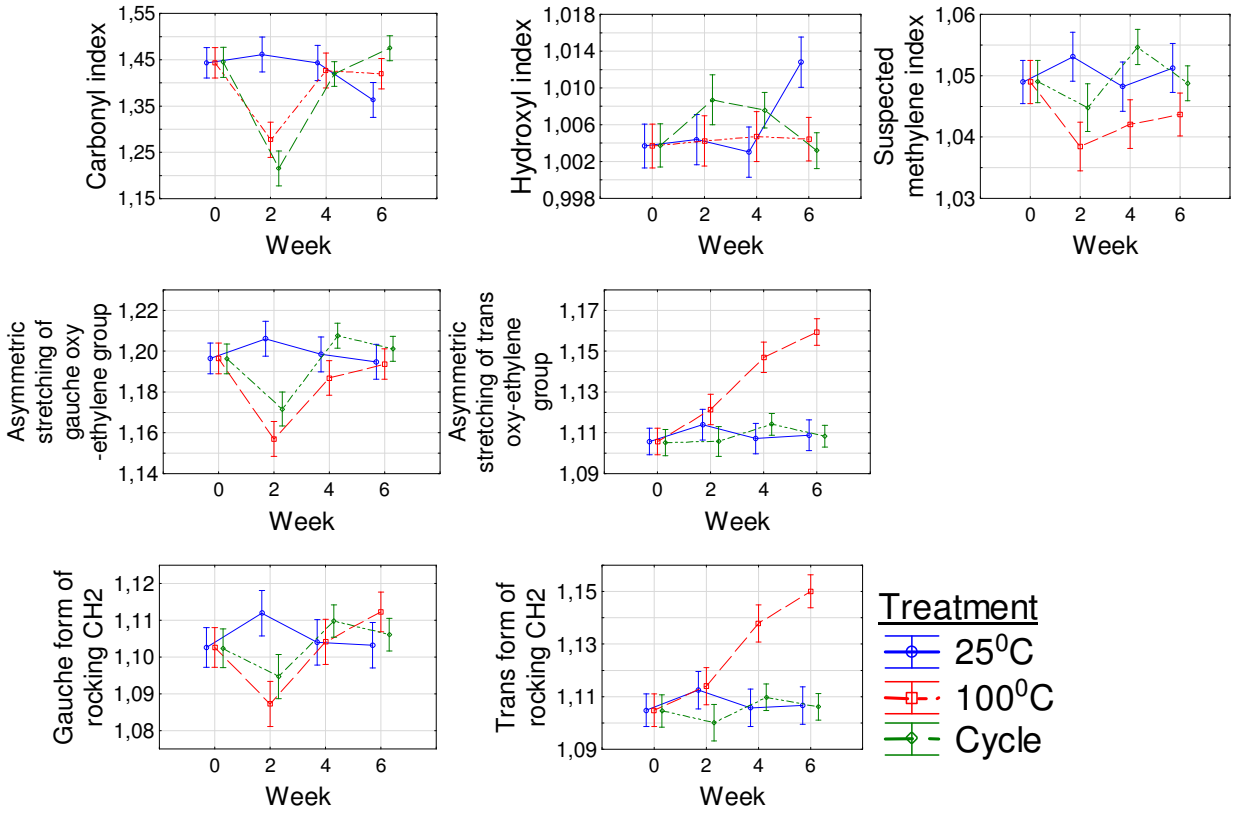

Figure 19: Mean graphs of FTIR indices for PET under initial treatment

For CPP, see Figure 20, increases in the carbonyl and hydroxyl indices along with decreases in the suspected methanetriyl and methyl indices are observed for the 100˚C and cycling temperature treatment. These trends are in correspondence with the changes expected during degradation, as can be seen in the mechanism in Figure 9, from section 2.2.1. Therefore, supporting the theory that degradation has occurred in CPP samples. The decrease in suspected methanetriyl indices could be an indication of side-chain stripping, which could explain the crystallinity increase for the 100˚C treatment. Variances in trends after initial observations could be due to secondary reactions and further degradation.

Considering the other CPP, PET and BPP results that did not exhibit significant crystallinity changes, the CPP hardness decreased, so it suggests degradation has occurred. From examining the functional group indices, it is observed that the cycling treatment had some variances. Indicating that change and possible degradation took place, supporting the hardness data, and appears to follow a similar trend to the 100˚C treatment, although lagging with a week or two. This would be expected as an increase in temperature generally increases the kinetic rate of reaction, in this case, the degradation. The BPP follows a similar trend to the CPP with regards to the different treatments, indicating that the BPP also experienced some degree of degradation following similar mechanisms to the CPP, see Figure 21 for BPP results. However, the BPP contains a photo stabiliser colour additive which could be the reason the deterioration of properties such as hardness is delayed or hindered.

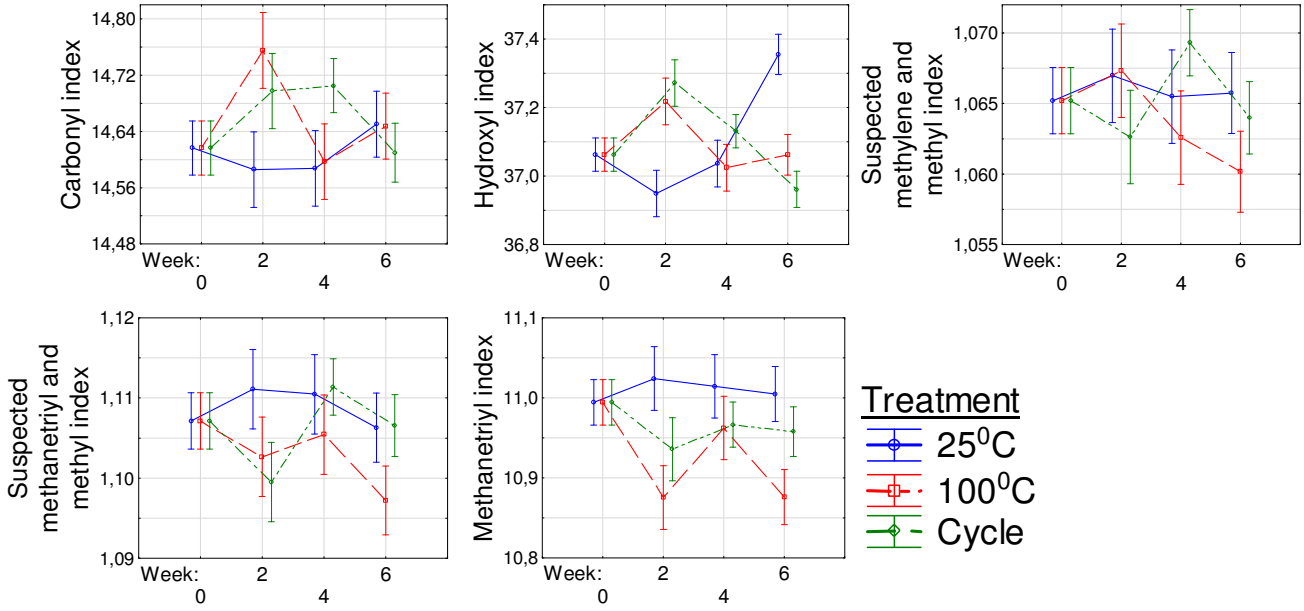

Figure 20: Mean graphs of FTIR indices for CPP under initial treatment

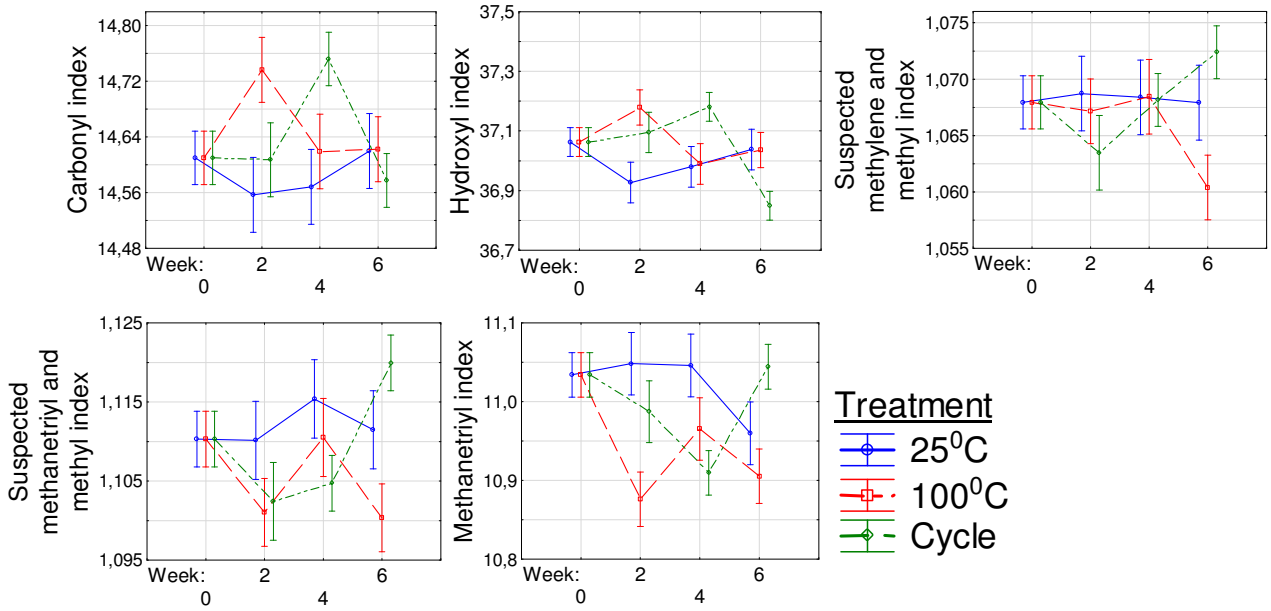

Figure 21: Mean graphs of FTIR indices for BPP under initial treatment

4.1.4 Analysis of variance

According to the ANOVA's on the individual factors, the initial treatment is significant for hardness, degree of crystallinity and all functional groups. The ANOVA results for the initial treatment can be seen in Table 8 (in Appendix C), where a 'p' value smaller than 0.05 refers to a significant effect. This means that the temperature had a statistically significant effect on all the results obtained (i.e. the null hypothesis is rejected, there is a significant variance in means between the 25˚C, 100˚C and cycle treatments). It also showed that the effects of time, plastic-type and initial treatment are independent of each other.

This effect was observed in the results as the higher temperatures tended to cause accelerated degradation (as predicted from kinetics and literature), as well as resulting in other reactions such as crystallization. The 100˚C initial treatment, as explained previously, caused a definitive crystallization in PET, followed by degradation, and is suspected of causing significant chemicrystallization in CPP and to some degree in BPP (although it is not significant in BPP). The cycling temperature appears to follow similar mechanisms as the 100˚C initial treatment, but not as substantial or significant. In contrast, the 25˚C treatment did not result in any significant variances, for all three plastics, which was anticipated since the degradation rate in normal or ambient conditions are extremely slow. Therefore, it was hypothesized that no significant degradation would occur this condition within six weeks.

Similarly, the plastic-type (i.e. PET vs CPP) and colour additive (i.e. CPP vs BPP) also proved to cause significant effects, as seen in the results and supported by the respective ANOVA's (see Table 9 and Table 10, pages 113 – 114, in Appendix C – ANOVA tables). The significant difference in plastic-type was anticipated as 100˚C exceeds the crystallization temperature for PET but the 25˚C treatment already exceeded the crystallization temperature for polypropylene. There was thus a significant difference in the variance of the degree of crystallinity between the plastic-types, which was supported by the difference in indices and hardness values which followed opposing trends, as discussed previously.

The effects of the colour additive were that the CPP initially had a slightly higher degree of crystallinity and hardness value. It is suspected to be due to the CPP being "purer" by not having the same additive as BPP. This allows the CPP molecular structure to be more crystalline. Although the more crystalline material generally exhibits less degradation (Izdebska & Thomas, 2016), it was not the observed case for the two lower temperature treatments. CPP exhibited greater increases in the degree of crystallinity and greater decreases in hardness along with similar trends in functional group indices when compared to BPP. It is theorized that this may be due to the additive added to BPP to prevent photo- and photo-oxidative degradation. It could be possible that the additive hinders the radical formation and is therefore also, to some lower extend, successful in hindering thermo-oxidative degradation or that the colour additive hinders the deterioration of the mechanical properties. However, for the 100˚C treatment, there was no significant difference between the two plastics for any index calculated from FTIR results. This combined with the crystallinity and hardness data suggests that the additive is de-activated at the high-temperature treatment, effectively nullifying its degradation prevention properties.

4.1.5 Investigating the effect of shape and size

An investigation into the magnitude and significance of the difference in degradation results because of shape or size was conducted. The FTIR results obtained from the samples of various shapes and sizes of BPP, CPP and PET are discussed below.

For the BPP samples, there were a few singular significant differences. The first of these was observed during the cycling treatment (as can be seen in Figure 22). The small circular shape exhibited a higher, and the large rectangular shape exhibited a lower, carbonyl index value where an increase in carbonyl

index is associated with degradation occurring. The large rectangular shape also exhibited a lower hydroxyl value at week four for the 25˚C and cycling treatment, but a higher hydroxyl and suspected methylene and methyl index value at week four for the 100˚C treatment.

Similarly, the large circular shape exhibited a higher hydroxyl index end value for the 25˚C treatment, where an increase in hydroxyl index is associated with the formation of degradation products. The small rectangular shape exhibits a lower suspected methyl and methanetriyl index tendency under the 25˚C treatment, during the first few weeks. Moreover, the small circular shape exhibited a lower methanetriyl index tendency at week four during cycling temperature treatment—both of which are associated with the formation of degradation products. The results are therefore random and not conclusive, suggesting that the period of the experiment was not long enough or the conditions not harsh enough to cause a significant distinction between the shapes.

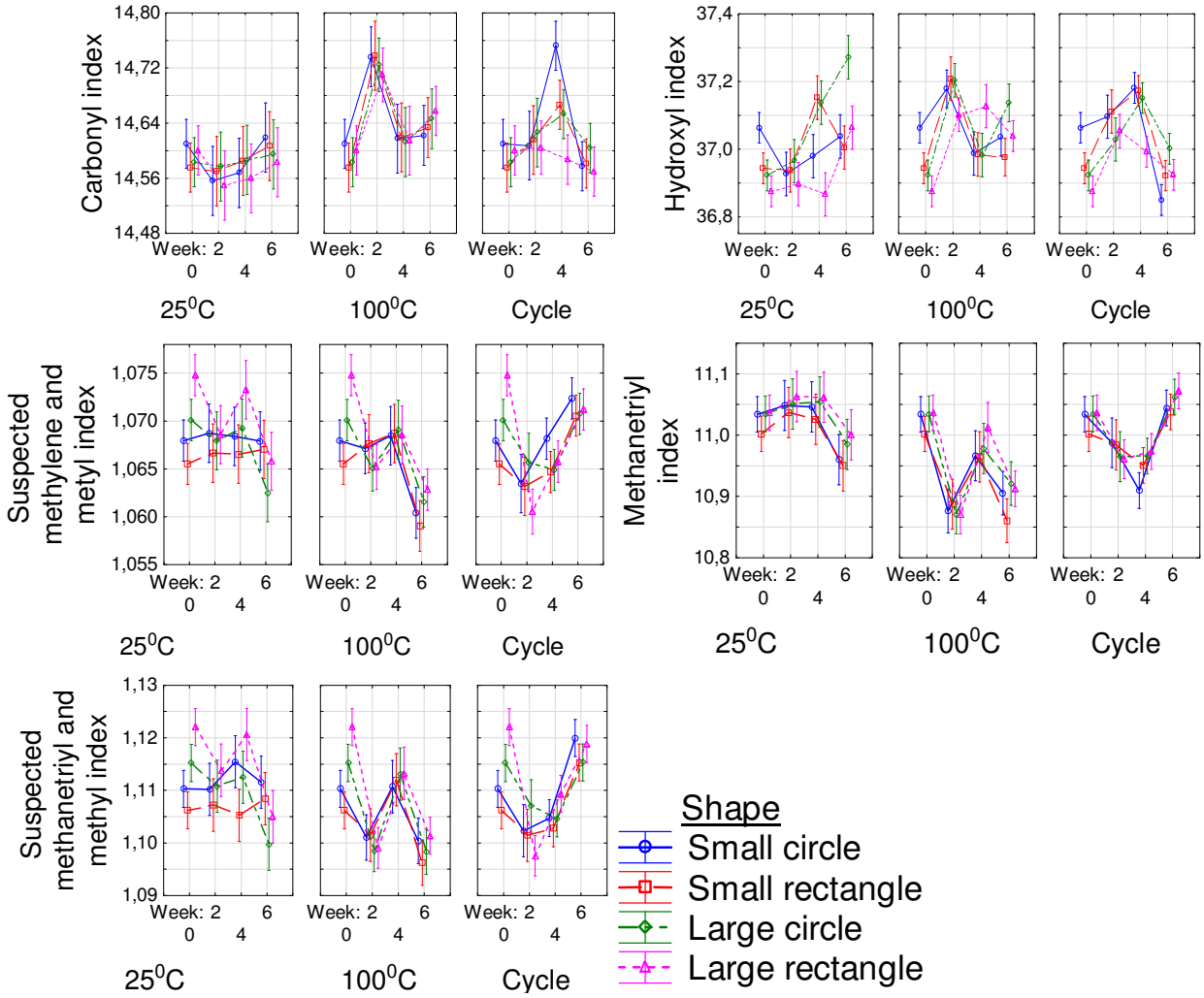

Figure 22: Mean graphs of FTIR indices for various shapes of BPP samples under initial treatment

For the CPP samples, the difference in trends was more consistent, with the smaller shapes exhibiting higher or tendencies to higher carbonyl and hydroxyl indices than the larger shapes. Moreover, the larger shapes exhibited higher suspected methyl and methanetriyl indices, especially the large rectangular

shape (as seen in Figure 23). Since increases in carbonyl and hydroxyl indices and decreases in suspected methyl, methylene and methanetriyl indices are associated with degradation, it appears as if the smaller shapes had undergone accelerated or increased degradation. The smaller shapes have a larger surface area to volume ratio, which is hypothesised to accelerate the degradation rate (Gewert *et al.*, 2015) and the observed results support this hypothesis. When comparing the two smaller shapes, there was no consistency on which one experienced greater or accelerated degradation, leading to the suggestion that six weeks is insufficient time to cause a significant distinction between the two shapes. However, should the time frame be extended, it is hypothesised that small rectangles will experience accelerated degradation since they have a higher surface area to volume ratio.

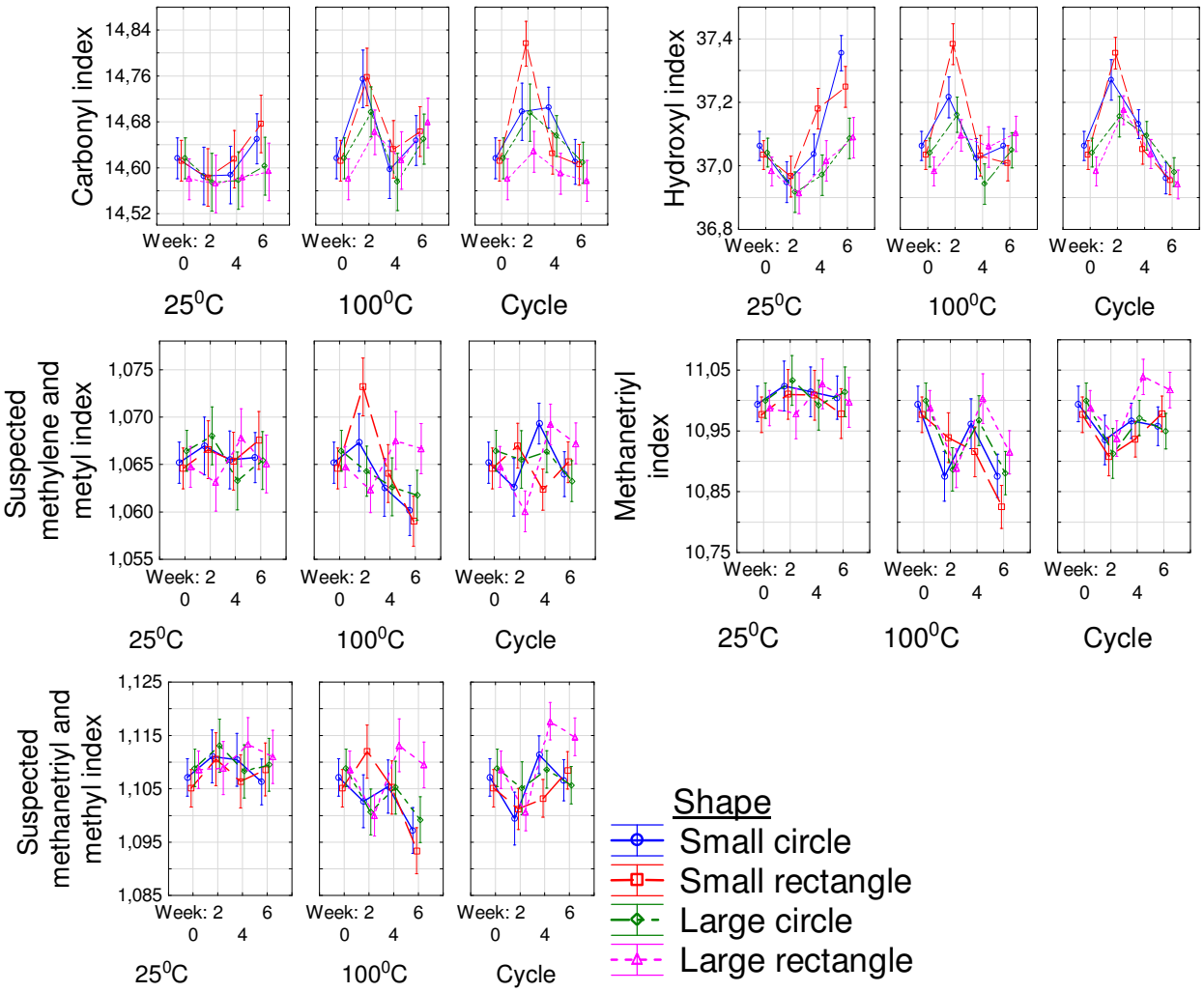

Figure 23: Mean graphs of FTIR indices for various shapes of CPP samples under initial treatment

Similar to BPP, the PET did not exhibit many significant differences between the various shapes and sizes, as can be seen in Figure 24. From the results in Figure 24, it appears as if the smaller PET shapes tended to result in lower hydroxyl and methylene indices when subjected to a treatment of 100˚C. However, as mentioned in 4.1.3, the decrease in the methylene index value at 100˚C is suspected of indicating crystallization rather than degradation. Nonetheless, it could still be an indication that the smaller shapes

experienced a greater or accelerated crystallization reaction and is hypothesised to replicate this phenomenon for degradation over a prolonged experiment as well.

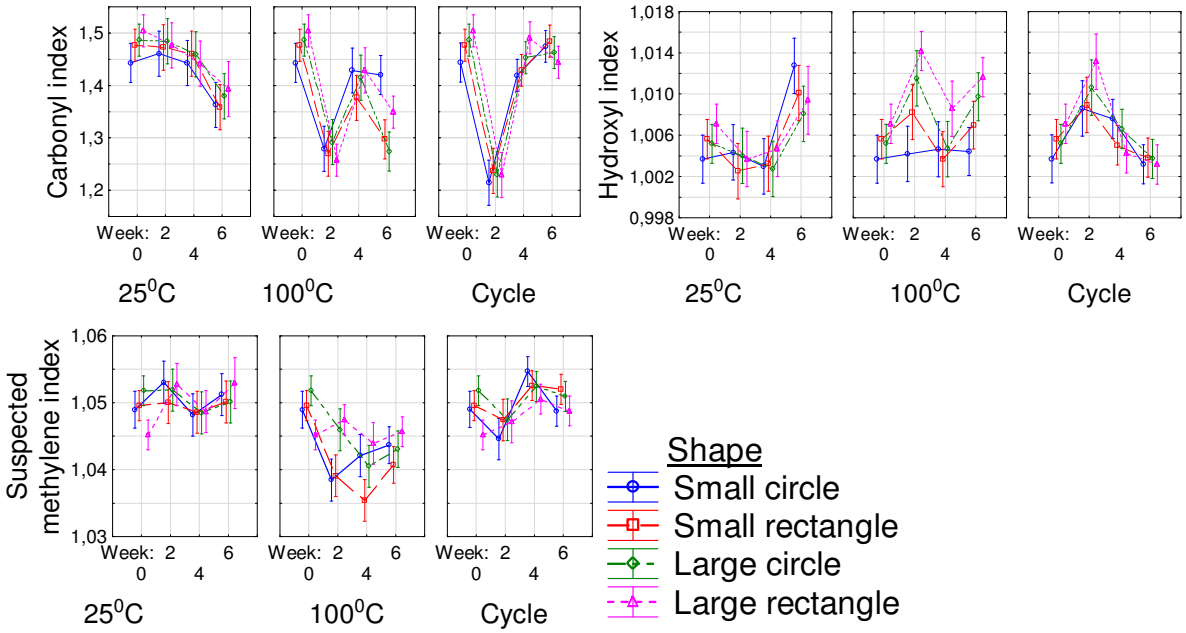

Figure 24: Mean graphs of FTIR indices for various shapes of PET samples under initial treatment

Understandably, CPP shapes were the only samples to exhibit an observable difference between the shape sizes, as from the previous section, it could be seen that CPP seems to be the most vulnerable to degradation. The results indicate that although it appears as if the smaller shapes undergo accelerated degradation, definitive conclusions on degradation rate with regards to shape could not be drawn. It is therefore advised to conduct another experiment on shapes that has a larger surface area to volume ratio difference or with harsher conditions and extend the experimental period.

4.2 Secondary experiments (Bench tests)

All bench tests were subjected to treatment while in seawater unless specifically stated that demineralised water (referred to as “fresh” water) was used. Also, in the bench tests samples that were not subjected to any of the three initial treatments will be referred to as “fresh” plastics.

4.2.1 BPP

4.2.1.1 Crystallinity

Figure 25 represents the variance in the degree of crystallinity for BPP samples during bench tests. It is observed that the degree of crystallinity, for samples subjected to the 60˚C treatment, regardless of the initial treatment, decreased significantly (between 2.5% ± 1.8 % and 3.7% ± 1.7 %). Similarly, for samples subjected to the 25˚C treatment, decreases or tendencies to decrease was observed (between 0.9% ± 1.8% and 3.1% ± 1.7%). At the same time, the lower radiance level of 65 W/m^2 (or UV2) exhibited no significant changes. The samples subjected to the high radiance of 130 W/m^2 (or UV1) exhibited

decreases in degree of crystallinity for fresh samples and samples initially treated at 25˚C (between 2% ± 1.6% and 1.5% ± 1.9%) and an increasing tendency for samples initially treated at 100˚C (about 1.3% ± 1.4%). This can be explained by the formation of a new peak on the DSC thermograms (see Figure 26), which is small enough at the moment to be irrelevant.

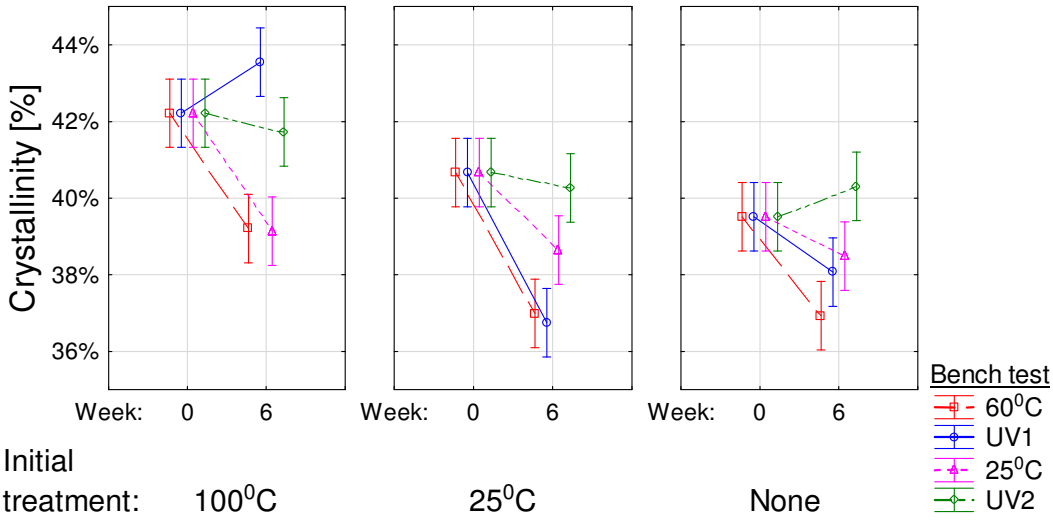

Figure 25: Mean graphs of percentage crystallinity for BPP bench tests

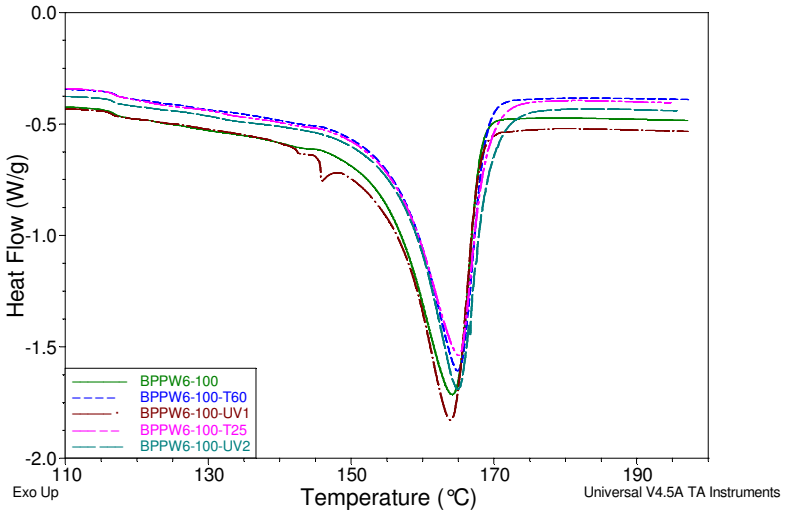

Figure 26: Thermograms for BPP initially treated at 100˚C before and after bench tests were completed

It was suspected that the BPP will exhibit slight or no degradation when subjected to UV radiance, as the colour additive hinders photooxidative degradation. Therefore, the insignificant changes in samples treated at 65 W/m^2 (or UV2) were anticipated. The tendency to increase (although not significant) in crystallinity for the higher UV radiance samples initially treated at 100˚C, is theorised to be due to the 100˚C treatment passivating the colour additive. This prevents the additive from hindering the photodegradation, which in turn, initiates chemicrystallization that results in slight crystallinity increases followed by significant decreases (Izdebska & Thomas, 2016; Rouillon *et al.*, 2016). The decreases in degree of crystallinity for the other 130 W/m^2 UV radiance treatments are theorised to be attributed to

causes similar to the temperature treatment since the UV radiance temperature would have been between 30°C and 40°C. One of the possible reasons for the decreases observed in Figure 25 is, therefore, that thermo-oxidative degradation occurred, through excessive crosslinks, chains scissions or other oxidation mechanisms. The degradation is expected to increase with an increase in temperature (Izdebska & Thomas, 2016; Gijsman, 2008). Thus the 60˚C treatment exhibiting the greatest decrease supports the degradation theory. Other possible reasons or contributions to the decreases in the degree of crystallinity are the increase of moisture absorption (Subramanian, 2017) and the saltwater; as Ma, *et al*. (2019) found that salt ions caused a weakening in the electrostatic repulsions of the molecular chains.

4.2.1.2 Hardness

Many studies found that during degradation hardness exhibits an increase preceding the decrease and that the observed trend is zig-zagging instead of linear (Izdebska & Thomas, 2016; Rouillon *et al*., 2016; O'Brine & Thompson, 2010; Signor *et al*., 2003). The BPP hardness data obtained from the bench tests see Figure 27, indicated that only the samples subjected to a temperature treatment of 60˚C exhibited any significant changes and that it was still in the first phase of increasing hardness. The samples subjected to 60˚C that were fresh exhibited an increase of 3.2% ± 2.4% and the samples initially treated at 100 ˚C exhibited an increase of about 4.8% ± 2.2% .Possible reasons why the other treatments did not exhibit any significant changes might be insufficient degradation or the softening or plasticizing effect of water on the polymer are at a rate similar to the degradation (Ghobadi, Marquardt, Zirdehi, Neuking, Varnik, Eggeler & Steeb, 2018; Andrady, 1990).

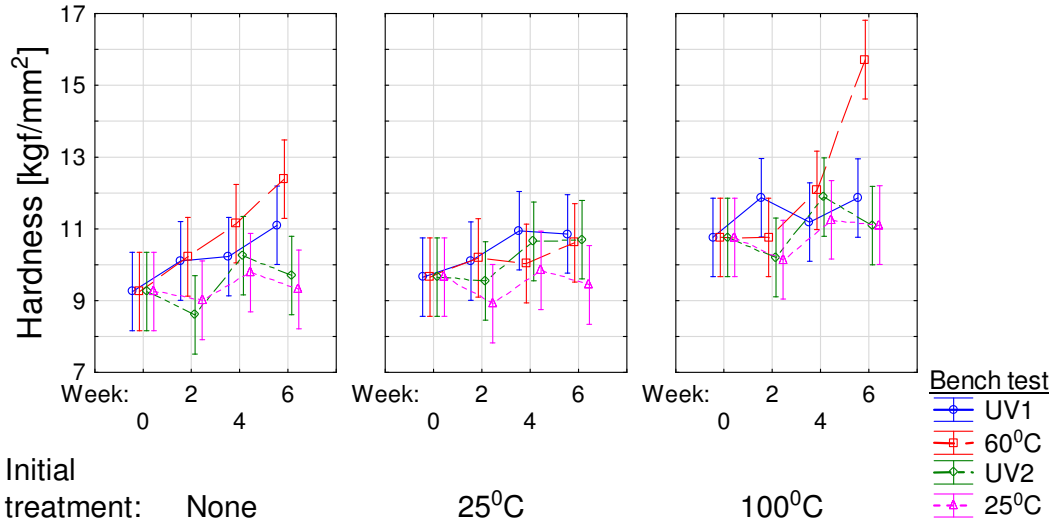

Figure 27: Mean graphs of hardness for BPP bench tests

4.2.1.3 FTIR indices

The BPP samples subjected to a UV radiation of 65 W/m^2 (or UV2) exhibited a few significant variances in indices over the course of the experiment (see Figure 28). The samples that did exhibit a significant variance was the samples subjected to initial treatment. The observed changes were slight increases at week two in the carbonyl and hydroxyl indices. Other variances were decreases in the suspected

methanetriyl, methylene and methyl indices at week four, followed by increases at week six, for the samples initially treated at 25˚C and fresh samples. As well as a significant increase in the methanetriyl index at week six, for samples initially treated at 100˚C. These indicate that degradation is occurring. However, when considering the amount and magnitude of variances, along with the hardness and crystallinity results (which exhibited no significant changes or degradation for the duration of the experiment), it is suggested that the degradation is extremely slow and not significant during six weeks.

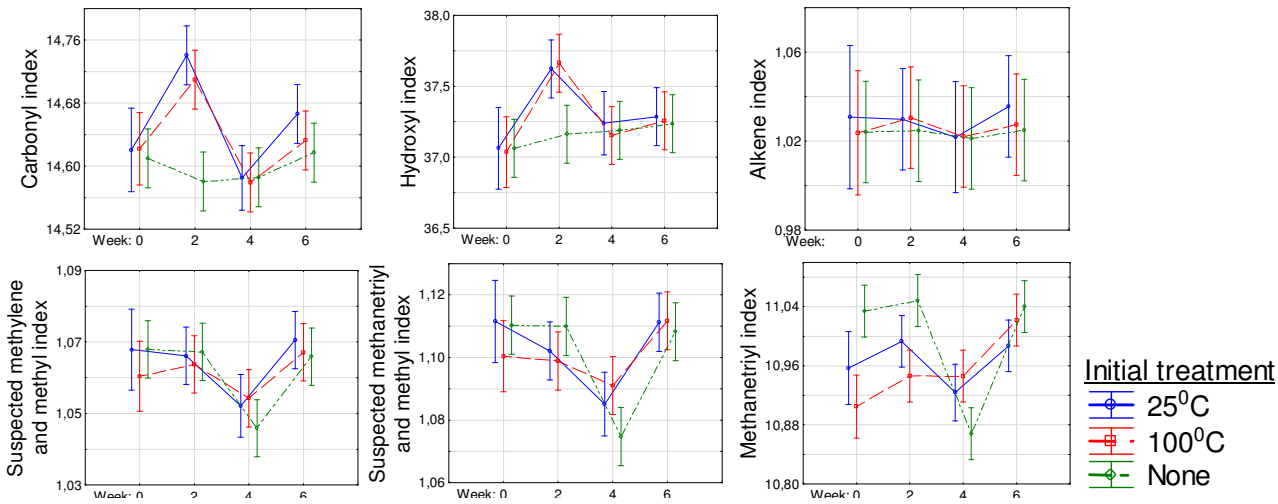

Figure 28: Mean graphs of FTIR indices for BPP bench tests subjected to 65 W/m^2 UV radiance

In Figure 29, the mean indices of BPP samples subjected to the 25˚C treatment are given. From these significant variances in the suspected methanetriyl, methylene and methyl indices during measurements at week four are observed, for fresh samples and samples initially treated at 25˚C. While increases in the carbonyl and hydroxyl indices are only observed at week six, for fresh samples and samples initially treated at 100˚C. It is hypothesised that this could be due to the 100˚C passivating the colour additive. It also indicates that the rate of oxidation degradation is very slow, as expected at low temperatures, since the primary products, generally used to signify oxidative degradation, only varies significantly at week six. The variances in the suspected methanetriyl, methylene and methyl indices, which signifies breakage of carbon-carbon bonds occurring (Kaczmarek *et al.*, 2004), during measurements of week two and four, is possibly due to degradation occurring via side-chain stripping, crosslinking or branching and is enhanced by the water absorption of the polymer (Ghobadi *et al.*, 2018). This supports the crystallinity results which suggest that slow, degradation is occurring, especially since crosslinking will cause a loss in degree of crystallinity and explain why hydroxyl and carbonyl indices do not form during the first stage of the experiment.

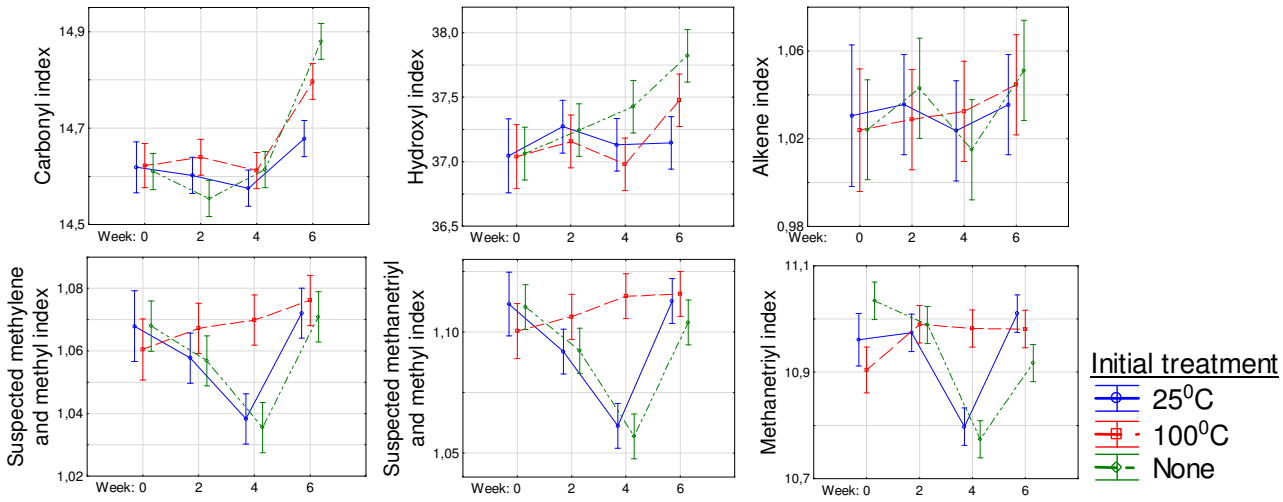

Figure 29: Mean graphs of FTIR indices for BPP bench tests subjected to 25˚C

The BPP samples subjected to the 130 W/m^2 UV radiance (or UV1) treatment had two different trends, as seen in Figure 30. The samples initially treated at 100˚C before being subjected to 130 W/m^2 UV radiance exhibited significant increases in carbonyl index, alkene index and hydroxyl index and significant decreases in the suspected methanetriyl and methyl indices at week two. This is consistent with changes expected during crosslinking, chain scission and oxidation, and is an indication that photo-oxidative degradation could have taken place as theorised. However, measurements at week four exhibited the reverse of this, even though most of the reverse changes are not significant. A possible theory is re-polymerization occurring from the alkenes produced by one of the degradation mechanisms. Studies have been completed indicating that recombination of macromolecules during UV-radiation treatment occurs and that polypropylene synthesis and copolymerization is achievable at atmospheric pressure, under a variety of temperatures from 20˚C – 45˚C (Zhang, Jiang, He, Fu, Xu & Fan, 2019; Liu, Niu, Li, & Dong, 2018; Naga, Sakai, Usui & Tomoda, 2010; Xio, Wang, Liu, Yu & Dong, 2008; Kaczmarek *et al*., 2004; Ye & Zhu, 2003). Therefore, it is speculated that due to the extended period, the temperature being between 30^{o}C and 40^{o}C and the pressure being around 1 atm, the possibility exists that the alkenes formed during degradation can recombine or react to re-polymerization or re-form polypropylene. The speculation is supported by the increase in crystallinity without the simultaneous decrease in hardness that generally accompanies the plasticizing effect, which could be due to the polymer rebuilding some of the previously degraded parts. However, another possibility is secondary reactions occurring, which utilises some of the products produced during degradation. It is also possible that the crystallinity results can be explained by chemicrystallization. Measurements at week six indicated a mixture of results usually associated with degradation mechanisms occurring and opposing trends, indicating that photo-degradation is continuing along with secondary reactions occurring.

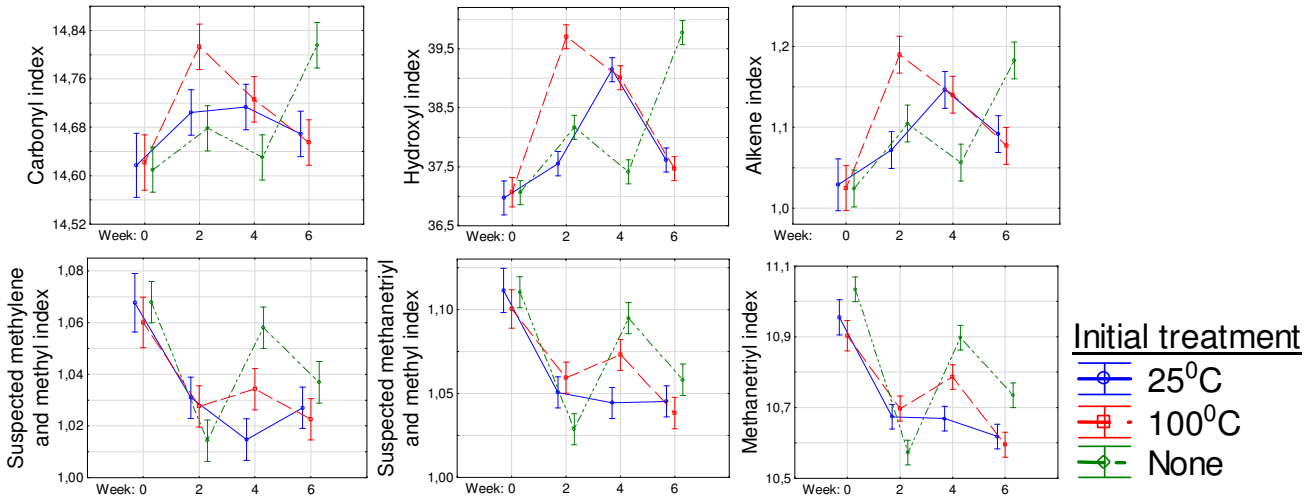

Figure 30: Mean graphs of FTIR indices for BPP bench tests subjected to 130 W/m^2 UV radiance

With regards to the fresh samples and samples initially treated at 25˚C of the BPP samples subjected to 130 W/m^2 UV radiance, the following was observed. Between the two, the fresh samples were the only samples to exhibit significant increases in the carbonyl index and only at week six. The fresh samples also exhibited significant increases in the hydroxyl and alkene indices at week two and week six. While the samples that were initially treated at 25˚C only exhibited a significant increase in the hydroxyl and alkene indices at week four. Followed by decreases, but with an overall increase at week six. This indicates that significant thermal- or photo-oxidative degradation is only observed at a later stage, and therefore occurs slowly.The suspected methanetriyl, methylene and methyl indices exhibit variances from week two already, for both. It indicates that breakage of carbon-carbon bonds take place, and thus that some form of degradation is occurring during that time (Kaczmarek *et al.*, 2004). Regarding all of the above-mentioned indices, it appears that degradation is occurring. This will support the observed decreases in crystallinity, although as previously stated these decreases can also be contributed to other factors such as the water absorption or salt ions (from the seawater) disrupting the electrostatic repulsions of the molecular chains (Ma *et al.*, 2019; Subramanian, 2017).

The BPP samples subjected to the 60˚C treatment, see Figure 31, exhibited increases in carbonyl, hydroxyl and alkene indices and decreases in suspected methanetriyl and methyl indices during the first few weeks of the experiment; indicating that thermo-oxidative degradation is occurring. Subsequently, some variances and various ups and downs are then observed. This could be similar to the re-polymerization explained for samples initially treated at 100˚C and subjected to 130 W/m^2 UV radiance. Another theory is that the variances in the different indices are due to secondary reactions occurring which utilizes some of the products produced during degradation. This theory is stated to be more likely because the alkene indices exhibits a steady upward trend without significant decreases, along with the crystallinity exhibiting significant decreases and the hardness exhibiting significant increases.

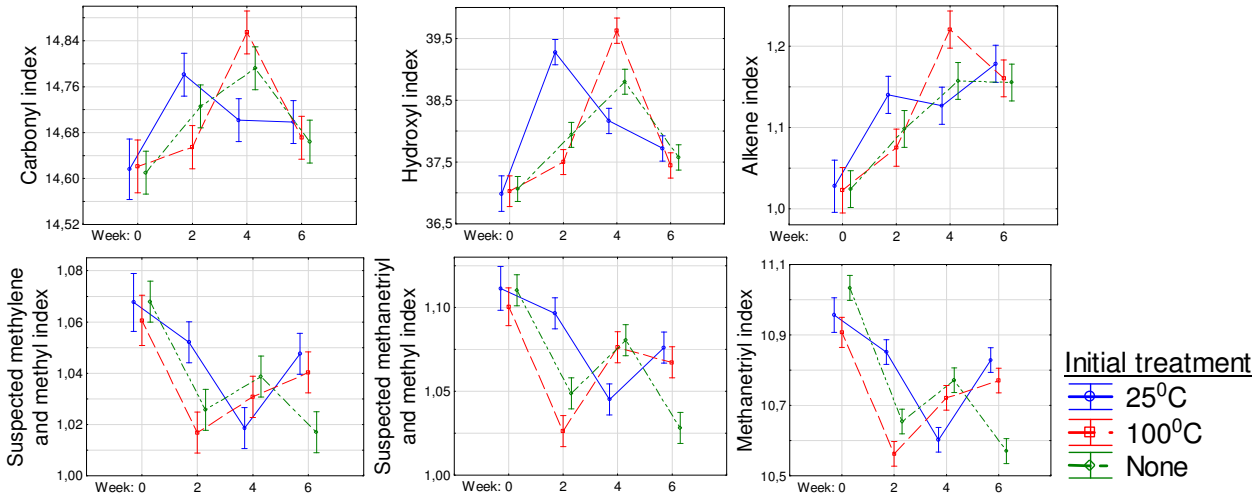

Figure 31: Mean graphs of FTIR indices for BPP bench tests subjected to 60˚C

4.2.2 CPP

4.2.2.1 Crystallinity

The CPP samples subjected to the 60˚C treatment exhibited decreases (between 2.9% ± 1.5% and 3.4% ± 1.8%) in the degree of crystallinity, regardless of the initial treatment, as seen in Figure 32, which could be an indication that significant degradation has occurred. At the same time, the CPP samples subjected to the 25˚C treatment exhibited a decrease (about 2.3% ± 1.8%) for samples initially treated at 100˚C, and tendencies (although not significant) to decrease for the other initial treatments. This indicates that degradation occurred at 25˚C, even if the rate was slower than at 60˚C. This was anticipated, since degradation rate should increase with temperature, based on reaction kinetics.

The CPP samples subjected to the lower UV radiance of 65 W/m^2 exhibited no significant variances, indicating that the photo-oxidation degradation rate was too slow to observe significant changes in six weeks. While most of the CPP samples subjected to the high UV radiance of 130 W/m^2 exhibited significant increases in the degree of crystallinity (between 0.8% ± 1.3% and 5.3% ± 1.5%). As previously stated the crystallinity is expected to increase during the first stage of degradation before exhibiting a decrease. Therefore, this can be an indication of degradation during that time.

From Figure 32, it is noted that CPP samples initially treated at 25˚C did not exhibit a significant increase in the degree of crystallinity under the 130 W/m^2 UV radiance (or UV1). Therefore, the thermogram of the samples was consulted. Comparing the thermograms of the samples initially treated at 25˚C (Figure 34), and the fresh samples (Figure 33), it can be observed that under 130 W/m^2 UV radiance (or UV1) similar changes occurred. It is therefore suspected that the reason the degree of crystallinity did not exhibit an increase, is due to the %crystallinity calculation method since significant differences in all CPP samples subjected to 130 W/m^2 can be observed in the thermograms.

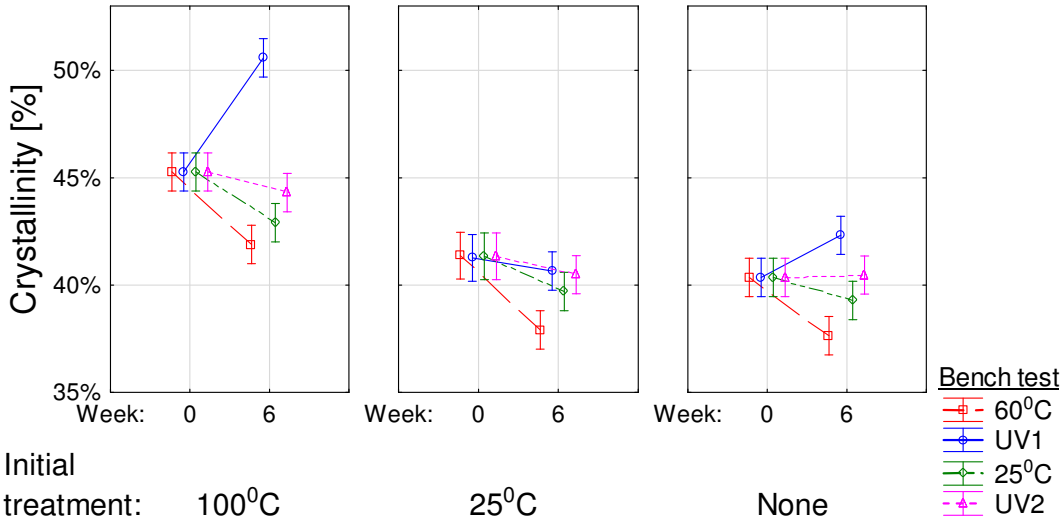

Figure 32: Mean graphs of percentage crystallinity for CPP bench tests

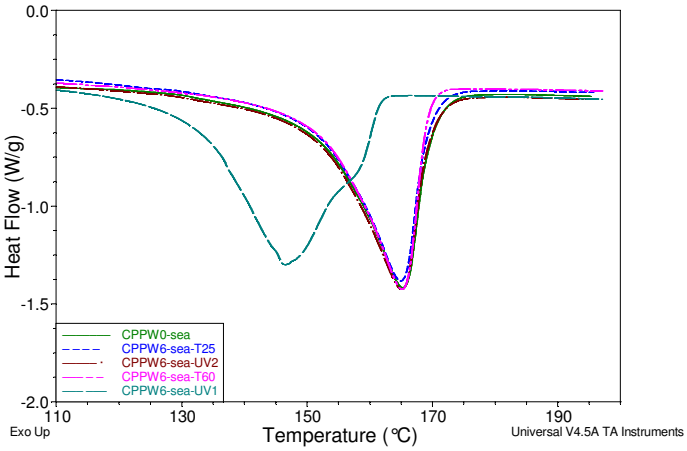

Figure 33: Thermograms for CPP not subjected to initial treatment before and after bench tests were completed

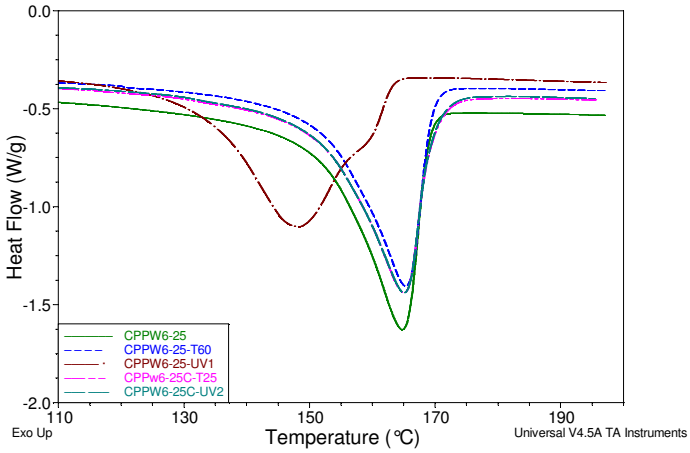

Figure 34: Thermograms for CPP initially treated at 25˚C before and after bench tests were completed

4.2.2.2 Hardness

The hardness data, as seen in Figure 35, supported the theories from the crystallinity data. Significant increases in hardness (between 2.2% ± 2% and 3.5% ± 1.9%) preceding decreases (between 2.2% ± 2.1% and 4.7% ± 2%) in hardness was observed for all samples subjected to 130 W/m^2 UV radiance (or UV1). The decrease was accompanied by formation of a network of cracks on the surface, as seen in Figure 36. This is in correspondence with degradation studies that found the ultimate decrease in hardness to be accompanied by crack formation on the surface (Rouillon *et al.*, 2016). The CPP was the only plastic that exhibited this visible network of cracks on the surface within 6 weeks.

Similar to the BPP data, the CPP samples subjected to the 25˚C and 65 W/m^2 UV radiance (or UV2) treatments did not exhibit significant variances. Even though a tendency to increase (less than 2%) was observed for the CPP samples subjected to the 65 W/m^2 UV radiance (or UV2) treatments. The increasing tendency was anticipated since polypropylene is very susceptible to photodegradation and the CPP does not contain the same colour additive as BPP to prevent the photodegradation.

The CPP samples subjected to the 60˚C treatment also behaved similarly to the BPP data. They exhibited increases of 4.7% ± 2% and 2% ± 1.8%, at week six for the 100˚C samples and samples that were not subjected to initial treatment. This is in correlation with the crystallinity data that exhibited significant changes and degradation for the UV1 and 60˚C treatments and little or no degradation for the UV2 and 25˚C treatment.

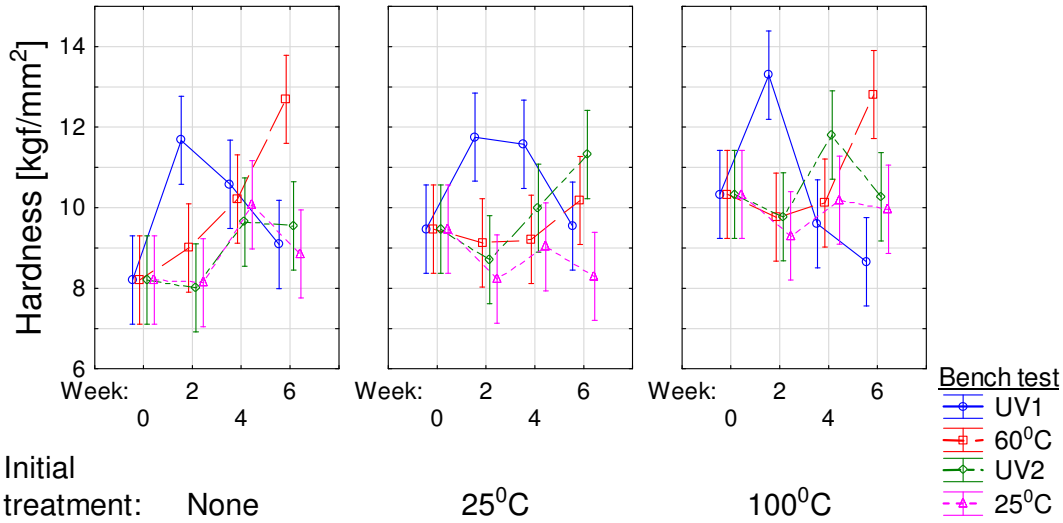

Figure 35: Mean graphs of hardness for CPP bench tests

Figure 36: Photo of the surface cracks on the CPP sample subjected to 130 W/m^2 UV radiance

4.2.2.3 FTIR indices

The CPP samples subjected to a UV radiation of 65 W/m^2 (or UV2), see Figure 37, exhibited almost no significant changes in indices over the course of the experiment, similar to the BPP data. The indices that did exhibit significant changes were some of the suspected methanetriyl, methylene and methyl indices, for the fresh samples and samples initially treated at 25˚C. The variances were at week four, around the same time the hardness started exhibiting an increasing tendency (even though not significant). This indicates that degradation by breakage of carbon-carbon bonds are occurring (Kaczmarek *et al.*, 2004), and possibly by crosslinking which is enhanced by the water absorption of the polymer (Ghobadi *et al.*, 2018). It signifies that, although reactions are occurring that might be degradation, the degradation is too slow to be significant and notable within six weeks. Therefore, it supports the hardness and crystallinity results, that exhibited no significant variances or degradation for the duration of the experiment.

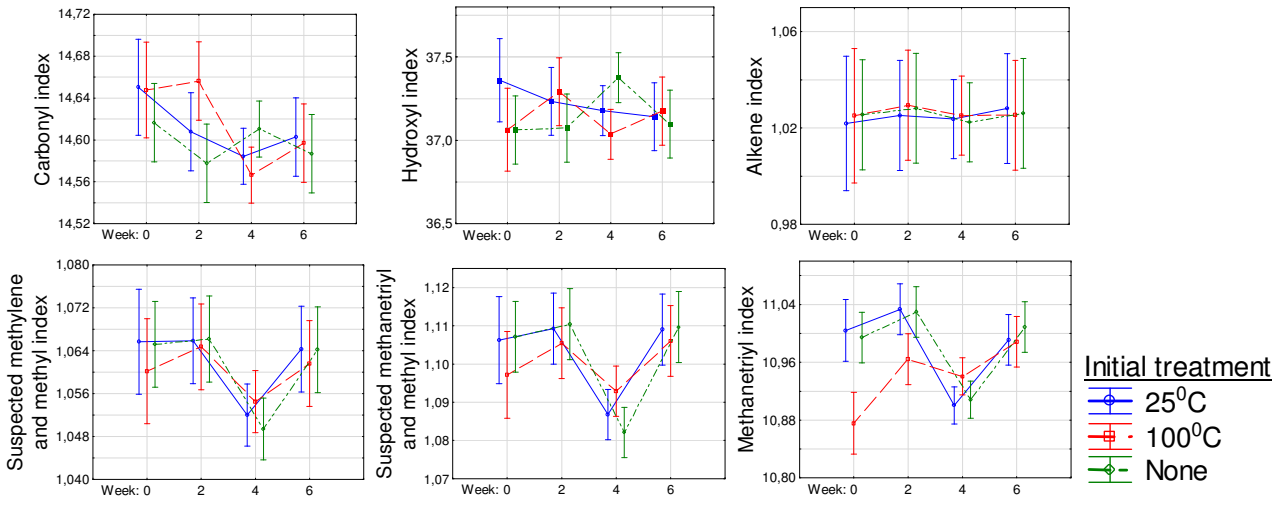

Figure 37: Mean graphs of FTIR indices for CPP bench tests subjected to 65 W/m^2 UV radiance

The CPP samples subjected to the temperature treatment of 25˚C, see Figure 38, also exhibited a few significant changes in indices throughout the experiment. The samples that exhibited significant variances in the primary expected oxidative degradation products were the fresh samples. Additionally, the exhibited increases in carbonyl and hydroxyl groups were only at week six. This signified the degradation

rate to be very slow. The suspected methanetriyl, methylene and methyl indices exhibited significant variances from week two onwards where the fresh samples and the samples initially treated at 25˚C exhibited initial decreases followed by increases.

In contrast, the samples initially treated at 100˚C exhibited a steady increase. It is suspected that this could be attributed to the degradation products formed during the 100˚C initial treatment, which promotes degradation and instigates secondary reactions. This theory would also support the observed crystallinity trend, with the samples initially treated at 100˚C exhibiting the greatest crystallinity decrease.

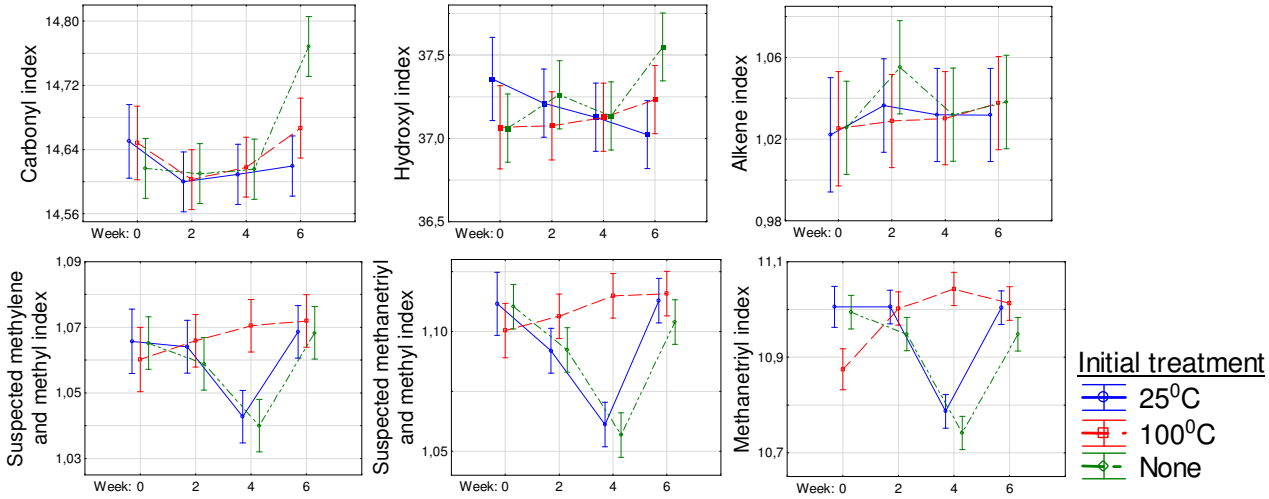

Figure 38: Mean graphs of FTIR indices for CPP bench tests subjected to 25˚C

The CPP samples subjected to the temperature treatment of 60˚C, see Figure 39, exhibited increases in alkene, carbonyl and hydroxyl indices over the first four weeks. In correspondence, the suspected methanetriyl and methyl indices exhibited decreases during the start of the experiment. This leads to the assumption that thermo-oxidative degradation is occurring. However, during week four and six, the carbonyl and hydroxyl indices exhibit a downward trend while the methanetriyl and methyl indices exhibit increasing tendencies.

Since the fresh samples and the samples initially treated at 100˚C also exhibit a decrease in alkene indices during that time, it could be an indication of re-polymerization; similar to the BPP data and with similar motivations regarding temperature and pressure. However, due to the samples initially treated at 25˚C not exhibiting a similar decrease in alkene indices during that time, the re-polymerization theory is deemed unlikely. Another theory is that the variances in trends are due to secondary reactions occurring. This is more probable, as it is supported by the crystallinity and hardness data, which indicates significant degradation occurring.

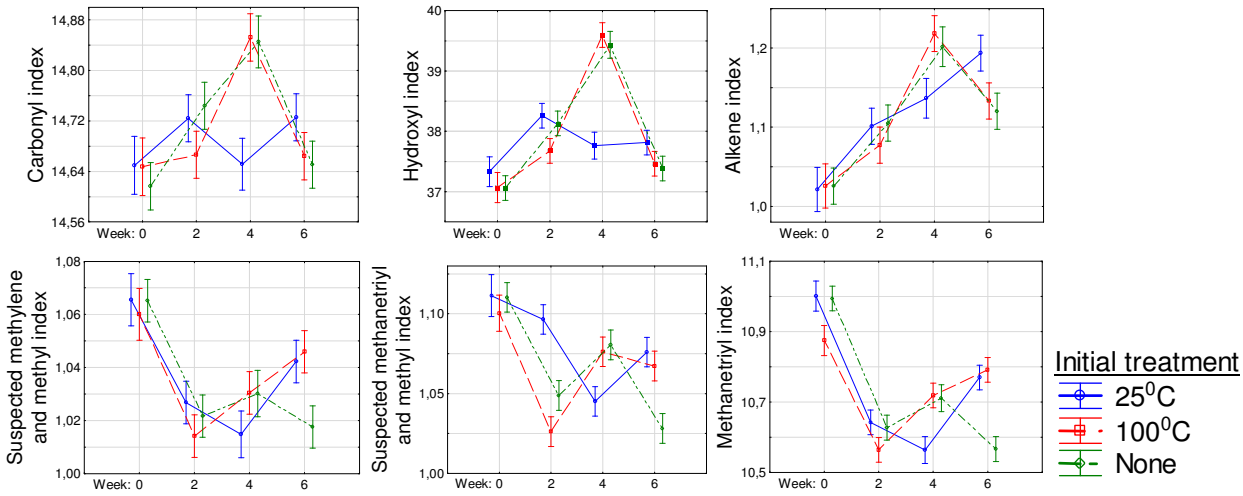

Figure 39: Mean graphs of FTIR indices for CPP bench tests subjected to 60˚C

Subjected to 130 W/m^2 UV radiance treatment (or UV1), see Figure 40, great variances in indices corresponding with photo-oxidative degradation was anticipated, since the hardness, DSC and physical data of the CPP samples under this condition exhibited degradation. The fresh samples and samples initially treated at 100˚C exhibited increases in alkene, carbonyl and hydroxyl groups during the first four weeks. This is in correlation with results expected from photo-oxidative degradation mechanism and indicates degradation has occurred as expected and therefore supports the hardness, DSC and physical data. While the samples initially treated at 25˚C exhibited no significant variances. This was surprising, since, with regards to hardness results, degree of crystallinity and suspected methanetriyl, methylene and methyl indices the samples initially treated at 25˚C exhibited similar trends to both the fresh samples and samples initially treated at 100˚C.

For all samples, the suspected methanetriyl, methylene and methyl indices exhibited decreases during the first few weeks, as well as ultimate overall decreases, which is in correlation with results expected from the photo-oxidative degradation mechanism. Therefore, the crystallinity, hardness and suspected methanetriyl, methylene and methyl indices indicate that photo-oxidative degradation has occurred. The fact that the 25˚C initially treated samples did not exhibit significant carbonyl, hydroxyl and alkene indices variances, therefore, suggests that a possible error in the analysis at week four has occurred, or the position in the UV chamber resulted in inadequate UV radiance.

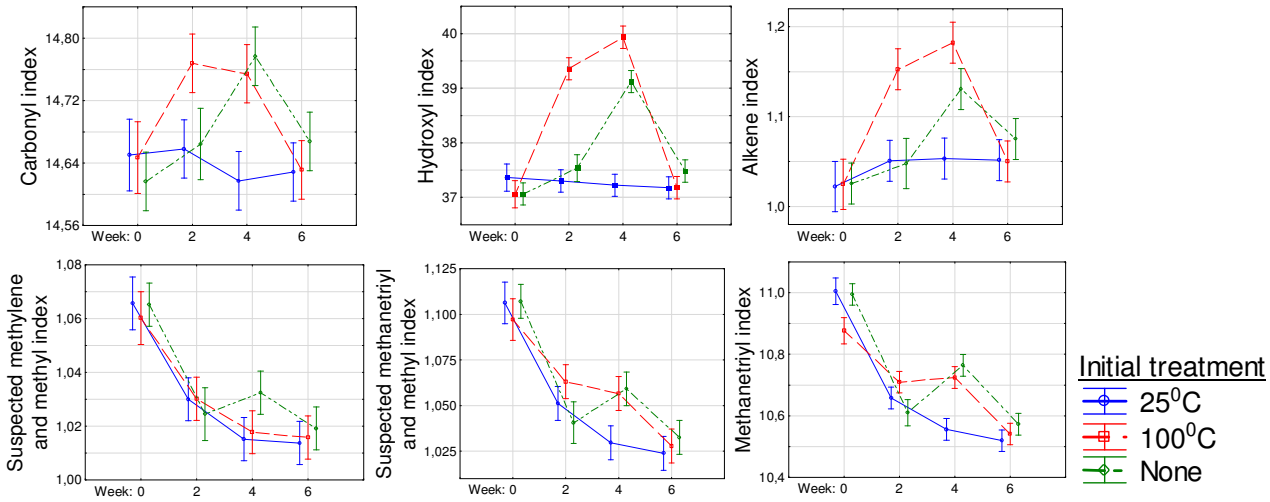

Figure 40: Mean graphs of FTIR indices for CPP bench tests subjected to 130 W/m^2 UV radiance

4.2.3 PET

4.2.3.1 Crystallinity

From Figure 41, it can be observed that the only crystallinity changes that were significant for PET, was the increases exhibited by the samples subjected to the 60˚C treatment that were not subjected to an initial treatment of 100˚C (with increase of about 4.7% ± 1.1% and 5.1% ± 1.2%). It is theorised that this is because of, similar to the initial cycling temperature treatment, some form of crystallization occurs at that temperature. And since the samples initially treated at 100˚C already underwent that crystallization it does not exhibit a similar increase. Another possibility is that the increase can be attributed to the plasticization effect of water or hydrolysis; and that it is only significant at the high temperature and less crystalline material since heat increases the water absorbance rate and crystalline regions hinder water absorbance (and thus hydrolysis) (Gok, 2016; Gewert *et al.,* 2015).

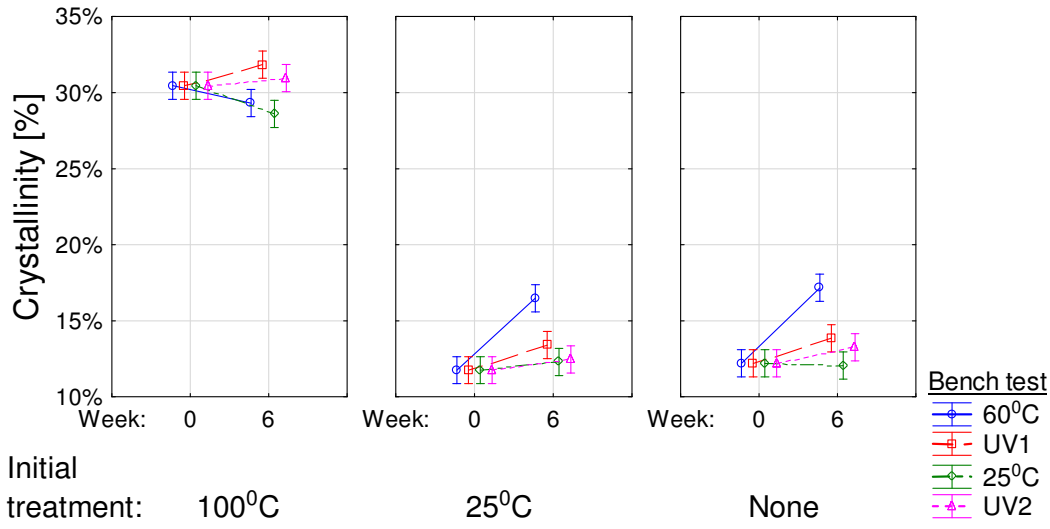

Figure 41: Mean graphs of percentage crystallinity for PET bench tests

4.2.3.2 Hardness

The hardness data, given in Figure 42, exhibited increases (between 2.2% ± 2.2% and 3.4% ± 1.3%) for all 65 W/m^2 UV radiance (or UV2) treatments. While the higher radiance level of 130 W/m^2 UV radiance (or UV1) treatments only exhibited a significant increase (about 2.25% ± 2.3%) for samples initially treated at 100˚C. Similarly, the samples subjected to the 25˚C treatment also only exhibited a significant increase (of about 3.5% ± 2.2%) for samples initially treated at 100˚C. While samples subjected to 60˚C exhibited increases (about 2.6% ± 2.3%) for fresh samples, and an increase (of about 4.1% ± 2.1%) preceding a decrease (of about 5.5% ± 2%) for samples initially treated at 100˚C. This trend is in correspondence with literature that found hardness increases initially before decreasing during degradation (Gok, 2016; Izdebska & Thomas, 2016; Rouillon *et al*., 2016; O'Brine & Thompson, 2010; Signor *et al*., 2003).

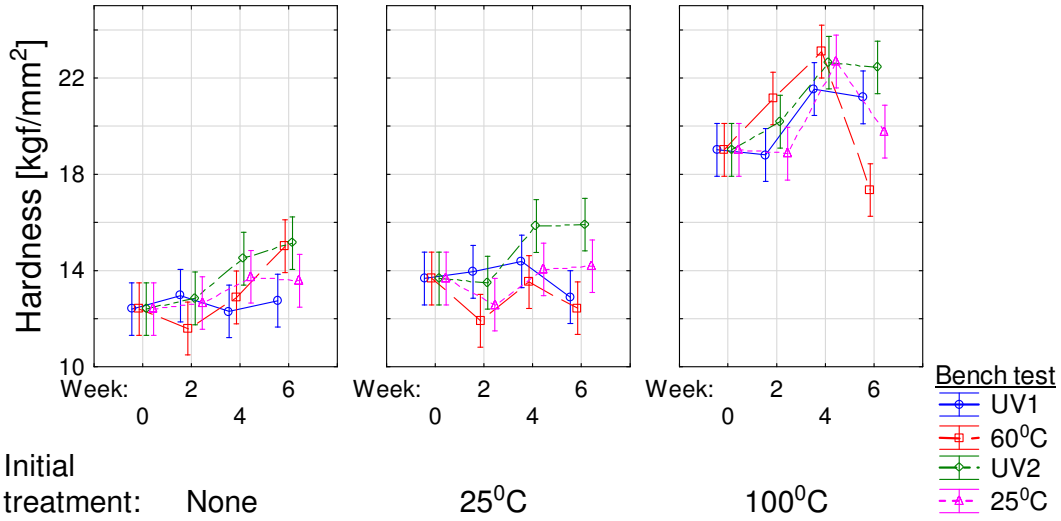

Figure 42: Mean graphs of hardness for PET bench tests

4.2.3.3 FTIR indices

It is difficult to gauge reactions from the FTIR data since PET has a complex molecular structure, and there are various mechanisms with different products that can occur for the same degradation type. During the bench tests, there is also the possibility of various degradation types being initiated and most of the time the degradation is due to a combination of the various types. It is also completely possible for intermediate products from the various mechanisms to interact with each other and form unanticipated products, causing the results to follow bewildering trends, as well as for secondary reactions to occur that consumes products usually formed during degradation. Therefore, when these trends are seen, it is not necessarily in contradiction with literature or expected trends, it might have occurred due to any of the reasons mentioned above. Therefore, a trend opposite to what was expected can also be an indication of degradation.

From PET samples subjected to the high UV radiance treatment of 130 W/m^2 (see Figure 43), it was observed that the hydroxyl indices increases sharply over the first four weeks followed by a steep decline, for the samples initially treated at 100˚C. While for the other samples, it increases sharply over the first

two weeks, followed by declines in the samples initially treated at 25˚C and a decrease preceding an increasing tendency for the fresh samples. The increase in hydroxyl index is an excellent indication of degradation occurring – and even though it can be contributed to all kinds of degradation, the greatest contributor is probably hydrolysis. The decrease in hydroxyl index can be contributed to secondary reactions (like the formation of CO and CO_2 gasses), the extraction of the hydroxyl groups by the surrounding water as found by Sugiura, Mitsuoka, Murase, Ueda (2000) and Cao (2016), or it could indicate that the amorphous region has been degraded and the crystalline region has been reached. This would act as a barrier for water absorption and thus hydrolysis and lower the photo-oxidation rate.

For PET samples initially treated at 100˚C and subjected to 130 W/m^2 UV radiance, it was observed that the hydrolysis rate is lagging, this is because the degradation products formed during the initial treatment does not promote hydrolysis, only oxidative degradation. The carbonyl groups exhibited a declining hyperbolic declining trend for samples initially treated at 100˚C or 25˚C, with 25˚C reaching its vertex point much more quickly, and a decrease preceding an increase for the fresh samples. The decrease in the carbonyl index indicates that oxidative degradation is occurring and that it is most likely via chain scission. A possible reason for the increase in the carbonyl index is the formation of carboxylic acid end groups, that can form during hydrolysis, crosslinking and auto-oxidation.

A decrease in the methylene index is anticipated under high UV radiance (as has been subjected to) as it indicates loss of carbonyl groups. The methylene index exhibited a steady decrease for both the 100˚C and 25˚C initial treated samples. Therefore, it corresponded with the trend observed in the carbonyl index. While the fresh samples exhibited a decrease in the first few weeks and an increase at week six, the increase could be a possible indication of hydrolysis dominating the degradation – and this theory is supported by the fresh samples' increasing hydroxyl index tendency at week six.

It has been stated that the 975 cm^{-1} region, linked to the "asymmetric stretching of the trans oxy-ethylene group in the ethylene glycol unit", is favoured by the crystalline regions. While the 1040 cm^{-1} region, linked to the "asymmetric stretching of the gauche oxy-ethylene group in the ethylene glycol unit", is favoured by the amorphous region (Gok, 2016; Scheirs & Gardette, 1997). A decrease in the index at 1040 cm^{-1} with a simultaneous increase in the index at 975 cm^{-1}, therefore, indicates a transition from amorphous to crystalline structure and thus an increase in the degree of crystallinity. Similarly, the 845 cm^{-1} region is linked to the trans form of the "CH_2 rocking of ethylene glycol", in comparison the 900 cm^{-1} region is linked to the gauche form of the "CH_2 rocking of ethylene glycol". Again, the trans form is favoured by the crystalline regions and the gauche form by the amorphous regions (Gok, 2016). The ethylene glycol unit is exceptionally susceptible to degradation. Thus, these indices should be good indications of degradation having occurred (Gok, 2016). Increases in the trans groups of the above mentioned can be linked-to photo- or thermal-oxidative degradation with chain scissions in the mechanism, while a decrease will indicate that the photo- or thermal-oxidative degradation is disturbing the crystalline region (Gok, 2016).

From the data obtained it would appear as if the 845 cm^{-1} region is a more sensitive index to use to obtain information about the crystallinity. Since the 845 cm^{-1} region exhibited a significantly higher index for the more crystalline PET (samples initially treated at 100˚C) at the start of the experiment and for the samples that did not undergo significant degradation.

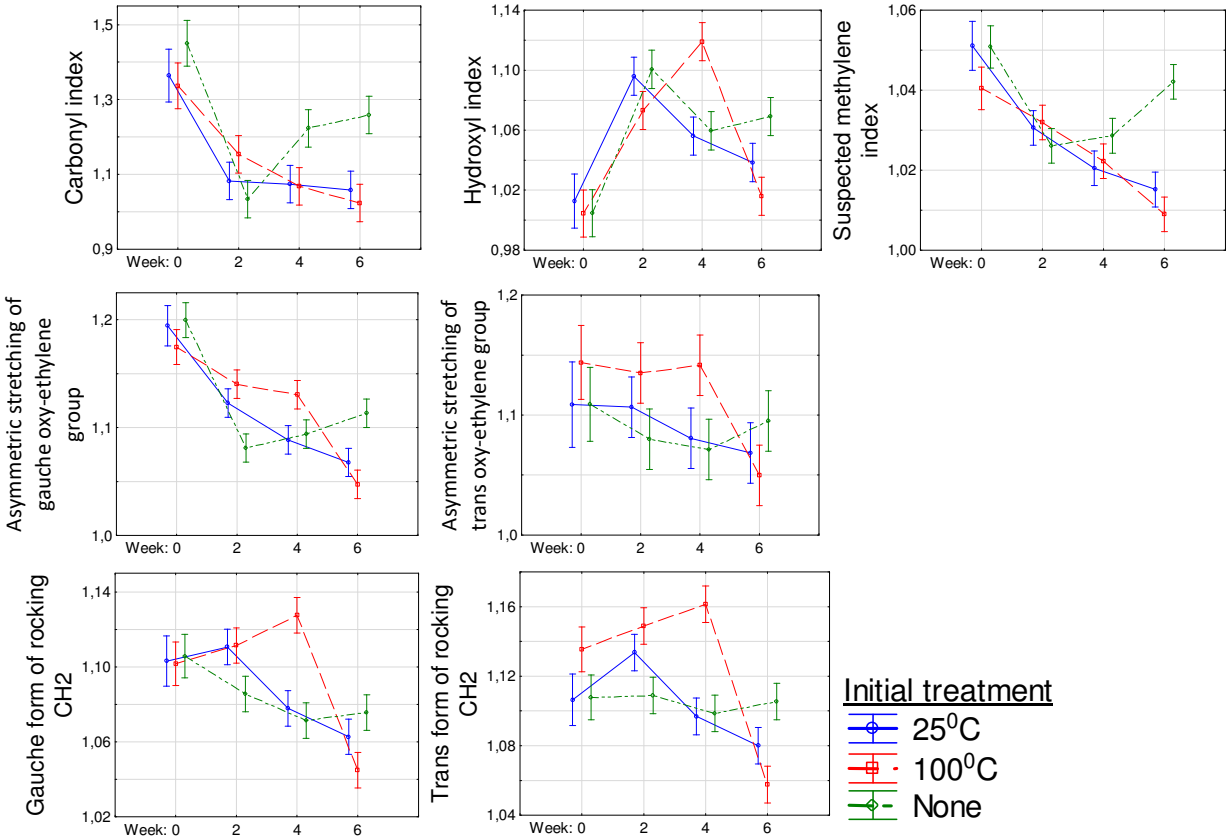

Figure 43: Mean graphs of FTIR indices for PET bench tests subjected to 130 W/m^2 UV radiance

Further investigation into the samples subjected to the high UV radiance showed that the index linked to the trans form of rocking ethylene glycol increased before exhibiting decreases, along with decreases in the index linked to the gauche form. This is an indication that degradation has occurred and would support the crystallinity data that tended to increase, but not significantly, as the FTIR data indicated that the crystallinity first increased and then decreased. The asymmetric stretch of the trans oxy-ethylene group, exhibited no significant differences until week six, in which case a significant decrease in this index for samples initially treated at 100˚C was observed. However, the gauche form had a steady decrease throughout the experiment. This indicates that the amorphous region is firstly degraded before the crystalline region undergoes degradation, which is in correspondence with literature that stated the amorphous region degrades more readily than the crystalline region (Izdebska & Thomas, 2016). This supports the idea formed from the hydroxyl index that the amorphous region has been degraded first and that the crystalline region only started degrading after week four. Understandably, only samples initially treated at 100˚C exhibit significant decreases since these samples have less amorphous regions due to the crystallization effect of the 100˚C treatment. The trend in the asymmetric stretch of trans oxy-

ethylene group index also supports the crystallinity data that exhibited no significant variances, since the index decreased only during the last stretch of the experiment. All of these indicate that photo- or thermal-oxidative degradation had occurred.

For samples subjected to the high-temperature treatment of 60˚C, see Figure 44, it was observed that the carbonyl index followed a zig-zag trend, with a decrease preceding an increase and ending in another decrease. The suspected methylene index follows a similar trend to the carbonyl group, as expected since a decrease in the methylene index is usually an indication of a decrease in carbonyl groups (Gok, 2016). Increases in carbonyl and methyl indices can occur during oxidative degradation, while the decreases in carbonyl and methyl indices can be indications of any degradation methods, especially hydrolysis, or it can indicate the occurrence of crystallization (Gok, 2016).

Hydroxyl indices exhibited steady increases throughout the experiment for samples initially treated at 25˚C and increases preceding decreases for the fresh samples and samples initially treated at 100˚C. Although increases in hydroxyl index can be contributed to any degradation mechanism, Gok (2016) found that hydroxyl index increased significantly only when hydrolysis occurred. Therefore, the observed trend is most likely an indication that hydrolysis is occurring continuously throughout the experiment. Decreases in the hydroxyl index are suspected to be due to similar reasons as the hydroxyl index decrease observed for the samples subjected to 130 W/m^2 UV radiance.

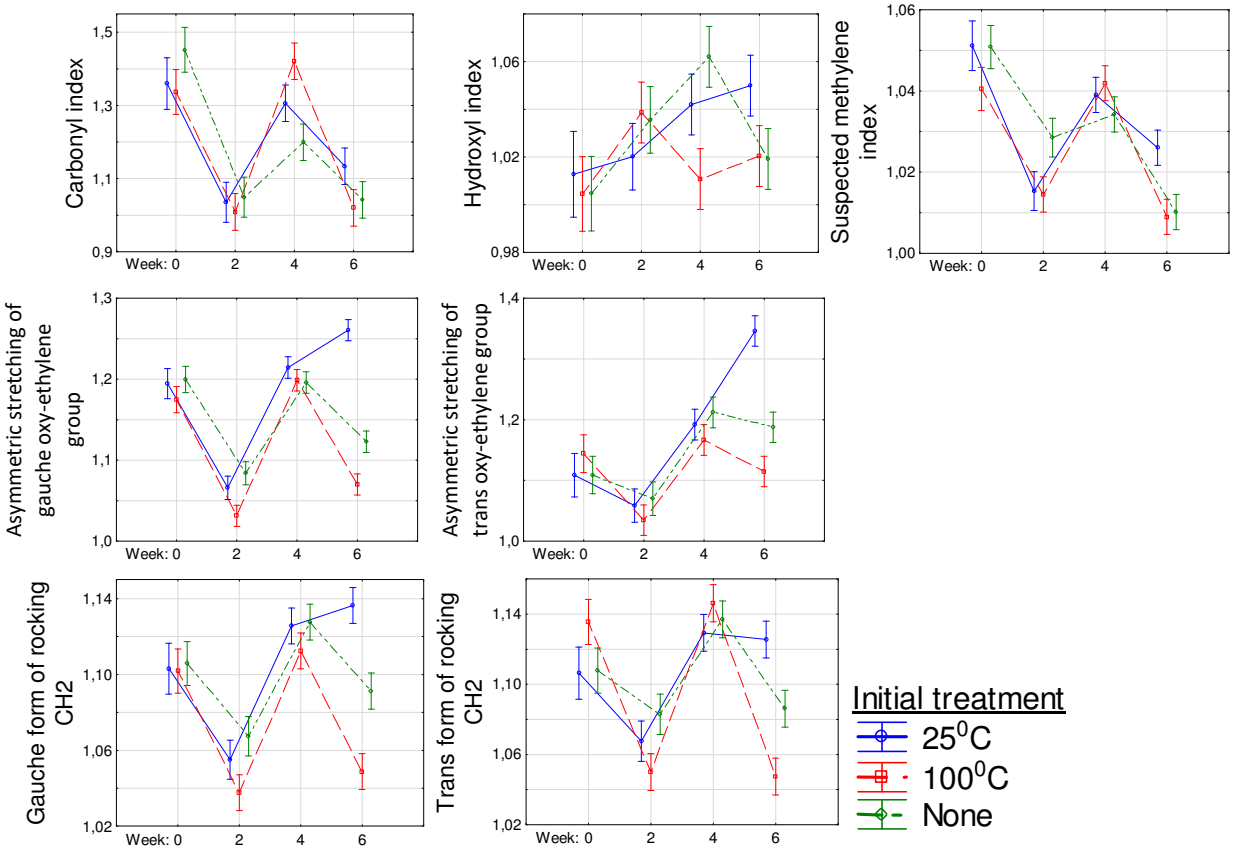

Figure 44: Mean graphs of FTIR indices for PET bench tests subjected to 60˚C

The trans form of rocking of CH_2 (which is linked to crystallinity as explained before) of the samples initially treated at 100˚C, exhibited a zigzag pattern similar to the carbonyl index which ended in an overall decrease. While the asymmetric stretch of the trans oxy-ethylene group exhibited a similar trend but had no significant difference overall. This supports the degree of crystallinity data of samples initially treated at 100˚C before being exposed to the 60˚C treatment, which exhibited an insignificant decreasing tendency. In both cases, the gauche form also exhibited an overall decrease indicating a loss of methylene groups, corresponding with the methyl index, and thus indicates degradation occurring.

Both trans and gauche form of the asymmetric stretching of the oxy-ethylene group in the ethylene glycol unit exhibited a zig-zag trend for the fresh samples and samples initially treated at 25˚C. Ending in overall, increases in the trans form and a decrease in the gauche form of the fresh samples, indicating a transition from gauche to trans and therefore supporting the increase in the degree of crystallinity data from the DSC. For the fresh samples, both the trans and gauche form of rocking CH_2 exhibited a significant zig-zag pattern. However, the overall variance was insignificant. In contrast, the trans form of the asymmetric stretch of the oxy-ethylene group exhibited an overall increase and the gauche form exhibited an overall decrease for the fresh samples, indicating a clear transition from gauche to trans and therefore supporting the increase in the degree of crystallinity data from the DSC.

The PET samples subjected to the 25˚C treatment, see Figure 45, exhibited a decrease in the carbonyl index at week four regardless of whether initially treated or not; and a return to original starting value limits at week six for samples subjected to initial treatment. While the fresh samples did not manage to reach the original limits. This was supported by the hydroxyl index that exhibited a significant increase for the fresh samples at week six, indicating that significant hydrolysis or oxidative degradation occurred during the last two weeks. The samples initially treated at 100˚C exhibited a slight increase in hydroxyl index at week four, but returned to limits of initial value at week six while the 25˚C samples exhibited no significant difference in hydroxyl index. This is surprising, as it was hypothesised that the hydroxyl index rather than the carbonyl index would vary significantly since hydrolysis is more likely to occur under these conditions than thermo-oxidative degradation. It is therefore suggested that this could be due to the plasticizing effect of water, opening up the matrix to be more accessible to oxidative degradation (Andrady, 1990).

The suspected methylene index corresponds with the loss in carbonyl groups by exhibited a similar trend to the carbonyl index. Indicating that the loss in carbonyl index at week four is more likely to oxidative degradation than hydrolysis, as also observed by the hydroxyl index. The index of the trans form of rocking CH_2 exhibited no significant difference. In contrast, the gauche form exhibited an increase at week four for the samples initially treated at 100˚C. Similarly, the index for the asymmetric stretch of the gauche oxy-ethylene group tended to increase in the samples initially treated at 100˚C while exhibiting decreases for the others. This will explain the degree of crystallinity data from the DSC, that exhibited no significant differences for the fresh samples and samples initially treated at 25˚C while exhibiting a decrease for the samples initially treated at 100˚C.

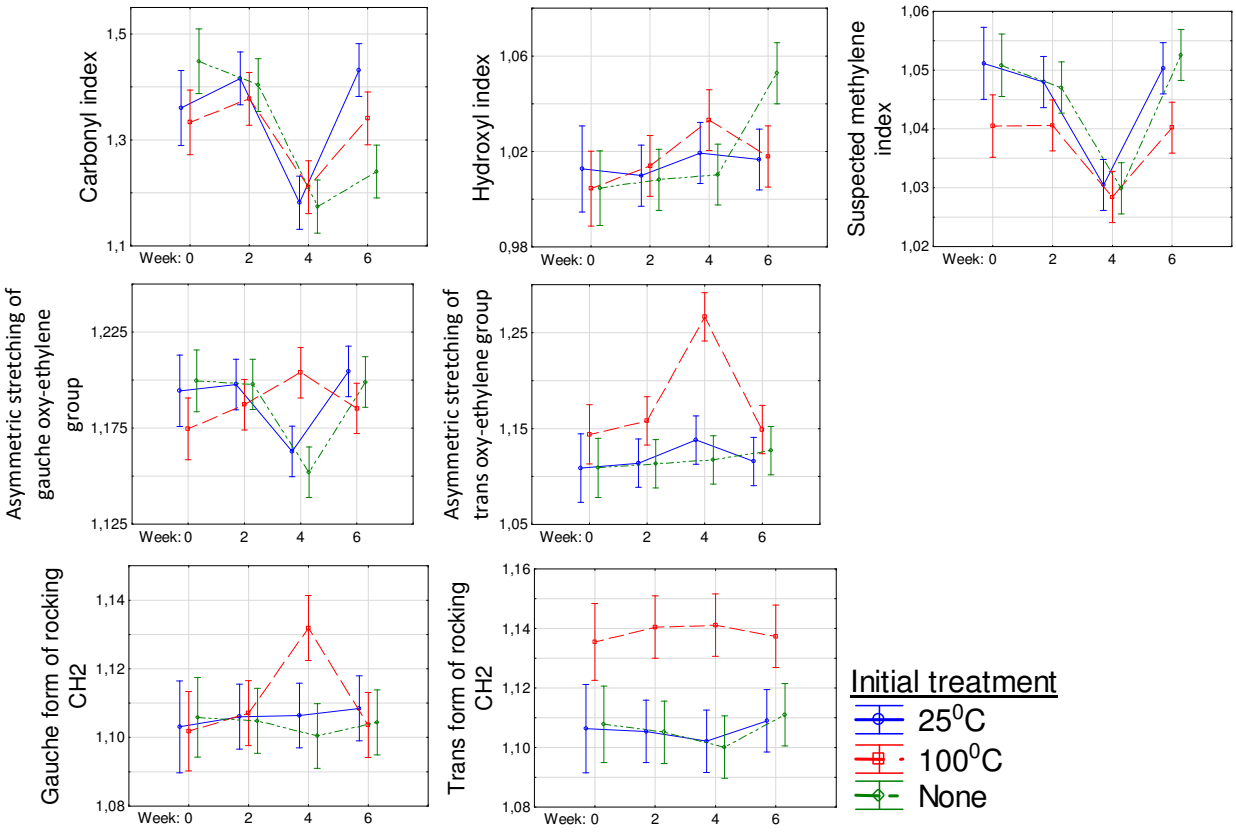

Figure 45: Mean graphs of FTIR indices for PET bench tests subjected to 25˚C

The PET samples subjected to the 65 W/m^2 UV radiance (or UV2), see Figure 46, exhibited decreases in carbonyl indices at week four and returns at week six for the fresh samples and samples initially treated at 25˚C. While the samples initially treated at 100˚C exhibited no significant differences. The hydroxyl indices exhibited no significant differences for fresh samples and samples initially treated at 25˚C. While the samples initially treated at 100˚C exhibited an increasing tendency over the course of the experiment. This could signify that photo- and thermal-oxidative degradation dominated for the fresh samples and samples initially treated at 25˚C. In comparison hydrolysis dominated the degradation for the samples initially treated at 100˚C. This would be in correspondence with literature which states the more crystalline the material, the better the resistance to degradation such as hydrolysis.

For the samples initially treated at 100˚C, the hydrolysis was therefore not significant enough to cause a definitive increase in hydroxyl index but was higher than the oxidative degradation since the conditions were too low to cause significant oxidative degradation, especially in the more crystalline material. The methylene index supports this by again mimicking the carbonyl index trend. Further investigation showed that neither the trans nor the gauche form of rocking CH_2 exhibited significant differences. This indicates that degradation was not significant as this area is very subjectable to degradation. It also supports the degree of crystallinity data from the DSC that also exhibited no significant variance. This is also supported by both forms of the asymmetric stretch of the oxy-ethylene group which also exhibited no overall difference.

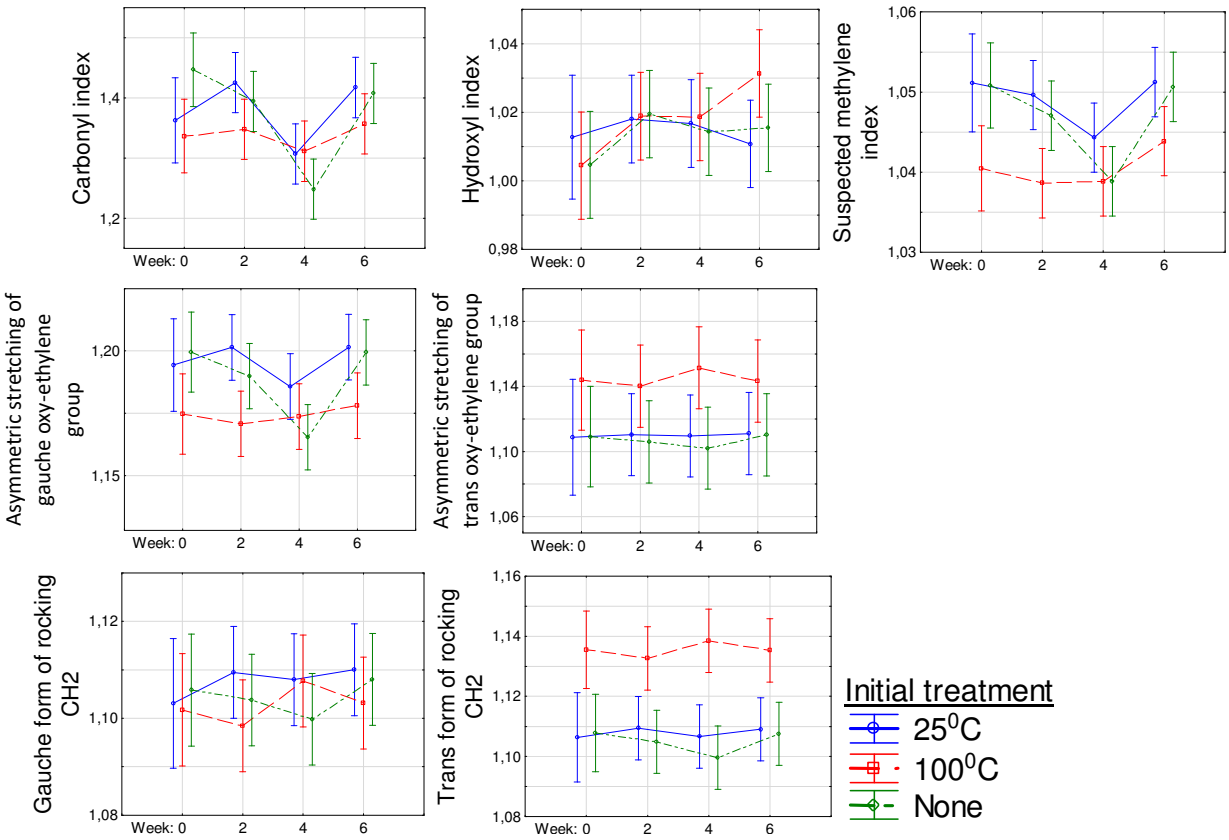

Figure 46: Mean graphs of FTIR indices for PET bench tests subjected to 65 W/m^2 UV radiance

4.2.4 Discuss initial treatment effects

4.2.4.1 Comparing the samples initially treated at 100˚C to the fresh and 25˚C initial treated samples

Subjected to the low UV radiance of 65 W/m^2 there were not many notable differences in trends or values for any of the plastics when comparing the samples initially treated at 100˚C to the fresh and/or 25˚C initial treated samples. One or both followed a similar trend and/or exhibited similar values to the samples initially treated at 100˚C. The instances where notable variances occurred were in PET, where values differed based on crystallinity changes (as explained in 4.1.4) and the hardness exhibited significant increases for samples initially treated at 100˚C.

Similarly, when subjected to the low-temperature treatment of 25˚C, not many notable differences were observed. However, there were slightly more than for the low UV radiance treatment. For the polypropylenes, these differences were only observed in the indices used as secondary indicators of degradation, which suggests that it is not as significant, while for PET it was in both the primary and secondary indicator indices. PET also exhibited variances in hardness, where a decrease followed the initial increase for the samples initially treated at 100˚C, while the others were still in the increasing phase.

Subjected to high UV radiance of 130 W/m^2, the there were observable differences between the samples initially treated at 100˚C, and the fresh samples and/or samples initially treated at 25˚C. For the

polypropylenes, the samples initially treated at 100˚C resulted in greater crystallinity variances. The CPP even exhibited opposing trends between the samples initially treated at 100˚C and the others. This was also reflected in the indices used as primary indicators for degradation, as the sample initially treated at 100˚C led to greater variances and/or accelerated trends in both polypropylenes. Similarly, for PET the hardness increased significantly for the samples initially treated at 100˚C, but not the others. However, the indices used as primary indicators of degradation exhibited similar values and trends between the samples initially treated at 100˚C and 25˚C, with the samples from the 100˚C treatment appearing to lag behind the others in the hydroxyl index trend.

Subjected to the high-temperature treatment of 60˚C, the polypropylenes exhibited similar trends and values between the samples initially treated at 100˚C and the fresh and/or 25˚C initial treated samples. The observable differences were in the hardness values, and the primary indicator indices for BPP, which followed similar trends, but the samples initially treated at 100˚C exhibited greater increases than the fresh and/or 25˚C initial treated samples. For PET, the crystallinity and hardness results exhibited accelerated degradation in samples initially treated at 100˚C compared to the fresh samples and/or samples initially treated at 25˚C.

It is suggested from these results that the 100˚C accelerated the degradation for polypropylene under all conditions and even for PET under low conditions. The acceleration in polypropylene degradation was anticipated, since the polypropylene initially treated at 100˚C is further degraded. As previously explained this enhances degradation. However, this was not initially anticipated for PET as the increased crystallinity from the 100˚C was expected to act as a barrier to degradation initiating factors. It is theorised that the trend observed can be attributed to the degradation occurring after crystallization, during the 100˚C treatment, since this would result in a PET that is further degraded. The further degraded PET would contain more degradation products than the fresh and/or 25˚C initial treated PET samples. As previously explained the degradation products promote oxidative degradation. At low conditions, where environmental degradation is not as significant, these products will help enhance the degradation while under high degrading conditions the degradation from the environment is significant enough to surpass this.

4.2.4.2 Comparing the fresh samples and samples initially treated at 25˚C

Subjected to the low UV radiance of 65 W/m^2 there were not many notable differences in trends or values for any of the plastics when comparing the fresh samples and samples initially treated at 25˚C. Only BPP exhibited some variances in the indices. This suggests that at low UV radiance over a short time there is not much difference between the fresh samples and samples initially treated at 25˚C and that variances observed might be due to repeatability issues or the positioning of the flask and the uneven distribution of UV radiation in the UV chamber.

Similarly to the low UV radiance, the treatment of 25˚C did not exhibit many notable differences. However, slightly more were observed for the 25˚C treatment than for the low UV radiance treatment.

All plastics exhibited some variances in values, between the fresh samples and samples initially treated at 25˚C, in the carbonyl and hydroxyl indices. With the fresh polypropylene samples ending in higher values in both instances and the fresh PET samples ending in higher hydroxyl and lower carbonyl index values. Although these are possible indications of the fresh samples experiencing accelerated degradation, the data is not adequate for a convincing argument. This indicates that at low temperatures over a short time there is not sufficient difference between the fresh samples and samples initially treated at 25˚C.

Subjected to the high UV radiance of 130 W/m^2 the BPP exhibited similar trends for crystallinity and hardness, between fresh samples and samples initially treated at 25˚C. However, different trends were observed in the indices. The CPP exhibited lower variances or no significant variances in crystallinity and indices for the samples initially treated at 25˚C, compared to the fresh samples. In comparison PET exhibited different trends at week six and in indices, between fresh samples and samples initially treated at 25˚C.

Subjected to the high-temperature treatment of 60˚C, the polypropylenes exhibited similar trends for crystallinity, between the fresh samples and samples initially treated at 25˚C. While the samples initially treated at 25˚C appeared to have a lower effect on the hardness compared to the fresh samples. For CPP, the variances in the indices suggested slower degradation for the samples initially treated at 25˚C. In contrast, for BPP, the variances in the indices suggested accelerated degradation for the samples initially treated at 25˚C. The PET exhibited similar hardness trends to the polypropylenes with the samples initially treated at 25˚C appearing to have a lower effect on the hardness compared to the fresh samples. In some indices, it appeared as if the samples initially treated at 25˚C lagged behind the fresh samples. However, in most indices similar trends were observed.

It was interesting to note that samples initially treated at 25˚C exhibited lower or no significant variances for CPP under both high conditions, compared to the fresh samples. Similarly, both polypropylenes exhibited increases in carbonyl and hydroxyl indices for fresh samples at 25˚C treatment while the samples initially treated at 25˚C did not vary significantly. The data, therefore, suggest that the fresh plastics degrade more readily than the samples initially treated at 25˚C. Originally this was not expected. It is speculated that the low storage temperature could have caused the trend, as polypropylene exhibits poor resistance to a variety of factors at low temperatures (Hindle, 2019; Crawford & Quinn, 2016; Rubin, 1990). It is also speculated to be only observed in CPP, as CPP does not have the same degradative preventative colour additive as BPP. However, as mentioned in the results section, it could also be attributed to an experimental error, and it is advised to repeat the experiment.

4.2.5 Discuss temperature and UV radiance effects

Various responses on the different bench test treatments were seen. These responses and the occurrences observed will be discussed in this section. The ANOVA results, as seen in Table 11 in Appendix C – ANOVA tables, indicate that these responses were significantly different. As the ANOVA's

indicated the secondary experiments (or bench tests) are significant for hardness, degree of crystallinity and all functional groups. This means that the temperature and UV radiation had a statistically significant effect on all the results obtained (i.e. the null hypothesis is rejected, there is a significant variance in means between the different treatments). It also showed that the effects of time, plastic-type, initial treatment and the secondary tests are independent of each other.

The low UV radiance exhibited no effects on any of the BPP samples, while it exhibited some variances for the CPP samples. This indicates that the CPP is more vulnerable to photo-oxidative degradation than the BPP, as anticipated due to the photo stabiliser in BPP. For PET, the low UV radiance resulted in increases in hardness and some variances in indices. It is suggested that the 65 W/m^2 only resulted in oxidative degradation for the fresh samples and samples initially treated at 25˚C. It is further suggested that hydrolysis is responsible for any degradation observed in the samples initially treated at 100˚C. However, in both cases, it is stated that the degradation is very slow and not necessarily significant.

The low-temperature treatment resulted in decreases in BPP crystallinity and some variances in primary oxidative investigative indices at week six, but no variance in hardness. Similarly, for the CPP, the low-temperature treatment also resulted in decreases or tendency to decrease for crystallinity and some variances in indices, but no variance in hardness. It is suggested that the occurrence of thermo-oxidative degradation is a possibility. However, it is very slow since the first significant differences are only observed late in the experiment. From the indices that varied, it is suggested that possible crosslinking occurred, which would also support the decrease in crystallinity. For PET subjected to the low-temperature treatment, no significant variance in the degree of crystallinity or hardness was observed. Moreover, significant index variances were only observed late in the experiment, which suggests that the low temperature has slow degradation that requires a more extended period to result in notable differences.

The high temperature and UV radiance resulted in significant effects on the samples. The CPP was significantly affected by the high UV radiance treatment. While it appears as if the higher temperature had a greater effect on the PET and BPP, however, this statement requires further investigation and more analysis to be stated conclusively. It also bears worthy to note that variance in radiance throughout the chamber existed. An attempted to minimize the effect by bi-weekly repositioning the beakers have been made. However, in cases were bewildering trends are observed, it could be due to the position of the beaker in the chamber.

The high-temperature treatment resulted in significant decreases in crystallinity, along with significant increases in hardness for both polypropylenes. It also caused significant variances early on in the indices. However, it also brought unexpected trends in the indices after the initial degradation. The possibility of re-polymerization of the polypropylenes due to the high temperature was considered. However, based on the decrease in crystallinity and the alkene index not exhibiting a decrease, it is suggested that the unexpected trends are due to secondary reactions occurring. When considering all the results for the PET samples initially treated at 100˚C, it is suggested that degradation, both hydrolysis and thermo-oxidative,

has occurred. The observed tendency to decrease in the degree of crystallinity could be due to either the amorphous regions degrading first before degradation in the crystalline regions start; or it could be that the crystallinity has, similarly to the hardness, exhibited an initial increase and is now in the decreasing phase causing the overall effect to not be significant yet. For the PET samples, both fresh and initially treated at 25˚C, the high-temperature treatment resulted in increases in the degree of crystallinity, along with increases or tendencies to increase in hardness. It was suggested that this could, similar to the initial treatment, be due to some crystallization occurring. Considering the indices, it is difficult to conclusively state what has transpired, since the indices yielded results generally associated with crystallization, while simultaneously yielding results indicating degradation has occurred.

The high UV radiance resulted in an increase in the degree of crystallinity for BPP samples initially treated at 100˚C. At the same time, decreases for the fresh samples and samples initially treated at 25˚C were observed. The thermograms also did not exhibit much difference for the fresh and 25˚C samples, which suggests that the oxidative degradation for these were possibly due to thermo-oxidative degradation. The indices also exhibited significant variances indicating degradation. However, the variances were at a later stage in the experiment indicating that the degradation is relatively slow. For the samples initially treated at 100˚C, the indices of the first few weeks exhibited significant trends that are associated with degradation. It is suspected that the initial treatment caused the stabiliser to be de-activated or accelerate the leaching of the stabiliser during the bench tests, which allowed the BPP to undergo photo-oxidative degradation. Another possibility is that thermo-oxidative degradation occurred, due to the temperature of the water that increased as a result of the energy emitted by the light. However, this is anticipated to be slow and low, as temperature should not have been more than 30˚C – 40˚C. At a later stage in the experiment unanticipated trends were observed, it was considered that this could be the result of re-polymerization since alkene index also decreases and the degree of crystallinity and hardness exhibits tendencies to increase. However, it is more likely to be secondary reactions occurring.

For CPP, the high UV radiance resulted in great degradation, and the physical embrittlement effect was observable with the human eye. It also resulted in notable variances in the thermograms and the anticipated degradation trend of the initial increase in hardness followed by a decrease. The indices also exhibited significant variances contributed to degradation. The samples initially treated at 25˚C exhibited a strange trend of not having a significant crystallinity, hydroxyl or carbonyl variance. Conversely, at the same time, the thermogram, hardness and suspected methanetriyl, methylene and methyl indices indicated significant degradation and followed similar trends to the fresh samples. Considering the PET results, the high UV radiance did not have a significant effect on the crystallinity. Even thought the results exhibited an increasing tendency (as generally occurs during the first phase of degradation). It also resulted in an increase in hardness for the samples initially treated at 100˚C. While all the indices calculated indicated that photo- or thermal-oxidative degradation is occurring along with continuous hydrolysis. From the results, it is suggested that the amorphous region is firstly degraded before the crystalline region undergoes degradation. It is therefore suggested that the high UV radiance also caused significant PET degradation. For PET samples initially treated at 100˚C and then subjected to 130 W/m^2

UV radiance, it was observed that the hydrolysis rate is lagging. This is suspected to be because the degradation products formed during initial treatment do not promote hydrolysis, only oxidative degradation.

Investigating the effect of plastic-type by considering these results, it was observed that CPP under high UV radiance exhibited the most physical visible degradation. This is supported by literature which states that polypropylene is more vulnerable to photo-oxidative degradation than PET. Other observable different reactions between the two plastic types were at high-temperature treatment, where PET exhibits what is suspected to be crystallization to some extent. However, at the lower temperature and UV radiance treatments, there are not such definitive observable variances. It is suspected that the time frame of six weeks is too short to be able to produce and identify significant differences in degradation between the two plastic types at low conditions.

Examining the effect of the colour additive by considering these results, the CPP exhibited increases in hardness and degree of crystallinity for the high UV radiance treatment. In contrast, BPP did not exhibit significant variances in hardness and exhibited decreases (except for the increase at the 100˚C initial treatment) in the degree of crystallinity – which was attributed to additive in the BPP and signifies that the additive prevents photo-oxidative degradation. For the secondary temperature treatments and all samples initially treated at 100˚C, similar trends are followed between CPP and BPP for FTIR indices, hardness and degree of crystallinity. This supports the theory as mentioned above, that the additive is de-activated at the initial high-temperature treatment, effectively nullifying its degradation prevention properties.

4.3 Comparing different environments

An investigation was conducted on the effect the environment has on plastic degradation. For the ensuing investigation, the environments “land” refers to the treatment of plastics at constant 25˚C in air (or no water medium), “sea” refers to the treatment of plastics in seawater and “fresh” refers to the treatment of plastics in demineralised water. For the investigation between land and water (both sea and fresh), the same constant temperature was used to focus on the effect of water vs no water. However, in a real-life scenario, the plastics in the marine environment will be subjected to a more regulated temperature. In contrast, plastics on land will be subjected to a higher variance in temperature, which could have a significant effect. Another factor in a real-life scenario that can influence these results, and should be considered in further studies, is sunlight or UV radiance. For the investigation on the effect of water salinity, thus sea water vs demineralised (or fresh) water, the same temperature and UV radiance treatments from the secondary experiments (or bench tests) were used. It was used to yield a better understanding of real-life scenarios but also accelerate some of the effects to obtain significant variances within six weeks.

From the graphs in Figure 47, it can be seen that the water decreased the polypropylenes’ degree of crystallinity significantly compared to the land environment. However, between the two water mediums

there was no significant difference for either PP or PET. This is supported by the ANOVA analysis that indicated a statistically significant variance between the 3 environments when subjected to a temperature of 25˚C (see Table 12, page 117 in Appendix C – ANOVA tables), but no statistical significance between the two water environments for the other treatments (see Table 13, page 118 in Appendix C – ANOVA tables) since no environment or environment interaction had a 'p' value lower than 0.05 for the degree of crystallinity in Table 13.

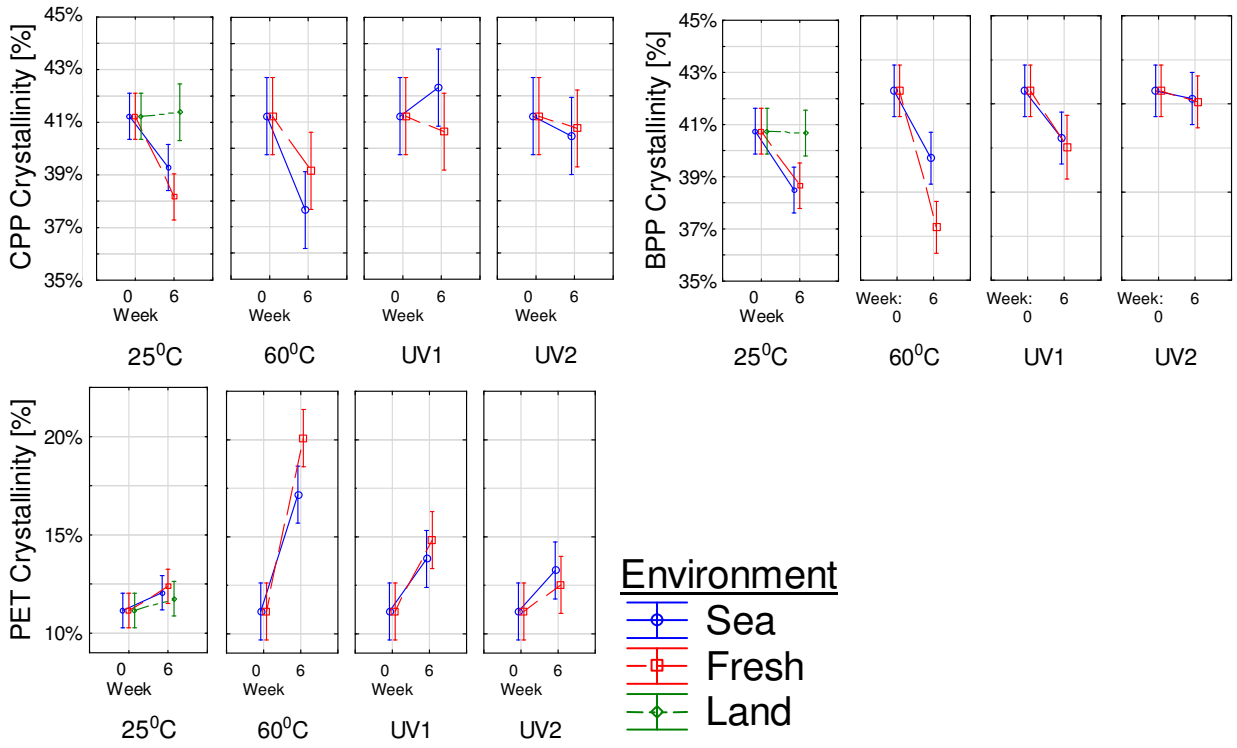

Figure 47: Mean graphs of percentage crystallinity comparing no water (land), seawater and demineralised (or fresh) water as mediums

It was anticipated that PET would be more susceptible to hydrolysis and effects from water absorption (such as plasticizing) than polypropylene. Since PET has the higher water absorption rate, of 0.1-0.2% weight gain compared to polypropylene with a rate of 0.01–0.03% weight gain, both in 24 hours at 21˚C (Crawford & Quinn, 2016; Omnexus, n.d.). However, as discussed above, it was the polypropylenes that exhibited a significant difference in the degree of crystallinity. It is theorised that this could be due to the water molecules and salt ions disrupting the crystalline region in the polypropylenes, while it would first diffuse through and attack the already amorphous region of the PET. Therefore, causing significant crystallinity changes in the polypropylenes but not in PET. The theory of the attack being firstly on the amorphous region of PET before disrupting the crystalline region is supported by the gauche form of the asymmetric stretch of the oxy-ethylene group in the ethylene glycol unit index. This index exhibited significant decreases at week four, for the 25˚C treatment (see Figure 51), while the trans form of this index stayed relatively constant throughout or exhibited a slight increase.

For the hardness, the only significant difference in environment occurred at a temperature of 60˚C, for all three plastics. For all other treatments, there were no significant differences in hardness, as can be seen in Figure 48. It is also supported by ANOVA results, as the ANOVA of the three environments at a temperature of 25˚C indicated no statistical difference for environment as neither environment nor environment interaction had a 'p' value lower than 0.05 (see Table 12, page 117 in Appendix C – ANOVA tables). While the ANOVA results for the water mediums indicated a statistically significant variance for the environment and some of the interactions between the sea and demineralised or "fresh" water (see Table 13, page 118 in Appendix C – ANOVA tables). Solubility is known to increase with temperature, and this could be a possible reason why the higher temperature had significant hardness variances between seawater and "fresh" water, as the higher temperature could increase or accelerate the effect of the salt ions present in the seawater.

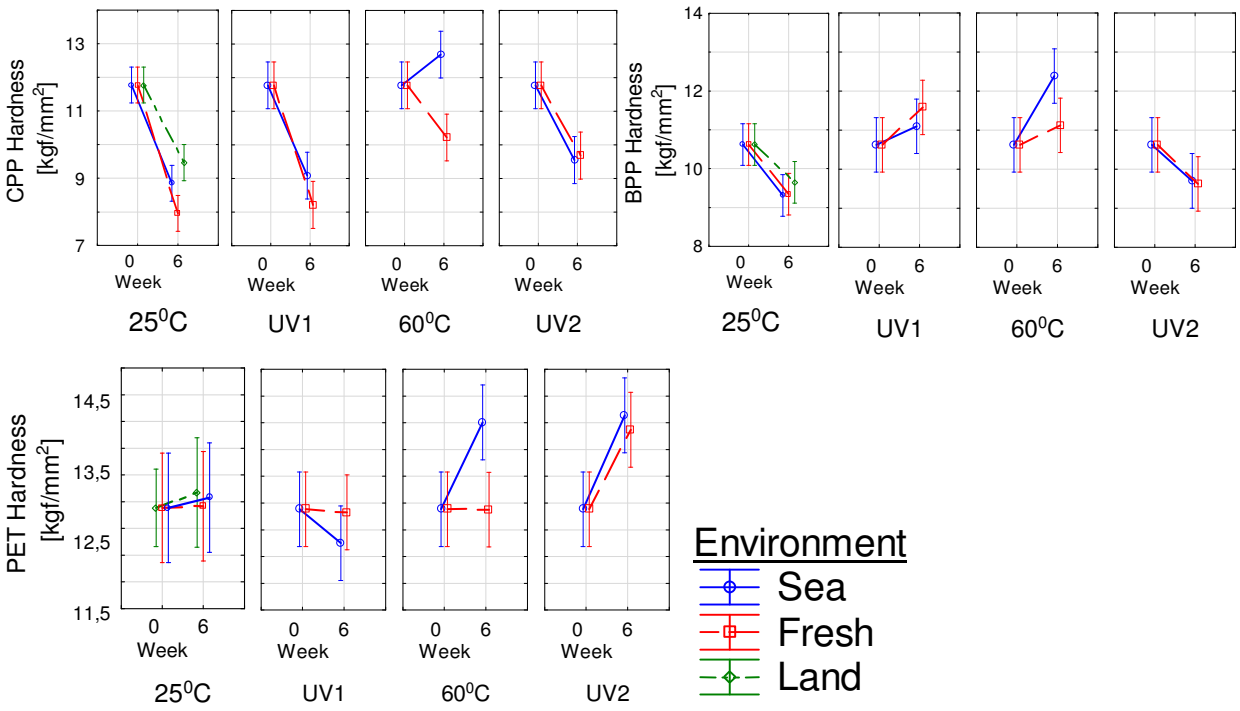

Figure 48: Mean graphs of hardness comparing no water (land), sea and demineralised (or fresh) water as mediums

For the polypropylenes, between the land and both water environments at 25˚C, the suspected methylene, methyl and methanetriyl indices were lower for the plastics in water mediums than for plastics on land. As previously mentioned, this is a possible way of tracking degradation and led to the suggestion that the water environments had greater degradation, indicating a significant effect. The carbonyl and hydroxyl indices support this theory for seawater as the carbonyl and hydroxyl indices from plastics in seawater were higher than the indices for plastics on "land". These indices can be viewed in Figure 49 for BPP and Figure 50 for CPP. Between the two water mediums at 25˚C, it was the sea environment that exhibited the higher carbonyl and hydroxyl indices and lower suspected methylene, methyl and methanetriyl indices. It suggests that seawater has an accelerating effect on degradation. This

is supported by the 60˚C and 130 W/m^2 (or UV1) treatments. In these the carbonyl, hydroxyl and alkene indices had higher variances or ended at a higher value, while the suspected methylene, methyl and methanetriyl indices were lower, for samples in seawater compared to samples in freshwater; for both BPP and CPP.

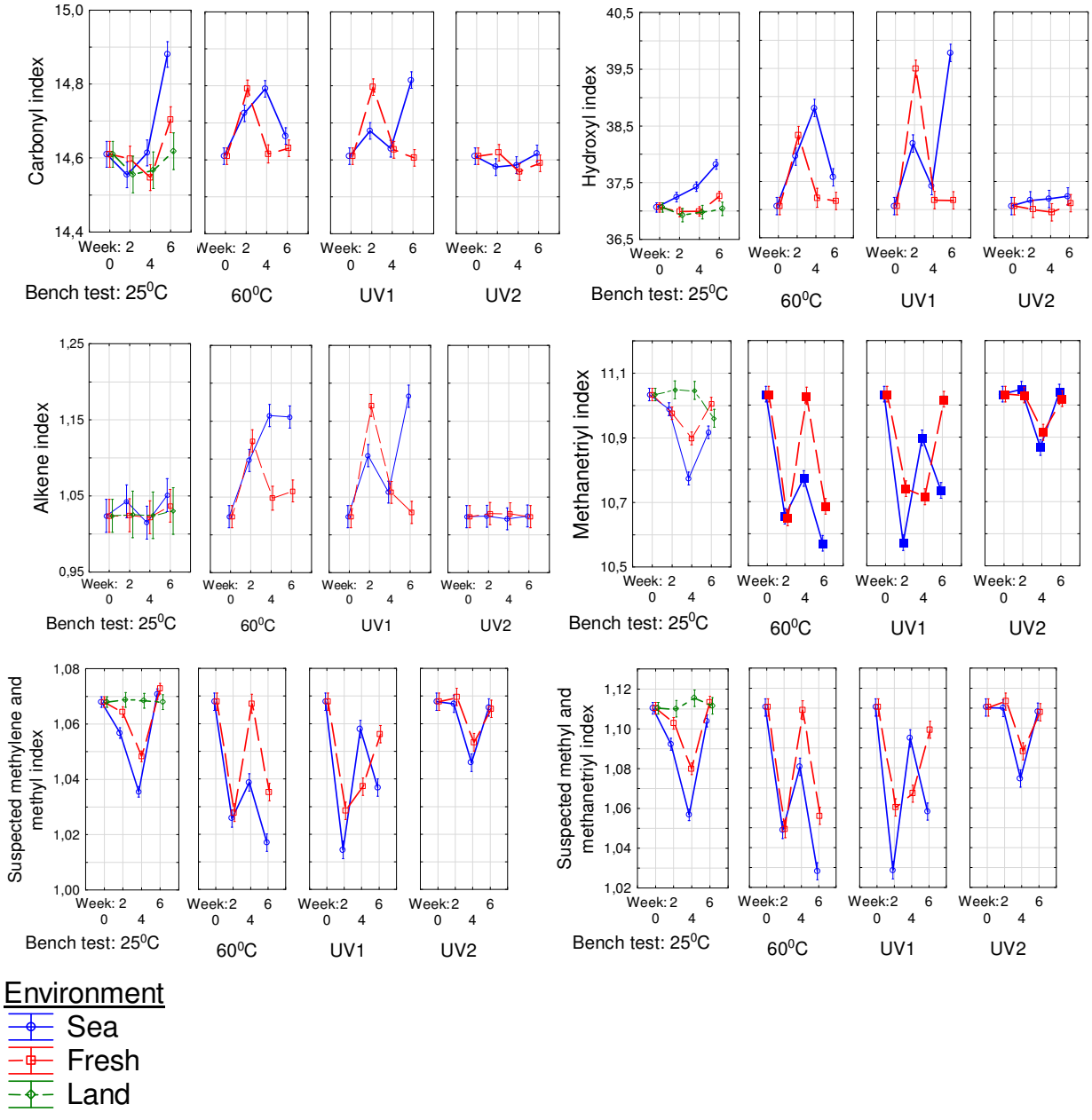

Figure 49: Mean graphs of FTIR indices for BPP comparing no water (land), sea and demineralised (or fresh) water as mediums

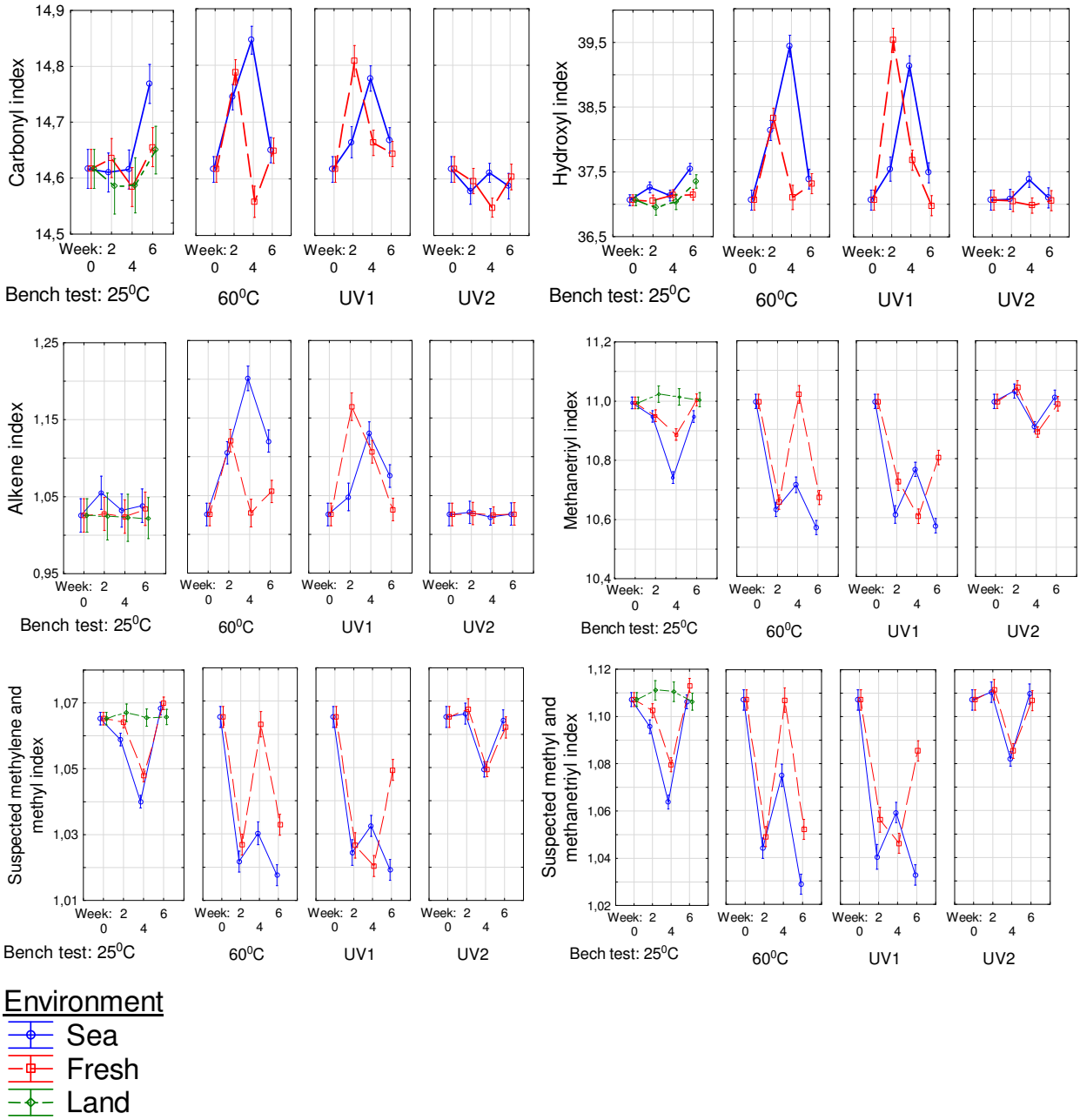

Figure 50: Mean graphs of FTIR indices for CPP comparing no water (land), sea and demineralised (or fresh) water as mediums

For PET the water environments exhibited a lower final value in carbonyl index, with greater variances in carbonyl, suspected methylene and asymmetric stretch of the gauche oxy-ethylene group compare to the land environment. At the same time the plastics from the sea environment exhibited significant increases in hydroxyl and asymmetric stretch of the trans oxy-ethylene group compare to the land environment, as seen in Figure 51. These are indications that the plastics in the water environment has undergone more degradation than those on land (without water), which is theorised to be due to the hydrolysis occurring.

For PET, between the two water mediums significant differences in the carbonyl index for all four treatments with seawater exhibiting the greater variance or ending lower than the freshwater was observed (see Figure 51). This was also observed for the gauche form of the asymmetric stretch of the oxy-ethylene group under 25˚C and 130 W/m^2, the gauche form of rocking ethylene under 130 W/m^2 and the methylene index under 60˚C. These are all indication of degradation, and suggests accelerated degradation in seawater since the gauche form is favoured by the amorphous region which is expected to degrade first. At the same time, the hydroxyl index at treatments 25˚C and 130 W/m^2 (or UV1) exhibited higher values for seawater samples compared to freshwater samples. This would support the suggestion of accelerated degradation in seawater. However, the evidence is not conclusive enough to state this definitely, since in most cases the indices from the seawater and freshwater samples overlap and exhibit insignificant differences.

It appears as if the water environments had greater degradation than the land environment for all plastic types. A possible explanation for the accelerated degradation in water can be the plasticizing effect of water even for polypropylene that does not undergo hydrolysis like PET. The plasticizing effect causes decreases in the crystallinity which could lead to greater degradation rates since the crystallinity of the material usually hinders the degradations such as hydrolysis (Gok, 2016; Gewert *et al*., 2015). The plasticizing effect can also lead to an increase in the accessibility of the polymer matrix to atmospheric oxygen and leaching of stabilisers and additives (Andrady, 1990), which will result in accelerated oxidative degradation rates. A distinctive difference between the two water environments was observed for the polypropylenes with the seawater resulting in an even greater acceleration in degradation than the fresh (or demineralised) water. Although the same tendency was observed for PET, it was not as definitive. A possible explanation of why the effect of salinity appears enhanced on polypropylene could be because PET undergoes hydrolysis in both fresh and seawater. The effect of the salt ions could, therefore, be less observable and only noticed when enhanced at higher temperatures. In contrast, polypropylene does not generally undergo hydrolysis and therefore the influence of the salt ions, that is said to cause a weakening in the electrostatic repulsions of the molecular chains are easier to observe in the polypropylenes (Ma *et al*., 2019).

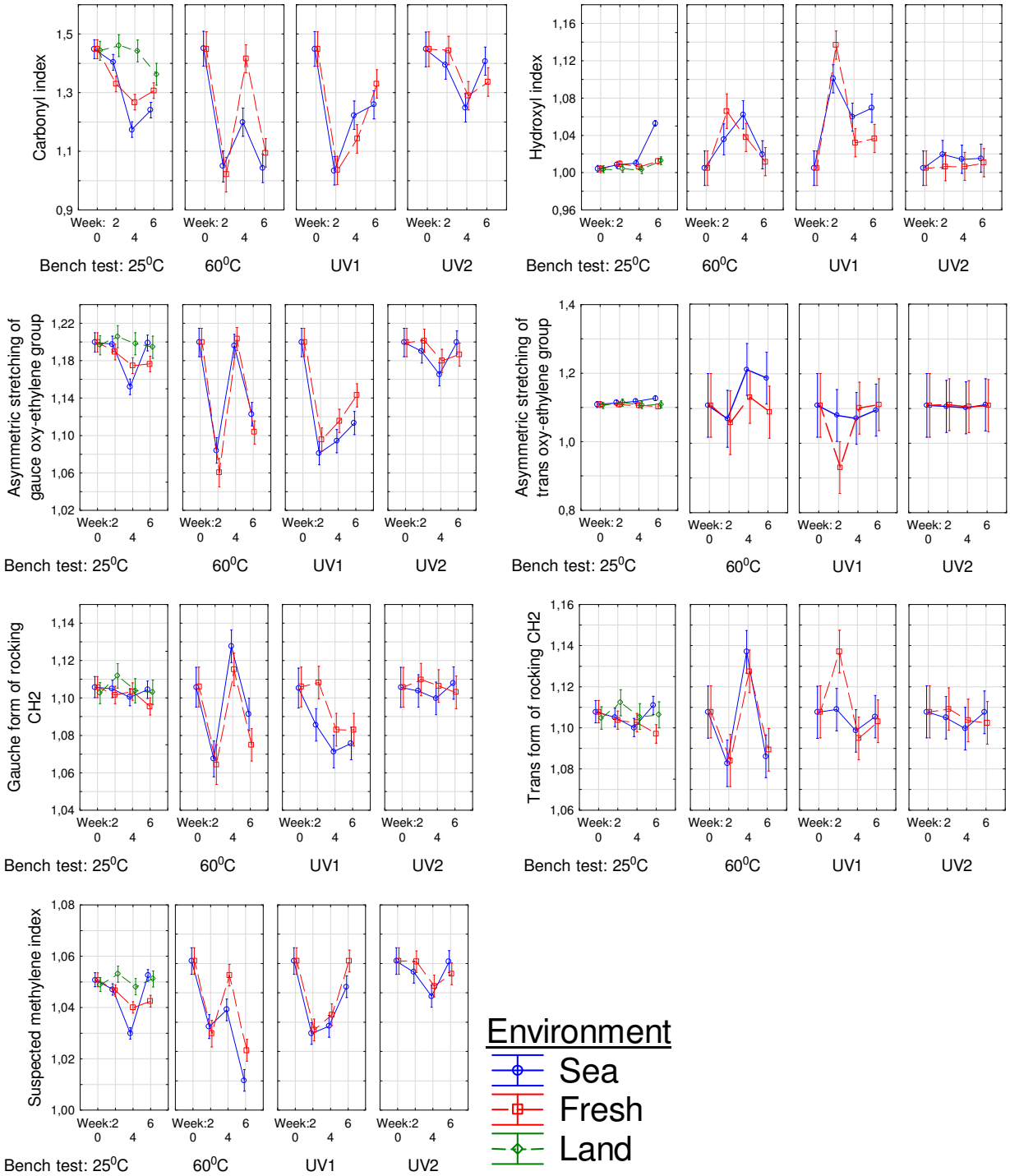

Figure 51: Mean graphs of FTIR indices for PET comparing no water (land), seawater and demineralised (or fresh) water as mediums

5 CONCLUSIONS AND RECOMMENDATIONS

5.1 Temperature associated plastic history study

The temperature associated plastic history study included an investigation into the effect of the temperature treatment. It was concluded that there is a difference in plastic behaviour with regards to the different initial temperature treatments. The 100˚C treatment resulted in crystallization and degradation for PET, suspected chemicrystallization for CPP and BPP and is also suspected of passivating the photo stabiliser in BPP. The cycling temperature treatment of 25˚C – 60˚C, also resulted in similar trends to the 100˚C treatment with some degree of crystallization (or annealing) in the PET along with some degree of degradation similar to the degradation from the 100˚C treatment although lagging with two weeks for the polypropylenes. In contrast, the 25˚C treatment did not have any significant effects. It is also suspected that the degradation underwent at 100˚C, for the polypropylenes and after crystallization for PET, was much higher than at the ambient temperatures.

The temperature associated plastic history study also included an investigation into the effect of the initial temperature treatment (or temperature associated plastic history) after the plastics are submerged in water. It was again concluded that the initial treatment or plastic history has a significant effect on the degradation rate, since it was observed that the samples initially treated at 100˚C resulted in increased oxidative degradation most of the time. This is theorised to be due to the degradation rate being enhanced by the degradation products formed during the initial treatment, and that 100˚C treated samples had increased levels of degradation products compare to the other initial treatments due to an increased degradation rate contributed to the elevated temperature (even for crystallized PET).

For the investigation on whether size and shape play a significant role in plastic degradation, it was found that the CPP samples were the only samples to have a distinctive difference between the large and small shapes, favouring degradation in the smaller shapes or shapes with a higher surface area to volume ratio. The PET samples also exhibited some variances favouring accelerated or greater reaction rates in the smaller samples. At the same time, there was not a significant difference for BPP samples. Therefore, from the size and shape analysis, it is hypothesised that degradation rates for smaller samples will be accelerated should the exposure or experimental time be prolonged. It is recommended to prolong the exposure or employ harsher conditions and/or utilise shapes that have a larger surface area to volume ratio difference, to validate this hypothesis.

Another recommendation for investigation on shape effects in plastic degradation is that along with FTIR analysis, other alternative plastic degradation tracking methods are applied that will accommodate samples of various sizes and shapes. It is also recommended that size and shape investigation is continued into the marine environment with applied mechanical stresses, as size could affect the probability of the plastic to turn over and expose more surface areas. This will affect photo-oxidative degradation rate, as photons only penetrate a short distance into the polymer surface.

5.2 Marine environment study

The marine environment study included an investigation into two UV radiance treatments that are associated with ambient conditions in the marine environment. During this investigation, it was found that the low UV radiance did not result in significant differences. It is thus concluded that the degradation occurring under these conditions are extremely slow, and a more prolonged exposure is recommended to investigate if it reflects the same trend as the extreme conditions. Conversely, the high UV radiance treatment resulted in significant degradation for all plastics, especially for CPP and BPP that were initially subjected to 100˚C. It is concluded that degradation for polypropylene is mostly photo initiated (photo-oxidative) and that summertime would exhibit increased degradation rates since the high UV radiance is closer to the summertime average.

The study also included an investigation into two temperature treatments. The low-temperature treatment, similar to the low UV-radiance treatment, did not result in significant differences. While the higher temperature, as seen in both the initial and secondary tests, generally resulted in accelerated or increased degradation. However, it also initiated other effects as seen by the crystallization of PET. It is stated that temperature is a very complex factor with regards to plastic degradation. High temperatures can cause crystallization or re-polymerization of plastics, that could have opposing effects and slows down degradation. At the same time, low temperatures can result in freezing of molecules and cycling temperature can cause annealing effects. Therefore, it is important to note that temperature effects are plastic specific and prone to variations.

For the marine environment investigation into the effect of different environmental factors, it was concluded that there is a difference in degradation behaviour between the UV and temperature treatments for extreme conditions (i.e. between the high UV and high-temperature treatments). As mentioned before, for the low conditions, a more prolonged exposure is recommended to investigate if it reflects the same trend as the extreme conditions. For the UV radiance treatment, an increase in crystallinity, which is suspected to be attributed to chemicrystallization, was observed. In contrast for the temperature treatment, a decrease in crystallinity was observed. It was also observed that for the extreme conditions, the UV radiance treatment had the greatest degrative effect on CPP in which case the embrittlement and crack formation was physically observable. It also had a tremendous degrative effect on BPP samples initially treated at 100˚C where it is suspected the photo stabiliser had been de-activate (or passivated). While the high-temperature treatment had the greatest effect on PET and is suspected of increasing hydrolysis. However, the high temperature is unnatural, but the high UV radiance is still within natural limits and led to significant degradation results in all plastics. It is, therefore, concluded that the UV radiance has a greater degradation effect compare to temperature, on plastics in the natural environment. It is noted though that monitoring effects of degradation proved difficult with various unexpected trends, such as secondary reactions and possible occurrences of crystallization or re-polymerization, which could have affected the results obtained under the extreme conditions.

Additionally, it was observed that neither polypropylenes exhibited significant variances in their alkene indexes under low conditions. In contrast, both exhibited significant increases in their alkene indices under the high UV and temperature conditions, which leads to the conclusion that alkene index can be a useful parameter for tracking significant degradation in polypropylene. It was also observed that from the data obtained the 845 cm^{-1} region appears to be a good index to obtain information about the crystallinity. The 845 cm^{-1} region exhibited a significantly higher index for the more crystalline PET and insignificant variances for the samples that did not undergo significant degradation.

5.3 Effect of the colour additive

Both the marine environment and the temperature associated plastic history study included an investigation into the effect of a colour additive. The investigation into the effect of a colour additive on the degradation behaviour in different environmental conditions showed that the photo stabilising colour additive effectively hindered the degradation of the BPP under UV treatment in the marine environment when compared to CPP. The colour additive is also suspected to be responsible for the hindering of deterioration of mechanical properties in BPP under temperature treatment in both marine and land environment. It is theorised that BPP and CPP underwent similar degradation but that the colour additive hindered the BPP, allowing CPP to degrade faster and causing BPP to lag.

The trend exhibited by the BPP exposed to initial treatment of 100˚C was different from the trends exhibited by the other initial treatments in the secondary tests. It resembled the trend exhibited by the CPP in the secondary tests. It is suggested that the additive is passivated during the high-temperature treatment, effectively nullifying its degradation prevention properties.

5.4 Effect of plastic-type

Both the marine environment and the temperature associated plastic history study included an investigation into the effect of plastic-type. The investigation to determine if different types of plastic react similarly to different environmental factors concluded that the polypropylene and PET did not react similarly. Polypropylene was much more sensitive to UV radiance and extremely low temperatures. At the same time, PET appeared to be more prone to exhibiting reaction or transformation at high temperatures compared to CPP. This is possibly due to the difference in crystallization temperatures. Not only did the molecular structural orientation, or degree of crystallinity, trend differ for these plastics under the high conditions, it was also observed that the common unit for degradation rate (namely carbonyl index) did not exhibit similar trends during degradation. This indicates that is might not be the best unit to determine degradation over a wide range of plastic types. It is therefore concluded that the FTIR indices should not be considered on their own but together, should it be used as a unit to measure degradation rate. Since, as observed, the mechanisms can result in a variety of functional groups, it is also advised to ensure that the indices used are viable on the specific plastics. For example, the alkene indices were not viable on PET samples but were useful for PP analysis. Similarly, it is also recommended

not to be solely dependant on indices but to include other variables and properties (e.g. hardness, crystallinity, chain length etc.) when considering degradation in plastics.

5.5 Effect of environment

The conclusion from the investigation of the effect of environment is that a water environment (such as marine or freshwater) has an increasing effect on the plastic degradation, possibly due to the absorbance of water that has a "plasticizing" effect and allows for greater oxidative degradation rates. The effect was observable on the molecular level and, depending on the type of plastic, the crystallinity as well. However, it is believed that if exposed to the marine environment for longer than the investigated period, results will exhibit significant effects on all plastic's crystallinity and hardness. It is recommended that this effect should be further investigated especially with varying or cycling temperature and light conditions to simulate a more life-like scenario. It was also suggested from this investigation that the phenomenon of lower degradation in the marine environment than on land, observed by previous studies, could be due to water regulating the temperature since the addition of water under identical temperature conditions resulted in increased degradation.

The effect of salinity or variance between the marine and the freshwater environment was observable for the polypropylene data, as the samples submerged in seawater exhibited accelerated or greater degradation than the fresh (or demineralised) water. Although the PET exhibited a similar trend, it was not definitive, possibly due to the effect of hydrolysis. It is thus recommended that the exposure time should be prolonged to yield a conclusive verdict on the effect of salinity of the environment.

5.6 Additional recommendations

Additional recommendations are that the experiments should be repeated at different times during the year to account for the variance in seasonal atmospheric humidity and other seasonal variances in the repeatability investigation. Alternatively, it is recommended to complete investigations in an environment where humidity and atmospheric compositions are controlled. Prolonged runs are recommended as well since plastic degradation can transpire over hundreds of years and six weeks might have been too short to allow for conclusive results that can be extrapolated, under ambient and natural conditions. It is also recommended to take absorbance readings rather than transmittance in future research.

REFERENCES

Ainbinder, S. B. & Laka, M. G. 1966. Hardness of polymers. *Polymer Mechanics,* 2(3), pp. 211-217. DOI: 10.1007/BF00860285.

Ambrogi, V., Carfagna, C., Cerruti, P. & Marturano, V. 2017. Additives in Polymers. In: *Modification of Polymer Properties.* s.l.: Elsevier, pp. 87-108. DOI: 10.1016/B978-0-323-44353-1.00004-X.

Andrady, A. L. 1990. Environmental degradation of plastics under land and marine exposure conditions. in R. S. Shomura Honolulu & M. L. Godfrey, *Proceedings of the Second International Conference on Marine Debris*, Honolulu, Hawaii, pp. 848-869.

Androsch, R. & Wunderlich, B. 2001. Reversible Crystallization and Melting at the Lateral Surface of Isotactic Polypropylene Crystals. *Macromolecules,* 34(17), pp. 5950-5960. DOI: 10.1021/ma010260g.

Ángeles-López, Y. G., Gutiérrez-Mayen, A. M., Velasco-Pérez, M., Beltrán-Villavicencio, M., Vázquez-Morillas, A. & Cano-Blanco, M. 2017. Abiotic degradation of plastic films. *Journal of Physics: Conference Series,* Volume 792. DOI: 10.1088/1742-6596/792/1/012027.

Beltrán-Sanahuja, A., Casado-Coy, N., Simó-Cabrera, L. & Sanz-Lázaro, C. 2020. Monitoring polymer degradation under different conditions in the marine environment. *Environmental Pollution,* p. 259. DOI: 10.1016/j.envpol.2019.113836.

Binuja, S. 2018. *Photo-oxidation.* [Online] Available at: https://www.slideshare.net/binujass1/photooxidation [2019, May 30].

Blaine, R. L. 1990. *Polymer Heats of Fusion,* New Castle, USA: TA Instruments. [Online] Available at: http://www.tainstruments.com/pdf/literature/TN048.pdf [2019, October 6].

Blaine, R. L. n.d. *Determination of Polymer Crystallinity by DSC.* [Online] Available at: http://www.tainstruments.com/pdf/literature/TA123new.pdf [2019, January 27].

Bletter, M. C. M., Ulla, M. A., Rabuffetti, A. P. & Garello, N. 2017. Plastic pollution in freshwater ecosystems: macro-, meso-, and microplastic debris in a floodplain lake. *Environmental Monitoring and Assessment,* 189(581), pp. 1-13. DOI: 10.1007/s10661-017-6305-8.

Bradley, M. 2013. *Introduction to FTIR spectroscopy.* [Online] Available at: https://www.thermofisher.com/za/en/home/industrial/spectroscopy-elemental-isotope-analysis/spectroscopy-elemental-isotope-analysis-learning-center/molecular-spectroscopy-information/ftir-information/ftir-basics.html [2020, June 9].

Brantley, W., Berzins, D., Iijima, M., Tufekçi, E. & Cai, Z. 2017. 1 - Structure/property relationships in orthodontic alloys. In: T. Eliades & W. A. Brantley, eds. *Orthodontic Applications of Biomaterials.* s.l.: Woodhead Publishing & Elsevier, pp. 3-38. DOI: 10.1016/B978-0-08-100383-1.00001-1.

Briscoe, B. J. & Sinha, S. K. 1999. Hardness and Normal Indentation of Polymers. In: *Swallowe G.M. (eds) Mechanical Properties and Testing of Polymers. Polymer Science and Technology Series.* s.l.: Springer, Dordrecht, pp. 113-122. DOI: 10.1007/978-94-015-9231-4_25.

Buxbaum, L. H. 1968. The Degrdation of Poly(ethylene terephthalate). *Angewandte Chemie International Edition,* 7(3), pp. 182-190. DOI: 10.1002/anie.196801821.

Callister, W. D. & Rethwisch, D. G. 2015. *Materials Science and Engineering.* 9th ed. Asia.: John Wiley & Sons.

Cambridge University Engineering Department. 2003 Materials Data Book. [Online] Available at: http://www-mdp.eng.cam.ac.uk/web/library/enginfo/cueddatabooks/materials.pdf [2020, November 14].

Cao, W. 2016. *Semiconductor Photocatalysis: Materials, Mechanisms and Applications.* Rijeka, Croatia: InTech.

Capone, C., Di Landro, L., Inzoli, F., Penco, M. & Sartore, L. 2007. Thermal and mechanical degradation during polymer extrusion processing. *Polymer Engineering & Science,* 28 September, 47(11), pp. 1813-1819. DOI: 10.1002/pen.20882.

Celina, M., Ottesen, D. K., Gillen, K. T. & Clough, R. L. 1997. FTIR emission spectroscopy applied to polymer degradation. *Polymer Degradation and Stability,* 58(1-2), pp. 15-31. DOI: 10.1016/S0141-3910(96)00218-2.

Chaisupakitsin, M., Chairat-utai, P. & Jarusiripot, C. 2019. Degradation of polyethylene terephthalate bottles after long sunlight exposure. *Songklanakarin Journal of Science & Technology*, 41(2), pp. 259-264. [Online] Available at: https://rdo.psu.ac.th/sjstweb/journal/41-2/2.pdf [2020, May 28]

Chamas, A., Moon, H., Zheng, J., Qui, Y., Tabassum, T., Jang, J.H., Abu-Omar, M., Scott, S.L. & Suh, S. 2020. Degradation Rates of Plastics in the Environment. *ACS Sustainable Chemistry & Engineering,* 8(9), pp. 3494-3511. DOI: 10.1021/acssuschemeng.9b06635.

Chelliah, A., Subramaniam, M., Gupta, R. & Gupta, A. 2017. Evaluation on the Thermo-Oxidative Degradation of PET using Prodegradant Additives. *Indian journal of science and technology*, 10(6). DOI: 10.17485/ijst/2017/v10i6/111212

Chen, Z. 2012. *The Crystallization of Poly(ethylene terephthalate) Studied by Thermal Analysis and FTIR Spectroscopy.* MA thesis. Birmingham: University of Birmingham.

Clearpak. 2017. Polyethylene Terethphalate (PET). [Online] Available at: http://www.clearpak.com/site/clear-plastic-packaging-materials/pet-polyethylene-terethphalate-plastic [2019, June 29].

Climates To Travel World Climate Guide. n.d. *Climate - South Africa.* [Online] Available at: https://www.climatestotravel.com/climate/south-africa [2019, June 29].

Crawford, C. B. & Quinn, B. 2016. Physiochemical properties and degradation. In: *Microplastic Pollutants.* s.l.: Elsevier, pp. 57-100.

Crawford, R. 1982. Microhardness testing of plastics. *Polymer Testing,* 3(1), pp. 37-54. DOI: 10.1016/0142-9418(82)90011-3.

Crawford, R. J. & Thorne, J. L. 2002. Chapter 2 – Rotational molding polymers. In: *Rotational Molding Technology.* s.l.: William Andrew Publishing, pp. 19-68. [Online] Available at: http://www.sciencedirect.com/science/article/pii/B9781884207853500046 [2020, November 12].

Crompton, T. R. 1993. Functional Groups in Polymers. In: *Practical Polymer Analysis*. Boston: Springer, pp. 241-255.

Deepa, A., Jayakrishna, K. & Rajiyalakshmi, G. 2018. 12 - Fracture surface morphologies in the understanding of composite structural behavior. In: *Structural Health Monitoring of Biocomposites, Fibre-Reinforced Composites and Hybrid Composites.* 256: Elsevier, p. 243.

Department of Environmental Affairs. 2018. *South African water quality guidelines for coastal marine waters - Volume 1: Natural Environment and Mariculture Use.* [Online] Available at: https://www.environment.gov.za/sites/default/files/docs/waterqualityguideline2018.pdf [2019, May 29].

Derraik, J. G. 2002. The pollution of the marine environment by plastic debris: A review. *Marine Pollution Bulletin,* 44(9), pp. 842-852. DOI: 10.1016/S0025-326X(02)00220-5.

Dony, A., Ziyani, L., Drouadaine, I., Pouget, S., Faucon-Dumont, S., Simard, D., Mouillet, V., Poirier, J.E., Gabet, T., Boulange, L., Nicolai, A. & Gueit, C. 2016.MURE National Project: FTIR spectroscopy study to assess ageing of asphalt. in *6th Eurasphalt & Eurobitume Congress,* Prague, Czech Republic. DOI: 10.14311/EE.2016.154.

Fayolle, B., Richaud, E., Colin, X. & Verdu, J. 2008. Review: degradation-induced embrittlement in semi-crystalline polymers having their amorphous phase in rubbery state. *Journal of Materials Science volume,* 43(22), pp. 6999-7012. DOI: 10.1007/s10853-008-3005-3.

Fioletov, V., Kerr, J. B. & Fergusson, A. 2010. The UV Index: Definition, Distribution and Factors Affecting It. *Canadian Journal Of Public Health,* 101(4), pp. 15-19. DOI: 10.1016/j.atmosres.2012.01.005.

Fotopoulou, K. N. & Karapanagioti, H. K. 2017. Degradation of Various Plastics in the Environment. In: *The Handbook of Environmental Chemistry.* s.l.: Springer, pp. 77-91. DOI: 10.1007/698_2017_11.

Friedrich, J. 2018. Functional Groups at Polymer surface and Their Reactions. In: *Metal-polymer Systems: Interface Design and Chemical Bonding.* s.l.: John Wiley & Sons, pp. 135-172. DOI: 10.1002/9783527679898.ch5.

Güçlü, G., Yalçınyuva, T., Özgümüş,, S. & Orbay, M. 2003. Hydrolysis of waste polyethylene terephthalate and characterization of products by differential scanning calorimetry. *Thermochimica Acta, 4*04(1-2), pp. 193-205. DOI: 10.1016/S0040-6031(03)00160-6

Gewert, B., Plassmann, M. M. & MacLeod, M. 2015. Pathways for degradation of plastic polymers floating in the marine environment. *Environmental Science Processes & Impacts,* 17(9), pp. 1513-1521. DOI: 10.1039/C5EM00207A.

Ghobadi, E., Marquardt, A., Zirdehi, E.M., Neuking, K., Varnik, F., Eggeler, G. & Steeb, H. 2018. The Influence of Water and Solvent Uptake on Functional Properties of Shape-Memory Polymers. *International Journal of Polymer Science*. DOI: 10.1155/2018/7819353.

Gijsman, P. 2008. Review on the thermo-oxidative degradation of polymers during processing and in service. *E-Polymers,* 8(1). DOI: 10.1515/epoly.2008.8.1.727.

Gok, A. 2016. *Degradation pathway model of poly(ethylene-terephthalate) under accelerated weathering conditions,* PhD thesis. Cleveland: Case Western Reserve University.

Gotro, J. 2013. *Bio-Based Polypropylene: Multiple Synthetic Routes Under Investigation*, *Polymer Innovation Blog*. [Online] Available at: https://polymerinnovationblog.com/bio-based-polypropylene-multiple-synthetic-routes-under-investigation [2019, March 20].

Green, D. W. & Perry, R. H. 2007. *Perry's Chemical Engineers' Handbook.* 8th ed. United States of America: McGraw Hill.

Griffin, J., Wilkins, J. & Bowen, D. 2018. *The plastic problem: How much plastic pollution is in our ocean?.* [Online] Available at: https://www.aquarium.co.za/blog/entry/The-plastic-problem-How-much-plastic-pollution-is-in-our-ocean [2019, May 29].

Guanyu Tube. 2008-2020. Hardness Conversion Chart. [Online] Available at: https://tubingchina.com/Hardness-Conversion-Calculator.htm [2020, November 14].

Heimowska, A., Krasowska, K. & Rutkowska, M. 2014. Degradability of Different Packaging Polymeric Materials in Sea Water. in *The 12th Annual General Assembly of IAMU*, s.l., s.n., pp. 154-163. [Online] Available at: https://pdfs.semanticscholar.org/2a09/3d15b0458f38c8799450e597a14cd14afb8a.pdf [2019, Febuary 12]

Herrmann, K. 2011. *Hardness Testing - Principles and Applications.* United States of America: ASM International.

Hindle, C. 2019 *Polypropylene (PP)*, *British Plastics Federation*. [Online] Available at: https://www.bpf.co.uk/plastipedia/polymers/pp.aspx [2019, March 20].

Hofko, B., Porot, L., Falchetto Cannone, A., Poulikakos, L., Huber, L., Lu, X., Mollenhauer, K., Grothe, H. 2018. FTIR spectral analysis of bituminous binders: reproducibility and impact of ageing temperature. *Materials and Structures,* 51(45). DOI: 10.1617/s11527-018-1170-7.

Holland, B. & Hay, J. 2002. The thermal degradation of PET and analogous polyester measured by thermal analysis-Fourier transform infrared spectroscopy. *Polymer,* 43(6), pp. 1835-1847. DOI: 10.1016/S0032-3861(01)00775-3.

Huang, S. J. 1989. Biodegradation. In: *Comprehensive Polymer Science and Supplemements, vol 6, Polymer Reactions.* s.l., s.n., pp. 597-606.

Hunt, I. 2006. *Chapter 3: Conformations of Alkanes and Cycloalkanes.* [Online] Available at: http://www.chem.ucalgary.ca/courses/351/Carey5th//Ch03/ch3-02.html [2020, June 25].

Izdebska, J. & Thomas, S. 2016. *Printing on Polymers: Fundamentals and Applications.* United States of America: William Andrew Publishing & Elsevier.

Jambeck, J. 2018. *Marine Plastics.* [Online] Available at: https://ocean.si.edu/conservation/pollution/marine-plastics [2019, May 30].

Jung, M. R., Horgen, F. D., Orski, S. V., Rodrigueez, V. C., Beers, K. L., Balazs, G. H., Jones, T. T., Work, T. M., Brignac, K. C., Royer, S. J., Hyrenbach, D. K., Jensen, B. A. & Lynch, J. M. 2018. Validation of ATR FT-IR to Identify Polymers of Plastic Marine Debris, including Those Ingested by Marine Organisms. *Marine Pollution Bulletin,* Volume 127, pp. 704-16. DOI: 10.1016/j.marpolbul.2017.12.061.

Kaczmarek, H., S´wic¸catek, M. & Kamin´ ska, A. 2004. Modification of polystyrene and poly(vinyl chloride) for the purpose of obtaining packaging materials degradable in the natural environment. *Polymer Degradation and Stability,* 83(1), pp. 35-45. DOI: 10.1016/S0141-3910(03)00202-7.

Kamrannejad, M.M., Hasanzadeh, A., Nosoudi, N.A., Mai, L. & Nanaluo, A.A. 2014. Photocatalytic degradation of polypropylene/TiO2 nano-composites. *Materials Research,* 17(4), pp. 1039-1046. DOI: 10.1590/1516-1439.267214.

Kaufmann, E. N. 2003. Mechanical testing. In: *Characterization of Materials.* US: John Wiley & Sons, pp. 279-336.

Kool-a-sun. n.d. *Ultra-Violet (UV) Radiation.* [Online] Available at: https://koolasun.co.za/UV-rays.html [2020, June 1].

Lee, R. & Coote, M. L. 2016. Mechanistic insights into ozone-initiated oxidative degradation of saturated hydrocarbons and polymers. *Physical Chemistry Chemical Physics*, Volume 18, pp. 24663-24671. DOI: 10.1039/c6cp05064f.

LibreTexts. 2019. *Infrared Spectroscopy Absorption Table.* [Online] Available at: https://chem.libretexts.org/Bookshelves/Ancillary_Materials/Reference/Reference_Tables/Spectroscopic_Parameters/Infrared_Spectroscopy_Absorption_Table [2020, May 4].

Liu, X., Niu, H., Li, Y. & Dong, J.Y. 2018. New effort to synthesize star isotactic polypropylene. *Polymer Chemistry,* 9(24), pp. 3347-3354. DOI: 10.1039/C8PY00318A.

Longo, C., Savaris, M., Zeni, M., Brandalise, R. N. & Grisa, A. M. C. 2011. Degradation Study of Polypropylene (PP) and Bioriented Polypropylene (BOPP) in the Environment. *Materials Research,* 14(4), pp. 442-448. DOI: 10.1590/S1516-14392011005000080.

Lopez, J. 1993. Microhardness Testing of Plastics: Literature Review. *Polymer Testing,* 12(5), pp. 437-458. DOI: 10.1016/0142-9418(93)90016-I.

Ma, J., Yu, P., Xia, B. & An, Y. 2019. Effect of salt and temperature on molecular aggregation behavior of acrylamide polymer. *e-Ploymers,* 19(1), pp. 594-606. DOI: 10.1515/epoly-2019-0063.

Mackenzie, F. T., Duxbury, A. C. & Byrne, R. H. 2018. *Seawater.* [Online] Available at: https://www.britannica.com/science/seawater [2019, May 29].

Mark, H. 1948. Purity and Identity of Polymers. *Analytical Chemistry,* 20(2), pp. 104-110. DOI: 10.1021/ac60014a005.

Marionnet, C., Tricaud, C. & Bernerd, F. 2015. Exposure to Non-Extreme Solar UV Daylight: Spectral Characterization, Effects on Skin and Photoprotection. *International Journal of Molecular Sciences,* 16(1), pp. 68-90. DOI: 10.3390/ijms16010068.

Mellor, D., Moir, A. & Scott, G. 1973. The effect of processing conditions on the U.V. stability of polyolefins. *European Polymer Journal,* 9(3), pp. 219-225. DOI: 10.1016/0014-3057(73)90129-8.

Merck KGaA, 2020. *IR Spectrum Table & Chart.* [Online] Available at: https://www.sigmaaldrich.com/technical-documents/articles/biology/ir-spectrum-table.html [2020, May 4].

Meteo Blue Climate Cape Town. 2020. *Climate Cape Town.* [Online] Available at: https://www.meteoblue.com/en/weather/historyclimate/climatemodelled/cape-town_south-africa_3369157 [2020, June 13].

Meyer, T. & Keurentjes, J. T. 2005. *Handbook of Polymer Reaction Engineering.* Weinheim: Wiley-VCH.

Michiels, Y., Van Puyvelde, P. & Sels, B. F. 2017. Barriers and Chemistry in a Bottle: Mechanisms in Today's Oxygen Barriers for Tomorrow's Materials. *Applied Sciences,* 7(7), pp. 1-30. DOI: 10.3390/app7070665.

Michler, G. H. 2008. Amorphous Polymers. In: Electron Microscopy of Polymers. Berlin: Springer Laboratory, pp. 277-293. DOI: 10.1007/978-3-540-36352-1_16.

Mohee, R. & Unmar, G. 2007. Determining biodegradability of plastic materials under controlled and natural composting environments. *Waste Management,* 27(11), pp. 1486-1493. DOI: 10.1016/j.wasman.2006.07.023.

Moore, C. J., Moore, S. L., Leecaster, M. K & Weisberg, S. B. 2001. A Comparison of Plastic and Plankton in the North Pacific Central Gyre. *Marine Pollution Bulletin*, 42(12), pp. 1297–1300. DOI: 10.1016/S0025-326X(01)00114-X.

Moss, G. 1996. Basic Terminology of Stereochemistry. *International union of pure and applied Chemistry,* 68(12), pp. 2193-2222. DOI: 10.1351/pac199668122193.

Muscato, C. 2015. *Organic Molecules: Functional Groups, Monomers & Polymers.* [Online] Available at: https://study.com/academy/lesson/organic-molecules-functional-groups-monomers-polymers.html [2020, May 4].

Mylläri, V., Ruoko, T.-P. & Syrjälä, S. 2015. A comparison of rheology and FTIR in the study of polypropylene and polystyrene photodegradation. *Journal of Applied Polymer Science,* 132(28). DOI: 10.1002/app.42246.

Naga, N., Sakai, H., Usui, C. & Tomoda, H. 2010. Synthesis of polyethylene and polypropylene containing fluorene units in the side chain. *Journal of Polymer Science Part A: Polymer Chemistry,* 48(16), pp. 3542-3552. DOI: 10.1002/pola.24131.

O'Brine, T. & Thompson, R. C. 2010. Degradation of plastic carrier bags in the marine environment. *Marine Pollution Bulletin,* 60(12), pp. 2279-2283. DOI: 10.1016/j.marpolbul.2010.08.005.

Olesen, K.B., van Alst, N., Simon, M., Vianello, A., Liu, F. & Vollertsen, J. 2018. *Analysis of Microplastics using FTIR Imaging.* USA: Agilent Technologies .

Omnexus. n.d. *Water Absorption 24 hours.* [Online] Available at: https://omnexus.specialchem.com/polymer-properties/properties/water-absorption-24-hours [2020, May 24].

Pires, H., Mendes, L., Cestari, S., Pita, V. 2015. Effect of Weathering and Accelerated Photoaging on PET/PC (80/20 wt/wt%) Melt Extruded Blend. *Material Research*, 18(4), pp. 763-768. DOI: 10.1590/1516-1439.010115

Pirzadeh, E., Zadhoush, A. & Haghighat, M. 2007. Hydrolytic and thermal degradation of PET fibers and PET granule: The effects of crystallization, temperature, and humidity. *Journal of Applied Polymer Science,* 106(3), pp. 1544-1549. DOI: 10.1002/app.26788.

Predecki, P. & Karr, P. H. 1978. An improved method for determining polymer melting temperatures. *Polymer Engineering and Science,* 18(1), pp. 1-5. DOI: 10.1002/pen.760180102.

Reich, L. & Stivala, S. S. 1971. *Elements of polymer degradation.* s.l.: McGraw-Hill.

Resmeriță, A., Coroaba, A., Darie, R., Doroftei, F., Spiridon, I., Simionescu, B & Navardb, P. (2018). Erosion as a possible mechanism for the decrease of size of plastic pieces floating in oceans. *Marine Pollution Bulletin,* 127, pp. 387–395. DOI: 10.1016/j.marpolbul.2017.12.025.

Robert, J. D. & Caserio, M. C. 2019. *Conformational Isomers.* [Online] Available at: https://chem.libretexts.org/Bookshelves/Organic_Chemistry/Book%3A_Basic_Principles_of_Organic_Chemistry_(Roberts_and_Caserio)/05%3A_Stereoisomerism_of_Organic_Molecules/5.03%3A_Conformational_Isomers [2020, June 25].

Rogeaux, A., Carter, A., Perraton, D. & Daoudi, A. 2019. Effect of artificial ageing on two different bitumen of different origin but same performance grade. In: L. D. Poulikakos, *et al*. eds. *RILEM 252-CMB Symposium: Chemo-Mechanical Characterization of Bituminous Materials.* s.l.: Springer, pp. 27-32. DOI: 10.1007/978-3-030-00476-7_5.

Romão, W., Franco, M.F., Corilo, Y.E., Eberlin, M.N., Spinacé, M.A. & De Paoli, M.A. 2009. Poly (ethylene terephthalate) thermo-mechanical and thermo-oxidative. *Polymer Degradation and Stability,* 94(10), pp. 1849-1859. DOI: 10.1016/j.polymdegradstab.2009.05.017.

Rosario, L. & Dell, E. 2010. *Biodegradability of plastics testing in an undergraduate materials laboratory course.* s.l.: American Society for Engineering Education. [Online] Available at: https://peer.asee.org/biodegradability-of-plastics-testing-in-an-undergraduate-materials-laboratory-course.pdf [2019, January 23].

Rouba, N., Sadoun, T., Boutagrabet, N., Kerrouche, D., Zadi, S. & Mimi, N. 2015. Thermo-Oxidation and Biodegradation Study of Low-Density Polyethylene /Starch Films by IR Spectroscopy. *Iranian Journal of Chemistry and Chemical Engineering ,* 34(4), pp. 69-78.

Rouillon, C., Bussiere, P.O., Desnoux, E., Collin, S., Vial, C., Therias, S. & Gardette, J.L. 2016. Is carbonyl index a quantitative probe to monitor polypropylene photodegradation? *Polymer Degradation and Stability,* Volume 128, pp. 200-208. DOI: 10.1016/j.polymdegradstab.2015.12.011.

RS Components, n.d. *Lighting Ignitors*. [Online] Available at: https://za.rs-online.com/web/c/lighting/lighting-components-accessories/lighting-ignitors/ [2020, October 30].

RTI Laboratories. 2015. *FTIR Analysis.* [Online] Available at: https://rtilab.com/techniques/ftir-analysis/ [2019, May 05].

Rubin, I. I. 1990. Handbook Of Plastic Materials And Technology. New York: John Wiley & Sons, Inc.

SA Weather (WX) Forecasts. 2020. *What is the UV Index?.* [Online] Available at: https://sawx.co.za/uv-index-south-africa/ [2020, June 27].

SADCO. 1999. *Combination Of Temperature And Salinity.* [Online] Available at: http://app01.saeon.ac.za/sadcofunstuff/TempSalinity.htm [2020, July 22].

Scheirs, J. & Gardette, J.L. 1997. Photo-oxidation and photolysis of poly(ethylene naphthalate). *Polymer Degradation and Stability,* 56(3), pp. 339-350. DOI: 10.1016/S0141-3910(96)00199-1.

Shah, V. 2007. Appendix 1. In: *Handbook of Plastics Testing and Failure Analysis*. 3rd ed. s.l.:John Wiley & Sons, Inc., pp. 560-617. [Online] Available at: https://onlinelibrary.wiley.com/doi/pdf/10.1002/9780470100424.app9 [2020, November 14].

Sichina, W. J. 2000. *DSC as Problem Solving Tool: Measurement of Percent Crystallinity of Thermoplastics,* Norwalk: PerkinElmer Instruments. DOI: 10.1007/BF00007115.

Signor, A.W., Chin, J.W. & VanLandingham, M.R. 2003. Effects of Ultraviolet Radiation Exposure on Vinyl Ester Matrix Resins: Chemical and Mechanical Characterization. Polymer Degradation and Stability, 79(2), pp. 359-368. DOI: 10.1016/S0141-3910(02)00300-2.

Silberg, M. 2013. Principles of General Chemistry. International edition ed. New York: McGraw-Hill.

Smallman, R. & Ngan, A. 2014. Chapter 5 - Characterization and Analysis. In: R. Smallman & A. Ngan, eds. *Modern Physical Metallurgy.* Eighth ed. s.l.: Butterworth-Heinemann, pp. 159-250.

Smith, B. C. 2017. The Carbonyl Group, Part I: Introduction. *Spectroscopy,* 32(9), pp. 31-35.

Sobków, D. & Czaja, K. 2003. Influence of accelerated ageing conditions on the process of polyolefins degradation. *Polimery,* 48(9), p. 627. DOI: 10.14314/polimery.2003.627.

Subramanian, M. N. 2017. Polymer Properties. In: *Polymer Blends and Composites Chemistry and Technology.* s.l.: John Wiley & Sons.

Sugiura, M., Mitsuoka, T., Murase, A. & Ueda, K. 2000. Distribution Analysis of Hydroxyl Groups in Polymers by Derivatization-Electron Probe X-ray Microanalysis. *Analytical Sciences,* 16(12), pp. 1313-1315. DOI: 10.2116/analsci.16.1313.

Summers, J., Rabinovitch, E., & Qeensbury, G. 1983. Predicting heat buildup due to the sun's energy. *Journal of Vinyl Technology, 5*(3), pp. 110. DOI: 10.1002/vnl.730050308.

Sundararajan, G. & Roy, M. 2001. Hardness Testing. In: *Encyclopedia of Materials: Science and Technology (Second Edition).* s.l.: Elsevier, pp. 3728-3736.

Tosin, M., Weber, M., Siotto, M., Lott, C. & Innocenti, F. 2012. Laboratory test methods to determine the degradation of plastics in marine environmental conditions. *Frontiers in Microbiology* 3(225). DOI: 10.3389/fmicb.2012.00225

UCLA College Chemistry & Biochemistry. 2001. *Infrared Spectroscopy Table.* [Online] Available at: https://www.chem.ucla.edu/~bacher/General/30BL/IR/ir.html [2020, May 4].

University of Cambridge. 2004-2020. *Crystallinity in Polymers.* [Online] Available at: doitpoms.ac.uk/tlplib/polymers/summary.php [2020, April 12].

University of Puget Sound. n.d. *Characteristic IR Absorption Frequencies of Organic Functional Groups.* [Online] Available at: www2.ups.edu/faculty/hanson/Spectroscopy/IR/IRfrequencies.html [2020, May 4].

Vaillant, D., Lacoste, J. & Dauphin, G. 1994. The oxidation mechanism of polypropylene: contribution of 13C-NMR spectroscopy. *Polymer Degradation and Stability,* 45(3), pp. 355-360. DOI: 10.1016/0141-3910(94)90205-4.

Venkatachalam, S., Nayak, S. G., Labde, J. V., Gharal, P.R., Rao, K. & Kelkar, A. K. 2012. Degradation and Recyclability of Poly (Ethylene Terephthalate). In: H. E. M. Saleh, ed. *Polyester.* s.l.: IntechOpen, pp.75-98.

Weather Atlas. n.d. *Monthly weather forecast and climate Cape Town, South Africa.* [Online] Available at: weather-atlas.com/en/south-africa/cape-town-climate [2020, June 3].

Weather Spark. n.d. *Average Weather in Cape Town South Africa.* [Online] Available at: https://weatherspark.com/y/82961/Average-Weather-in-Cape-Town-South-Africa-Year-Round [2020, June 3].

Webb, H. K., Arnott, J., Crawford, R. J. & Ivanova, E. P. 2013. Plastic Degradation and Its Environmental Implications with Special Reference to Poly(ethylene terephthalate). *Polymers,* 5(1), pp. 1-18. DOI: 10.3390/polym5010001.

Wellfair, S. T. 2008. Testing the Degradation Rates of Degradable, Non-degradable and Bio-degradable Plastics Within Simulated Marine Environments. *The Plymouth Student Scientist,* 1(2), pp. 243-301.

World Sea Temperature. 2020. *South Africa Sea temperatures.* [Online] Available at: seatemperature.org/africa/south-africa/ [2019, May 29].

World Weather Online. 2020. *Cape Town Historical Weather.* [Online] Available at: https://www.worldweatheronline.com/cape-town-weather-history/western-cape/za.aspx [2020, June 13].

Xio, A., Wang, L., Liu, Q., Yu, H. & Dong, X. 2008. Synthesis of Low Isotactic Polypropylene Using MgCl2/AlCl3-supported Ziegler–Natta Catalysts Prepared Using the One-Pot Milling Method. *Designed Monomers and Polymers,* 11(2), pp. 139-145. DOI: 10.1163/156855508X298044.

Xu, W., Yin, X., He, G., Zhao, J. & Wang, H. 2012. Photografted temperature-sensitive poly(N-isopropylacrylamide) thin film with a superfast response rate and an interesting transparent-opaque-transparent change in its deswelling process. Soft Matter, 8(11), pp. 3105-3111. DOI: 10.1039/C2SM07404D.

Yan, C., Xiao, F., Huang, W. & Lv, Q. 2018. Critical matters in using Attenuated Total Reflectance Fourier Transform Infrared to characterize the polymer degradation in Styrene–Butadiene–Styrene-modified asphalt binders. *Polymer Testing,* Volume 70, pp. 289-296. DOI: 10.1016/j.polymertesting.2018.07.019.

Ye, Z. & Zhu, S. 2003. Synthesis of branched polypropylene with isotactic backbone and atactic side chains by binary iron and zirconium single-site catalysts. *Journal of Polymer Science Part A: Polymer Chemistry,* 41(8), pp. 1152-1159. DOI: 10.1002/pola.10653.

Zhang, Z., Jiang, B., He, F., Fu, Z., Xu, J. & Fan, Z. 2019. Comparative Study on Kinetics of Ethylene and Propylene Polymerizations with Supported Ziegler–Natta Catalyst: Catalyst Fragmentation Promoted by Polymer Crystalline Lamellae. *Polymers,* 11(2). DOI: 10.3390/polym11020358.

Zhao, X., Li, Z., Chen, Y., Shi, L. & Zhu, Y. 2007. Solid-phase photocatalytic degradation of polyethylene plastic under UV and solar light irradiation. *Journal of Molecular Catalysis A: Chemical*, 268(1-2), pp. 101-106. DOI: 10.1016/j.molcata.2006.12.012.

APPENDIX A – SAMPLE CALCULATIONS

Degree of crystallinity

a) For PET:

Open melting endotherm for PET sample and run: "Sigmoidal Horizontal Peak Integration" between 110˚C – 150˚C and 200˚C – 270˚C, the software will yield a figure with values as seen below.

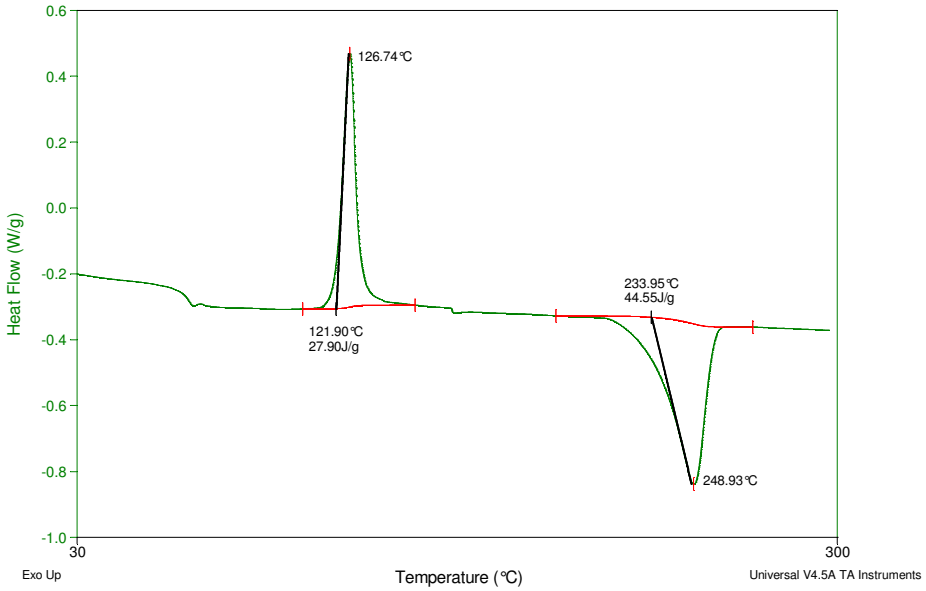

From the figure obtain the necessary values as seen in the table:

Onset T	ΔH_m (J/g)	Peak T (in ˚C)	Onset T_C	ΔH_c (J/g)	Peak T_c (in ˚C)	ΔH_m^o (J/g)	H_f (J/g)
233.95	44.55	248.93	121.9	27.9	126.74	140.1	140

Apply values to crystallinity formula and obtain %crystallinity:

$$\%Crystallinity = \frac{\Delta H_m - \Delta H_c}{\Delta H_m^o} \times 100\%$$

$$\%Crystallinity = \frac{44.5 - 27.9}{140.1} = 11.8844 \approx 12\%$$

b) For polypropylene:

Open melting endotherm for PET sample and run: "Sigmoidal Horizontal Peak Integration" between 120˚C – 180˚C, the software will yield a figure with values as seen below.

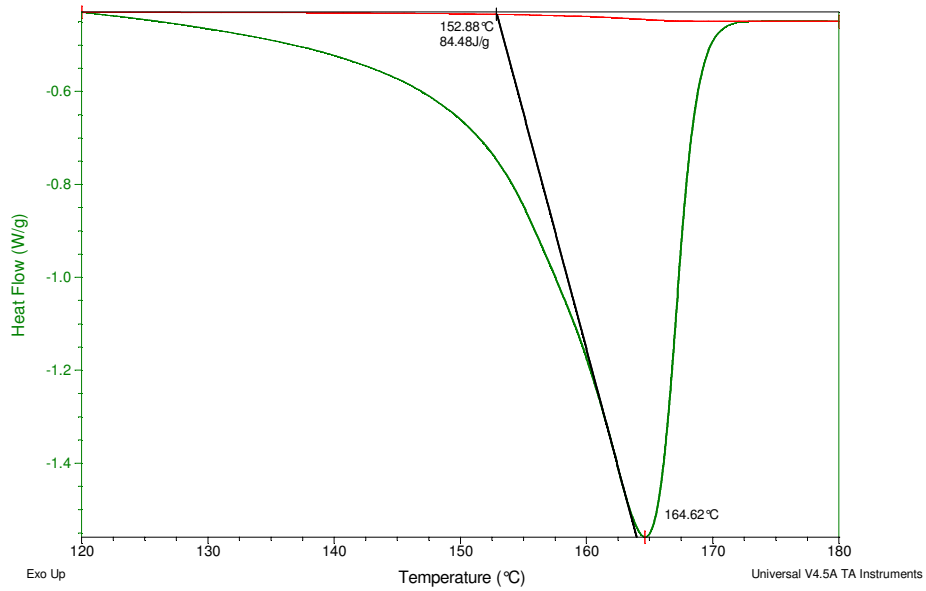

From the figure obtain the necessary values as seen in the table:

Onset T	ΔH_m (J/g)	Peak T (in ˚C)	ΔH_m^o (J/g)	H_f (J/g)
152.1	85.39	164.53	207.1	207

Apply values to crystallinity formula and obtain %crystallinity:

$$\%Crystallinity = \frac{\Delta H_m - \Delta H_c}{\Delta H_m^o} \times 100\%$$

$$\%Crystallinity = \frac{85.39 - 0}{207.1} = 41.2313 \approx 41\%$$

Reference to validate % crystallinity sample calculations: (Blaine, n.d.)

Hardness:

Apply diagonal lengths, as seen in table, to formula:

Sample	D1	D2
PETW0-25C-None-1	217.71	214.78

$$HV = \frac{300}{1000} \div \left(\left(\frac{217.71}{1000} \times \frac{214.78}{1000}\right) \times 0.5\right) = 12.8315 \approx 12.83$$

Functional group indices

a) Peak method

Sample: PETW0-25C-None-1

Obtain excel spreadsheet of FTIR graph data as explained in analysis procedure, this will yield a data set similar to the following table but with wavelengths from 400 cm^{-1} to 4000 cm^{-1}:

Wavelength in cm^{-1}	Transmittance value
2156.508	99.99%
2156.99	99.95%
2157.472	99.88%
2157.954	99.77%
2158.436	99.63%
2158.918	99.46%
2159.401	99.28%
2159.883	99.10%
2160.365	98.95%
2160.847	98.84%
2161.329	98.78%
2161.811	98.77%
2162.293	98.78%
2162.775	98.80%
2163.258	98.81%
2163.74	98.81%
2164.222	98.79%
2164.704	98.79%
2165.186	98.80%
2165.668	98.84%
2166.15	98.90%
2166.632	98.96%
2167.115	99.02%
2167.597	99.08%
2168.079	99.13%
2168.561	99.18%
2169.043	99.23%
2169.525	99.29%
2170.007	99.35%
2170.489	99.40%
2170.971	99.44%
2171.454	99.46%
2171.936	99.48%
2172.418	99.50%
2172.9	99.52%
2173.382	99.56%
2173.864	99.59%
2174.346	99.61%
2174.828	99.60%
2175.311	99.58%

From table determine lowest value in the specific region of the functional group under investigation as well as lowest value region of reference.

For sample calculation the reference region of 2156.5 cm^{-1} – 2175 cm^{-1} was given as this was the smallest region and from this sample region in this specific sample the lowest value was 98.77% at 2161.811 cm^{-1}.

When both the functional group lowest value and reference lowest value is obtained – for example let us investigate the hydroxyl index. The lowest value in the hydroxyl region of 3000 – 3700 cm^{-1} was 96.58%.

Now obtain the absorbance values for both:

$$A_{OH} = 2 - \log(0.9658) \approx 2.015$$
$$A_{referance} = 2 - \log(0.9877) \approx 2.005$$

Using the index formula determine the hydroxyl index:

$$Functional\ group\ index = \frac{Max\ peak\ value\ in\ functional\ group\ range}{Max\ peak\ value\ in\ reference\ \ range}$$

$$\therefore OH\ index = \frac{2.015}{2.005} \approx 1.005$$

b) Area method

Similar to peak method obtain table of FTIR transmittance data with wavelengths from 400 cm^{-1} to 4000 cm^{-1}:

Wavelength in cm^{-1}	Transmittance value	Bar area
2156.508	99.99%	0.964011
2156.99	99.95%	0.964065
2157.472	99.88%	0.964184
2157.954	99.77%	0.964371
2158.436	99.63%	0.964627
2158.918	99.46%	0.96495
2159.401	99.28%	0.967322
2159.883	99.10%	0.965703
2160.365	98.95%	0.966055
2160.847	98.84%	0.966331
2161.329	98.78%	0.966506
2161.811	98.77%	0.96658
2162.293	98.78%	0.96658
2162.775	98.80%	0.966546
2163.258	98.81%	0.968521
2163.74	98.81%	0.96651
2164.222	98.79%	0.966526
2164.704	98.79%	0.966543
2165.186	98.80%	0.966533
2165.668	98.84%	0.966479
2166.15	98.90%	0.96638
2166.632	98.96%	0.966253
2167.115	99.02%	0.968123
2167.597	99.08%	0.965994
2168.079	99.13%	0.965882
2168.561	99.18%	0.965777
2169.043	99.23%	0.965667
2169.525	99.29%	0.965547
2170.007	99.35%	0.965423
2170.489	99.40%	0.965307
2170.971	99.44%	0.965214
2171.454	99.46%	0.967152
2171.936	99.48%	0.965107
2172.418	99.50%	0.965071
2172.9	99.52%	0.965025
2173.382	99.56%	0.964965
2173.864	99.59%	0.964898
2174.346	99.61%	0.964846
2174.828	99.60%	0.964829
2175.311	99.58%	0.966858

Calculate the area under the curve for the specific region with numerical integration using the midpoint rectangle method in combination with the Riemann sum.

For example, area of rectangular bar between 2161.329 cm^{-1} and 2161.811cm^{-1}:

First convert to absorbance:

$$A_1 = 2 - \log(0.9878) \approx 2.005331$$
$$A_2 = 2 - \log(0.9877) \approx 2.005375$$

Calculate midpoint:

$$Midpoint = \frac{2.005331 + 2.005375}{2} \approx 2.005353$$

Determine absorbance bar area:

$$Area = 2.005353 \times (2161.811 - 2161.329) \approx 0.96658$$

Apply this to whole of wavelength spectrum and then calculate Riemann sum of specific region of the functional group under investigation as well as region of reference.

For example, Riemann sum of reference region given in table is:

$$Absorbance\ area_{reference} = \sum_{2156.508}^{2175.311} Bar\ area_i = 0.964011 + 0.964065 + \cdots + 0.966858 \approx 38.63$$

Now determine index, for example hydroxyl absorbance area was 1406.81 thus hydroxyl index is:

$$Functional\ group\ index = \frac{Absorbance\ area_{Functional\ group}}{Absorbance\ area_{reference}}$$
$$\therefore OH\ index = \frac{1406.81}{38.63} \approx 36.4$$

Hardness to tensile strength

Using conversion table obtained from Guanyu Tube (2020) plot tensile strength against Vickers microhardness and obtain linear regression line (see Figure 52).

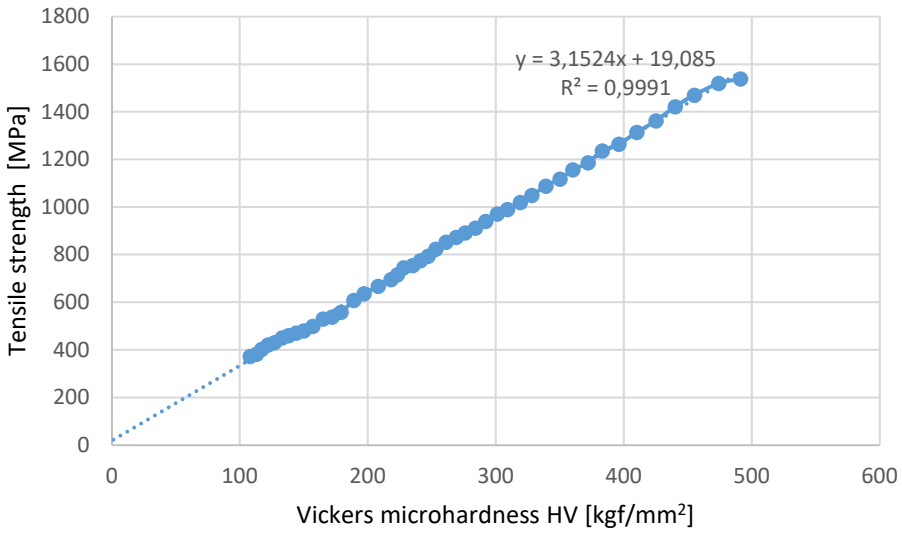

Figure 52: Plot of tensile strength against Vickers microhardness

Using the linear regression line a conversion can be made from hardness to tensile strength.

For example, covert 11.2 kgf/mm^2 to tensile strength in MPa:

$$Tensile\ strenght = 3.1524 \cdot x + 19.085$$
$$Tensile\ strenght = 3.1524 \cdot 11.2 + 19.085$$
$$Tensile\ sstrenght = 54.39188 \approx 54.4\ MPa$$

For example, covert 48.3 MPa to hardness in kgf/mm^2:

$$Tensile\ strenght = 3.1524 \cdot x + 19.085$$
$$48.3 = 3.1524 \cdot x + 19.085$$
$$\frac{48.3 - 19.085}{3.1524} = x$$
$$x = 9.267542 \approx 9.27 \frac{kgf}{mm^2}$$

APPENDIX B – INDEX CALCULATION METHODS SELECTION

Investigating the difference in calculation methods of FTIR indices, showed that for the most part, the trends stayed constant between the two methods. See Figure 53 for an example where the hydroxyl index calculated with area and peak method are compared.

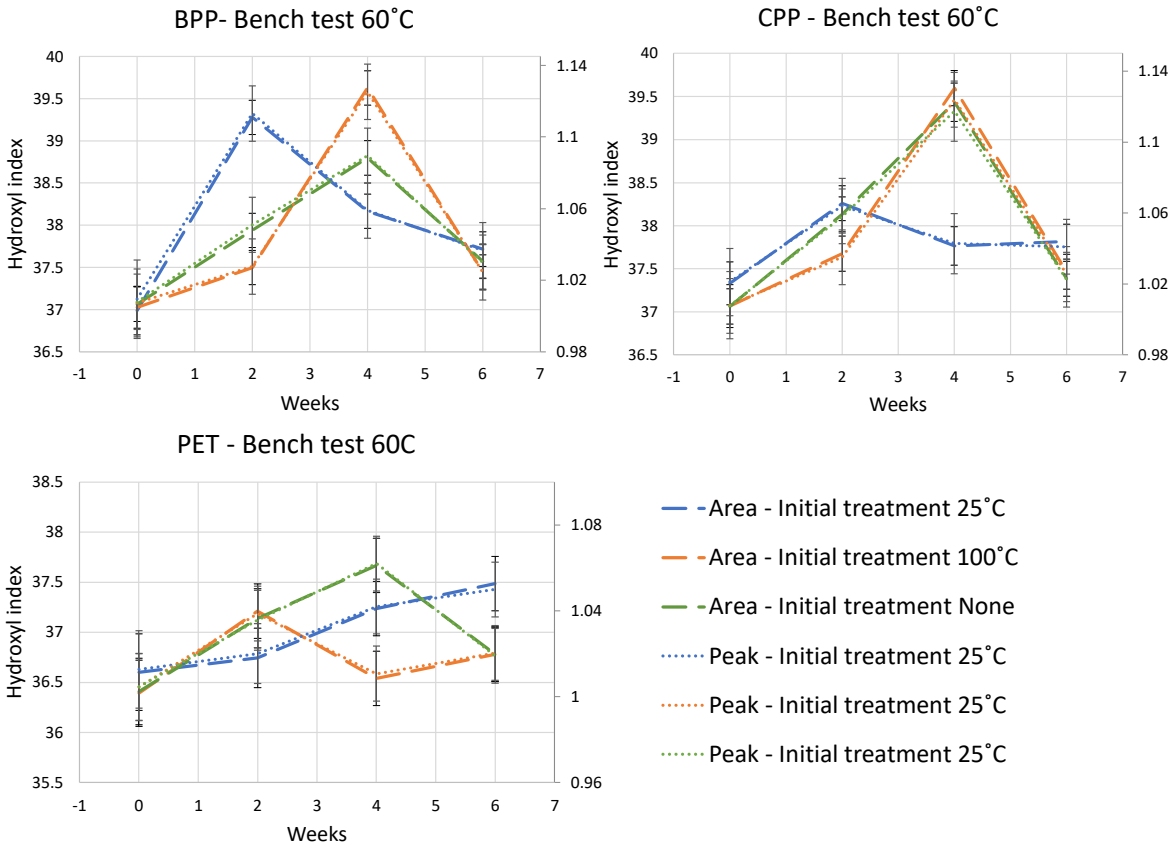

Figure 53: Comparison of area and peak method for calculating hydroxyl indices of samples from bench test treatment of 60˚C

Although the trends were similar the FTIR spectrum for each index were considered to determine if one method can be expected to be slightly more accurate than the other. From this investigation it was decided to use the area method for calculating the carbonyl and hydroxyl indices of polypropylene and the methanetriyl index of both PET and polypropylene. In most conditions both methods produced identical results, however under harsh conditions a slight difference was observed, see for example below explanation of carbonyl index.

For BPP and PET there were no observable differences in carbonyl index between the two methods, the only observation was that BPP exhibted greater uncertainty (larger error bars) when using the peak method. CPP also exhibited no difference between the two methods at the lower treatments, however, at UV radiance of 130 W/m^2, the area method exhibited more distinctive and greater differences in the index values compared to the peak method, see Figure 54.

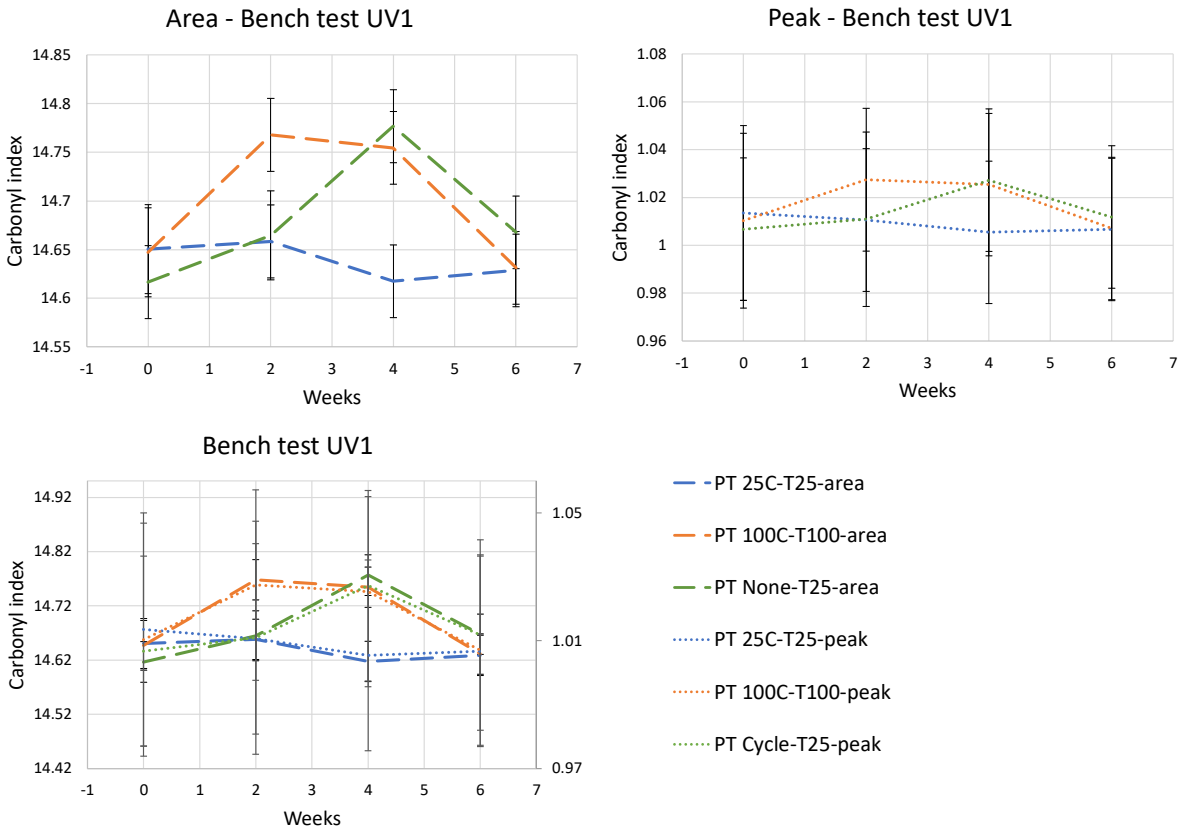

Figure 54: Comparing area and peak method for calculating carbonyl indices of CPP samples from bench test treatment of 130 W/m^2 UV radiance

This phenomenon can be explained by viewing Figure 55. The carbonyl index region for polypropylene exhibited a broadening of area rather than forming a dominant peak, as seen in Figure 55 with the red representing CPP. It is therefore suspected to be more reliable to use the area method for calculation of the carbonyl index for polypropylene than the peak method. Since the difference in peak height might not necessarily be significant while the difference in the area, which is larger, could be. In contrast, the PET exhibited a significant dominant carbonyl peak and exhibited secondary smaller peaks, as seen in Figure 55 (with the blue representing PET), which could influence the area method value at lower peak heights. It is therefore suspected that it would be more reliable to use the peak method for calculation of the carbonyl index for PET than the area method. Since the peak method will only include the main height of the carbonyl peak while the area method includes the additional error of the secondary peaks' area.

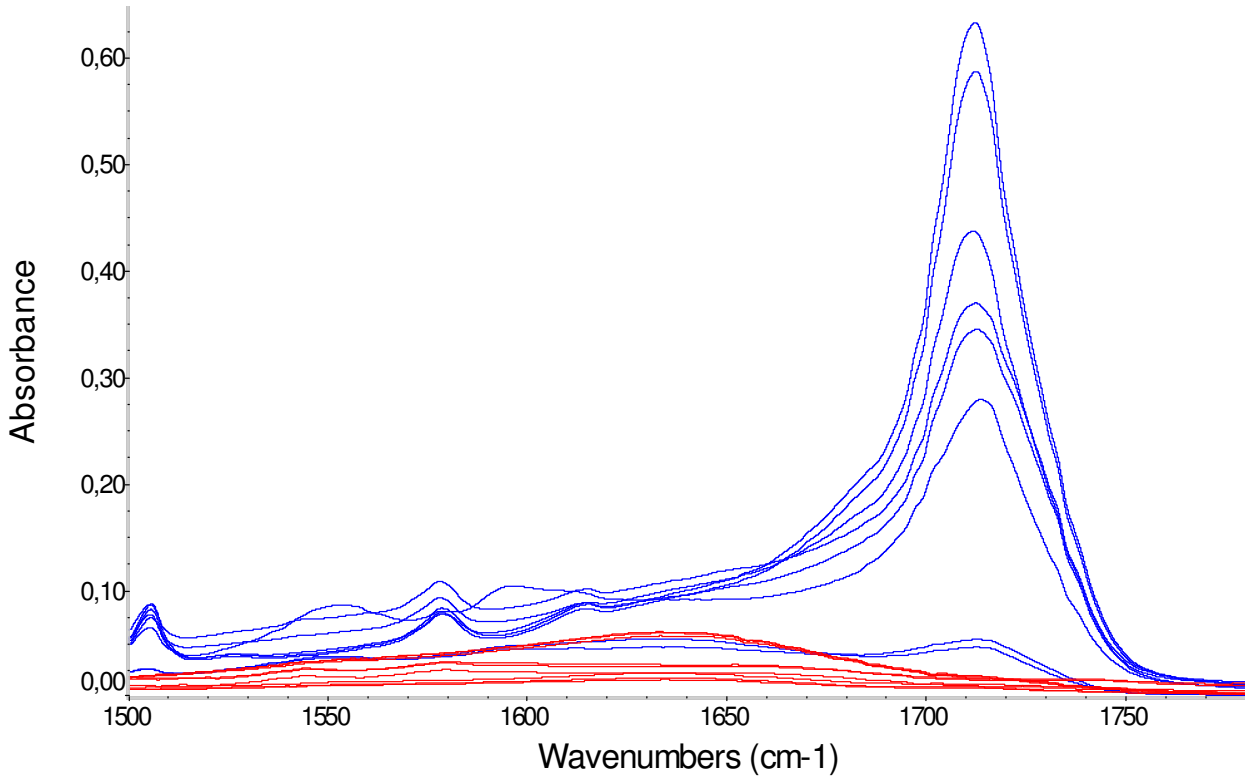

Figure 55: FTIR absorbance graphs for carbonyl region

In instances where differences was observed between the two methods, it was noted that the differences were mostly insignificant since the uncertainty (or error bars) intersected. It was therefore concluded that either method can be applied as long as it is kept constant, for that specific index, throughout the study.

APPENDIX C – ANOVA TABLES

Initial treatment

Table 8: ANOVA results for initial treatments

	%Crystallinity				Hardness			
Effect	Num. DF	Den. DF	F	p	Num. DF	Den. DF	F	p
Week	1	17	263	9.00E-12	1	45	0.01	9.13E-01
Plastic	2	18	8985	0.0E+00	2	45	279	0.0E+00
Initial treatment	2	18	196.4	6.00E-13	2	45	20.7	4.00E-07
Week*Plastic	2	17	143.8	2.00E-11	2	45	79.9	2.00E-15
Week*Initial treatment	2	17	196.4	2.00E-12	2	45	23.6	1.00E-07
Plastic*Initial treatment	4	18	81.8	3.00E-11	4	45	7.4	1.00E-04
Week*Plastic*Initial treatment	4	17	81.8	7.00E-11	4	45	8.4	4.00E-05
	Carbonyl index				Hydroxyl index			
Effect	Num. DF	Den. DF	F	p	Num. DF	Den. DF	F	p
Week	3	74	4.4	6.80E-03	3	74	3.5	1.87E-02
Plastic	2	41	3996.9	0.0E+00	2	41	34.6	2.00E-09
Initial treatment	2	41	0.6	5.33E-01	2	41	1.1	3.29E-01
Week*Plastic	6	74	14.1	1.00E-10	6	74	5.9	5.00E-05
Week*Initial treatment	6	74	10.3	3.00E-08	6	74	45.1	0.0E+00
Plastic*Initial treatment	4	41	7.7	1.00E-04	4	41	2.9	3.15E-02
Week*Plastic*Initial treatment	12	74	9.4	1.00E-10	12	74	3.9	1.00E-04
	Suspected methylene and methyl index				Suspected methanetriyl and methyl index			
Effect	Num. DF	Den. DF	F	p	Num. DF	Den. DF	F	p
Week	3	74	1.2	3.30E-01	3	74	1.2	3.01E-01
Plastic	2	41	7.8	1.30E-03	2	41	9.3	5.00E-04
Initial treatment	2	41	4.8	1.36E-02	2	41	3.5	3.82E-02
Week*Plastic	6	74	1.3	2.69E-01	6	74	1.7	1.25E-01
Week*Initial treatment	6	74	11.2	8.00E-09	6	74	8.8	3.00E-07
Plastic*Initial treatment	4	41	2.3	7.42E-02	4	41	1.4	2.51E-01
Week*Plastic*Initial treatment	12	74	2.4	1.00E-02	12	74	2.6	6.30E-03

Table 8 continued: ANOVA results for initial treatments

	Methanetriyl index			
Effect	Num. DF	Den. DF	F	p
Week	3	74	17.3	1.00E-08
Plastic	2	41	1850.4	0.0E+00
Initial treatment	2	41	25.6	6.00E-08
Week*Plastic	6	74	2.3	4.08E-02
Week*Initial treatment	6	74	11.4	6.00E-09
Plastic*Initial treatment	4	41	2	1.07E-01
Week*Plastic*Initial treatment	12	74	5.6	1.00E-06

Table 9: ANOVA table for initial treatment comparing CPP and BPP for colour additive effect investigation

	%Crystallinity				Hardness			
Effect	Num. DF	Den. DF	F	p	Num. DF	Den. DF	F	p
Week	1	11	44.7	3.45E-05	1	30	54.9	2.93E-08
Colour	1	12	41.5	3.21E-05	1	30	1.5	0.231207
Initial treatment	2	12	35.4	9.29E-06	2	30	2.4	0.104484
Week*Colour	1	11	19.9	0.000959	1	30	27.1	1.31E-05
Week*Initial treatment	2	11	59.1	1.3E-06	2	30	3.4	0.0485
Colour*Initial treatment	2	12	4.9	0.027098	2	30	0.8	0.475447
Week*Colour*Initial treatment	2	11	8.2	0.006589	2	30	1	0.362962
	Carbonyl index				Hydroxyl index			
Effect	Num. DF	Den. DF	F	p	Num. DF	Den. DF	F	p
Week	3	51	8	0.000187	3	51	3.8	0.016123
Colour	1	30	6.2	0.018493	1	30	19.2	0.000132
Initial treatment	2	30	21.9	1.35E-06	2	30	1.5	0.230281
Week*Colour	3	51	3.7	0.018303	3	51	9.4	4.82E-05
Week*Initial treatment	6	51	29	8.22E-15	6	51	36.4	1.11E-16
Colour*Initial treatment	2	30	0.4	0.665659	2	30	2.2	0.129812
Week*Colour*Initial treatment	6	51	1.4	0.244151	6	51	4.7	0.000683
	Suspected methylene and methyl index				Suspected methanetriyl and methyl index			
Effect	Num. DF	Den. DF	F	p	Num. DF	Den. DF	F	p
Week	3	51	2.7	0.055196	3	51	1.2	0.315847
Colour	1	30	4.8	0.036716	1	30	12.7	0.001231
Initial treatment	2	30	6.8	0.003778	2	30	5.5	0.008954
Week*Colour	3	51	1.3	0.296759	3	51	1.3	0.286902
Week*Initial treatment	6	51	13.9	2.83E-09	6	51	10.5	1.42E-07
Colour*Initial treatment	2	30	0.1	0.942431	2	30	0	0.973662
Week*Colour*Initial treatment	6	51	1.1	0.3926	6	51	1.4	0.228738
	Methanetriyl index							
Effect	Num. DF	Den. DF	F	p				
Week	3	51	16	1.81E-07				
Colour	1	30	4.5	0.041747				
Initial treatment	2	30	21.9	1.4E-06				
Week*Colour	3	51	2	0.131956				
Week*Initial treatment	6	51	13.6	3.99E-09				
Colour*Initial treatment	2	30	0.3	0.72989				
Week*Colour*Initial treatment	6	51	3.7	0.003749				

Table 10: ANOVA table for initial treatment comparing CPP and PET for plastic-type effect investigation

	%Crystallinity				Hardness			
Effect	Num. DF	Den. DF	F	p	Num. DF	Den. DF	F	p
Week	1	11	286.2	3.19E-09	1	30	0.6	4.57E-01
Plastic type	1	12	10676.6	0.0E+00	1	30	287.2	1.11E-16
Initial treatment	2	12	195.6	6.94E-10	2	30	17.3	1.01E-05
Week*Plastic type	1	11	134.1	1.68E-07	1	30	114.2	9.50E-12
Week*Initial treatment	2	11	195.6	2.53E-09	2	30	19.5	3.68E-06
Plastic type*Initial treatment	2	12	79.4	1.20E-07	2	30	7.7	1.98E-03
Week*Plastic type*Initial treatment	2	11	79.4	2.91E-07	2	30	8.7	1.04E-03
	Carbonyl index				Hydroxyl index			
Effect	Num. DF	Den. DF	F	p	Num. DF	Den. DF	F	p
Week	3	48	4.7	6.04E-03	3	48	7.7	2.57E-04
Plastic type	1	26	4852.4	0.0E+00	1	26	78	2.64E-09
Initial treatment	2	26	1.1	3.35E-01	2	26	2.7	8.66E-02
Week*Plastic type	3	48	22.8	2.50E-09	3	48	1.6	2.01E-01
Week*Initial treatment	6	48	4.4	1.33E-03	6	48	40.7	0.0E+00
Plastic type*Initial treatment	2	26	8.9	1.16E-03	2	26	1	3.69E-01
Week*Plastic type*Initial treatment	6	48	12.5	1.98E-08	6	48	4.1	2.21E-03
	Suspected methylene and methyl index				Suspected methanetriyl and methyl index			
Effect	Num. DF	Den. DF	F	p	Num. DF	Den. DF	F	p
Week	3	48	0.5	6.59E-01	3	48	0.8	4.98E-01
Plastic type	1	26	14.1	8.70E-04	1	26	14.6	7.43E-04
Initial treatment	2	26	3	6.64E-02	2	26	2.1	1.48E-01
Week*Plastic type	3	48	2.1	1.13E-01	3	48	3.1	3.47E-02
Week*Initial treatment	6	48	6.3	6.65E-05	6	48	5.3	3.09E-04
Plastic type*Initial treatment	2	26	3.5	4.62E-02	2	26	1.9	1.77E-01
Week*Plastic type*Initial treatment	6	48	3	1.33E-02	6	48	3.6	5.21E-03
	Methanetriyl index							
Effect	Num. DF	Den. DF	F	p				
Week	3	48	7.3	4.09E-04				
Plastic type	1	26	4677.2	0.0E+00				
Initial treatment	2	26	23.1	1.74E-06				
Week*Plastic type	3	48	2	1.32E-01				
Week*Initial treatment	6	48	4.9	5.73E-04				
Plastic type*Initial treatment	2	26	6.2	6.40E-03				
Week*Plastic type*Initial treatment	6	48	2.1	6.68E-02				

Secondary treatment (bench tests)

Table 11: ANOVA table for secondary treatment (bench tests) comparing all plastic types in sea water

	%Crystallinity				Hardness			
Effect	Num. DF	Den. DF	F	p	Num. DF	Den. DF	F	p
Week	1	68	24.2	5.73E-06	3	540	35.4	0.0E+00
Plastic	2	72	19071.9	0.0E+00	2	180	1621.7	0.0E+00
Initial treatment	2	72	2441.1	0.0E+00	2	180	470.4	0.0E+00
Bench test	3	72	22.2	2.80E-10	3	180	11.9	3.95E-07
Week*Plastic	2	68	96.5	0.0E+00	6	540	3.3	3.58E-03
Week* Initial treatment	2	68	2.2	1.16E-01	6	540	3.2	4.24E-03
Plastic* Initial treatment	4	72	883	0.0E+00	4	180	182.4	0.0E+00
Week* Bench test	3	68	22.2	3.97E-10	9	540	11.6	1.11E-16
Plastic* Bench test	6	72	19.2	3.22E-13	6	180	8.6	3.18E-08
Initial treatment * Bench test	6	72	11.7	4.36E-09	6	180	5.2	5.58E-05
Week*Plastic* Initial treatment	4	68	15.6	4.16E-09	12	540	4	5.65E-06
Week*Plastic* Bench test	6	68	19.2	6.07E-13	18	540	4.5	2.57E-09
Week* Initial treatment * Bench test	6	68	11.7	6.08E-09	18	540	1.7	4.22E-02
Plastic* Initial treatment * Bench test	12	72	2.5	8.62E-03	12	180	0.7	7.34E-01
Week*Plastic* Initial treatment * Bench test	12	68	2.5	9.05E-03	36	540	2.9	1.06E-07

Table 11 continued: ANOVA table for secondary treatment (bench tests) comparing all plastic types in sea water

	Carbonyl index				Hydroxyl index			
Effect	Num. DF	Den. DF	F	p	Num. DF	Den. DF	F	p
Week	3	487	33.9	0.0E+00	3	487	216.4	0.0E+00
Plastic	2	180	5647.7	0.0E+00	2	180	11.7	1.68E-05
Initial treatment	2	180	2	1.34E-01	2	180	7.3	8.59E-04
Bench test	3	180	41.1	0.0E+00	3	180	269.2	0.0E+00
Week*Plastic	6	487	87.7	0.0E+00	6	487	12.7	2.28E-13
Week*Initial treatment	6	487	18.8	0.0E+00	6	487	28.5	0.0E+00
Plastic*Initial treatment	4	180	6.9	3.70E-05	4	180	5.7	2.50E-04
Week*Bench test	9	487	86.1	0.0E+00	9	487	64.5	0.0E+00
Plastic*Bench test	6	180	152.2	0.0E+00	6	180	13.6	1.07E-12
Initial treatment*Bench test	6	180	6.3	4.44E-06	6	180	13.2	2.39E-12
Week*Plastic*Initial treatment	12	487	6.4	1.65E-10	12	487	11.3	0.0E+00
Week*Plastic*Bench test	18	487	50.4	0.0E+00	18	487	10.1	0.0E+00
Week*Initial treatment*Bench test	18	487	17.1	0.0E+00	18	487	23.6	0.0E+00
Plastic*Initial treatment*Bench test	12	180	3.8	4.16E-05	12	180	4.9	4.90E-07
Week*Plastic*Initial treatment*Bench test	36	487	8.1	0.0E+00	36	487	14	0.0E+00

	Suspected methylene and methyl index			
Effect	Num. DF	Den. DF	F	P
Week	3	487	645.8	0.0E+00
Plastic	2	180	156.3	0.0E+00
Initial treatment	2	180	0.5	5.95E-01
Bench test	3	180	169.1	0.0E+00
Week*Plastic	6	487	59.3	0.0E+00
Week*Initial treatment	6	487	30.2	0.0E+00
Plastic*Initial treatment	4	180	3.3	1.30E-02
Week*Bench test	9	487	211.8	0.0E+00
Plastic*Bench test	6	180	11.8	4.18E-11
Initial treatment*Bench test	6	180	17.3	8.88E-16
Week*Plastic*Initial treatment	12	487	11	0.0E+00
Week*Plastic*Bench test	18	487	23.2	0.0E+00
Week*Initial treatment*Bench test	18	487	23.9	0.0E+00
Plastic*Initial treatment*Bench test	12	180	3.7	5.65E-05
Week*Plastic*Initial treatment*Bench test	36	487	4.6	2.33E-15

Comparing different environments

Table 12: ANOVA table for comparing environments at 25˚C

	%Crystallinity				Hardness			
Effect	Num. DF	Den. DF	F	p	Num. DF	Den. DF	F	p
Week	1	17	14.7	1.33E-03	1	45	115.1	0.0E+00
Plastic	2	18	8629	0.0E+00	2	45	314.3	0.0E+00
Environment	2	18	5.3	1.56E-02	2	45	2.5	8.94E-02
Week*Plastic	2	17	18.9	4.70E-05	2	45	54.3	0.0E+00
Week*Environment	2	17	6.2	9.27E-03	2	45	2.5	8.94E-02
Plastic*Environment	4	18	2.8	5.74E-02	4	45	1	4.41E-01
Week*Plastic*Environment	4	17	3.3	3.52E-02	4	45	1	4.41E-01
	Carbonyl index				Hydroxyl index			
Effect	Num. DF	Den. DF	F	p	Num. DF	Den. DF	F	p
Week	3	105	64	0.0E+00	3	105	153.5	0.0E+00
Plastic	2	43	6107.6	0.0E+00	2	43	4.3	2.00E-02
Environment	2	43	37.3	0.0E+00	2	43	131.4	0.0E+00
Week*Plastic	6	105	80.5	0.0E+00	6	105	2.5	2.92E-02
Week*Environment	6	105	15.6	0.0E+00	6	105	42.9	0.0E+00
Plastic*Environment	4	43	58.4	0.0E+00	4	43	6.7	2.84E-04
Week*Plastic*Environment	12	105	20.7	0.0E+00	12	105	8.1	0.0E+00
	Suspected methylene and methyl index							
Effect	Num. DF	Den. DF	F	p				
Week	3	105	383.1	0.0E+00				
Plastic	2	43	601.5	0.0E+00				
Environment	2	43	111.6	0.0E+00				
Week*Plastic	6	105	13.8	0.0E+00				
Week*Environment	6	105	95.4	0.0E+00				
Plastic*Environment	4	43	7.2	1.55E-04				
Week*Plastic*Environment	12	105	7.9	0.0E+00				

Table 13: ANOVA table for comparing environments of water salinity

	%Crystallinity				Hardness			
Effect	Num. DF	Den. DF	F	p	Num. DF	Den. DF	F	p
Week	1	35	0	9.86E-01	2	90	203.7	0.0E+00
Plastic	2	36	4339.1	0.0E+00	1	90	4.8	3.11E-02
Environment	1	36	0.1	7.78E-01	2	90	10	1.17E-04
Treatment	2	36	0.5	6.20E-01	1	90	5.4	2.24E-02
Week*Plastic	2	35	62.5	2.84E-12	2	90	0.8	4.70E-01
Week*Environment	1	35	0.1	7.78E-01	4	90	7.6	2.69E-05
Plastic*Environment	2	36	1.9	1.63E-01	2	90	4.7	1.09E-02
Week*Treatment	2	35	0.5	6.20E-01	2	90	39.7	4.43E-13
Plastic*Treatment	4	36	13.7	6.84E-07	1	90	5.6	1.97E-02
Environment*Treatment	2	36	0.1	9.09E-01	2	90	11.8	2.84E-05
Week*Plastic*Environment	2	35	1.9	1.64E-01	4	90	0.4	7.95E-01
Week*Plastic*Treatment	4	35	13.7	7.93E-07	2	90	0.9	4.12E-01
Week*Environment* Treatment	2	35	0.1	9.09E-01	4	90	8.9	4.33E-06
Plastic*Environment* Treatment	4	36	1.9	1.36E-01	2	90	5.6	5.20E-03
Week*Plastic*Environment * Treatment	4	35	1.9	1.36E-01	4	90	0.5	7.41E-01
	Carbonyl index				Hydroxyl index			
Effect	Num. DF	Den. DF	F	p	Num. DF	Den. DF	F	p
Week	3	260	1.7	1.73E-01	3	260	231.7	0.0E+00
Plastic	2	90	262793.8	0.0E+00	2	90	1290169	0.0E+00
Environment	1	90	2.6	1.12E-01	1	90	69.9	7.24E-13
Treatment	2	90	2.1	1.25E-01	2	90	195.1	0.0E+00
Week*Plastic	6	260	11.2	4.53E-11	6	260	124.1	0.0E+00
Week*Environment	3	260	1	3.87E-01	3	260	229.3	0.0E+00
Plastic*Environment	2	90	0	9.74E-01	2	90	17	5.65E-07
Week*Treatment	6	260	4.8	1.08E-04	6	260	82.4	0.0E+00
Plastic*Treatment	4	90	13	2.02E-08	4	90	61.2	0.0E+00
Environment*Treatment	2	90	2.3	1.09E-01	2	90	13.2	9.75E-06
Week*Plastic*Environment	6	260	4	7.03E-04	6	260	98.6	0.0E+00
Week*Plastic*Treatment	12	260	6.5	4.63E-10	12	260	53.1	0.0E+00
Week*Environment* Treatment	6	260	2.4	2.83E-02	6	260	102.1	0.0E+00
Plastic*Environment* Treatment	4	90	0.5	7.68E-01	4	90	6.6	1.00E-04
Week*Plastic*Environment * Treatment	12	260	2.4	4.94E-03	12	260	41.3	0.0E+00

Table 13 continued: ANOVA table for comparing environments of water salinity

	Suspected methylene and methyl index			
Effect	Num. DF	Den. DF	F	p
Week	3	259	58.1	0.0E+00
Plastic	2	90	1276.8	0.0E+00
Environment	1	90	21.7	1.10E-05
Treatment	2	90	45.3	2.48E-14
Week*Plastic	6	259	31	0.0E+00
Week*Environment	3	259	4.9	2.60E-03
Plastic*Environment	2	90	0.4	6.90E-01
Week*Treatment	6	259	52.6	0.0E+00
Plastic*Treatment	4	90	28	4.00E-15
Environment*Treatment	2	90	5.2	7.32E-03
Week*Plastic*Environment	6	259	5	7.23E-05
Week*Plastic*Treatment	12	259	22.3	0.0E+00
Week*Environment*Treatment	6	259	7.4	2.54E-07
Plastic*Environment*Treatment	4	90	1.2	2.98E-01
Week*Plastic*Environment*Treatment	12	259	4.1	6.23E-06